Investigating the Role of Reactor Design to Maximise the Environmental Benefit of Algal Oil for Biodiesel

A thesis submitted to the University of Cape Town in partial fulfilment of the requirements for the degree of Master of Science in Engineering

Christine Richardson

March 2011

Centre for Bioprocess Engineering Research
Department of Chemical Engineering
University of Cape Town

Synopsis

While initially thought to be promising, crop based biofuels are an inadequate alternative to fossil energy due to the unrealistic space requirement, competition with food crops for land use and greenhouse gas release on clearing for crop land several times greater than biofuels provide through displacing fossil fuels, a factor inadequately accounted for in past studies. In contrast, biodiesel from microalgae is of interest due to the lower spatial requirements, much higher oil productivity, no requirement for arable land and rapid growth and harvesting cycles. To ensure the oversights of crop based biofuels are not repeated, there is a need to explore the sustainability of an algal biorefinery in the context of biodiesel production in this early phase of process development. An integrated biorefinery approach for the production of multiple products has been seen to improve the overall efficiency of biomass utilization in biofuel systems, contributing to both economic success and environmental sustainability and is of interest for microalgal biodiesel production.

A recent Life Cycle Assessment (LCA) study completed within the Centre for Bioprocess Engineering Research (CeBER) has shown that, in bioprocesses, the environmental impact of overall bioprocesses is strongly dependent on the bioreactor. This was shown for several heterotrophic microbial systems, but algal systems were not investigated. Improvements to the bioreactor phase can be made through changes in the microalgal species and bioreactor configuration. Species choice is an area of contention in the literature at present as, while data are available across most species, much of these data are not comparable due to inconsistencies in scale, reactor type and environmental conditions. Factors affecting this species choice include the lipid content, biomass concentration, productivity and ease of downstream processing. Lipid productivity has been shown to be the desirable criterion in species choice for algal biodiesel over growth rate and lipid content alone. There is also debate in the literature over the choice of open or closed reactor systems for the cultivation of microalgal biodiesel. While open systems are cheaper both in terms of construction costs and energetic efficiency, closed photobioreactors achieve much higher biomass concentrations and productivities and allow for better control of the culture conditions.

The main objectives of this study were therefore:

- To select, design and model a process flow-sheet representing a suitable biorefinery for the production of microalgal biodiesel and suitable co-products
- To collect appropriate data to inform the material and energy inventory of this flow-sheet

- To use the process simulation model to investigate several microalgal species and bioreactor configurations and generate material and energy inventories for the production of a functional unit of microalgal biodiesel
- To assess the system dependence on bioreactor design in terms of fossil energy requirement overall environmental impact using Life Cycle Analysis (LCA)

A process flow-sheet simulation model was developed to facilitate the rational design of a biorefinery for the production of microalgal biodiesel. The flow-sheet included algal cultivation, concentration of the algal suspension and dewatering, oil extraction, refining and its transesterification for biodiesel production and anaerobic digestion of residual biomass. These unit processes were modelled by means of material and energy balances informed by chemical engineering fundamentals, using MATLAB. The model was then used for the investigation of several microalgal species and bioreactor configurations, using experimental and literature data respectively. Inventory data generated by the model, according to the flow-sheet selected for the production of 1000 kg of biodiesel, was used to facilitate energy analysis and Life Cycle Assessment of three species of microalgae and three reactor configurations.

The impact of species choice was investigated using experimental data for *Chlorella vulgaris*, *Scenedesmus* sp. and *Tetraselmis suecica,* grown in 3.2 L CeBER Laboratory Vertical Airlift Reactors under identical nitrogen starved cultivation conditions. These species were selected from a laboratory study within CeBER investigating the growth and settling characteristics of 11 microalgal species grown under nitrogen replete and limited conditions. This addressed the problem of data quality in the algal literature prior to this study. Energy analysis showed an unrealistic negative energy balance, with the majority of the process energy requirement attributed to the reactor, particularly due to the supply of compressed air. This airlift reactor configuration was thus shown not to be suitable for scale-up. Sensitivity analysis on the reactors revealed air compression and connecting reactors in series to be key operational variables, offering order of magnitude reductions in reactor energy input per unit volume.

Lipid productivity was shown to be inversely proportional to reactor energy and thus the key variable in species choice. *Scenedesmus* sp. achieved the highest lipid productivity and thus, production of biodiesel from this species resulted in the lowest fossil energy requirement.

The environmental impact of the production of biodiesel from algae was found to be predominantly due to reactor energy requirements and the production of nitrogen fertiliser. Due to the dominance of reactor energy, the lowest environmental impact was again achieved by *Scenedesmus* sp., due to

its superior lipid productivity. All impact categories showed marked decrease when the digestate following anaerobic digestion was allocated as a fertiliser equivalent.

The impact of reactor configuration was analysed using three possible reactor configurations: raceway ponds and horizontal and vertical tubular reactor systems. The investigation showed raceway ponds to be the most energetically favourable, showing a net energy ratio (NER) of 1.5. Further sensitivity analysis revealed that the raceway, despite low concentrations and productivities, provides a net energy gain over the entire range of reasonable conditions. Neither of the airlift reactor systems investigated showed a net energy gain. The horizontal tubular airlift reactor was approximately energy neutral, with a NER of 0.97, contrasting to the vertical tubular airlift reactor which showed an NER of only 0.12. This airlift configuration was thus considered unsuitable for algal biodiesel production systems and not investigated on a life cycle basis.

A life cycle assessment of the production of microalgal biodiesel using raceway and horizontal tubular reactors was performed. Notably, raceway systems were shown to perform favourably in the global warming impact category due to the CO_2 utilised for growth. While the horizontal tubular reactor also utilised CO_2, this benefit was offset by the large reactor energy requirement.

For all three systems, the reactor was the dominant contributor to the overall process energy requirement. In raceway systems, however, the pumping contribution was also notable due to the low biomass concentrations. Sensitivity analysis showed the pumping energy requirement in raceways to decrease by an order of magnitude as the biomass concentration increased from 0.1 to 0.5 g/L. Further increases in biomass concentration showed less pronounced changes.

The sensitivity analysis also considered biomass productivity, lipid content and lipid productivity. In all three reactor cases, increases in these three variable resulted in process energy reduction. Both biomass productivity and lipid content translate into increased lipid productivity and thus a decreased reactor volume and, to a lesser extent, pumping requirement. The closed reactor systems show a more significant decrease over the achievable range for the given reactor system due to their higher power input per unit volume.

For raceways, a lipid productivity of greater than 0.005 g/L/day was shown to lead to a net energy gain at 0.5 g algal biomass/L. Cultivation in horizontal and vertical tubular reactors was estimated to require lipid productivities above 0.4 and 0.5 g/L/day respectively at the concentrations of ~4 and 1 g algal biomass/L. Vertical tubular reactors are therefore well short of the requirements for large scale biodiesel production, while raceways are energetically feasible over the entire range of reasonable conditions.

Acknowledgements

I would like to thank my supervisor, Professor Sue Harrison for all her input and the long hours put into this thesis. Also for giving me the opportunity to take a portion of this work to the RRB6 conference in Germany in 2010 and for making the transition from science to engineering such a good one. Thank you also to my co-supervisor, Associate Professor Harro von Blottnitz for all your assistance, advice and input to the LCA portion of the thesis and for setting me up with such an amazing job post-thesis.

I also wish to thank Mel and Nick for putting up with all my questions. Particularly to Mel, thank you for all your help in the beginning of this project and for showing me the ropes so well. To all the CeBER staff and students who assisted me during my time in Chemical Engineering, a big thank you for all your help and for being nice people. A big thank you also to Candice, for all the running around and mind-numbing tasks I gave you on the final day of this project and for the sometimes confusing enthusiasm with which you tackled them.

To John and Gaby, thank you for your editing help as well as the general support you provided during this project. It really was invaluable. John, thank you for teaching me how to be an engineer and to use MATLAB. Also, for always being available for anything from small questions to lengthy discussions to vending machine breaks.

In addition, acknowledgement is given to the Department of Science and Technology and National Research Foundation (NRF) for funding through the South African Research Chair Initiative and SABI and the Centre for Bioprocess Engineering Research (CeBER) (Department of Chemical Engineering, UCT), for providing the necessary funding to complete the project.

Plagiarism Declaration

I know the meaning of plagiarism and declare that all of the work in the document, save for that which is properly acknowledged, is my own.

Table of Contents

Synopsis i

Acknowledgements iv

Plagiarism Declaration v

Table of Contents vi

List of Figures xi

List of Tables xiv

Nomenclature xvi

Greek Letters xviii

Abbreviations xix

1. Introduction 1

1.1. Microalgal Biodiesel in Context 1

1.1.1. First Generation Biofuels 1

1.1.2. Biodiesel from Microalgae: a 2nd Generation Biofuel 2

1.1.3. Environmental Considerations and the Concept of a Biorefinery 2

1.2. Previous Work: Large-Scale, Low-Value, Low Concentration Processes 4

1.3. Considerations for the Production of Algal Biomass 5

1.3.1. Light for Photosynthesis 5

1.3.2. Gas Exchange 6

1.3.3. Mixing 8

1.3.4. Temperature Control 8

1.3.5. Salinity, Nutrients and pH control 9

1.3.6. Strain Selection 9

1.4. Photobioreactors 9

1.4.1. Open Pond Systems 10

1.4.2. Enclosed Photobioreactors 11

1.4.3. Hybrid Systems 16
1.4.4. Scale Up 17
1.4.5. Capital Cost 17
1.5. Harvesting 18
1.5.1. Initial concentration methods 18
1.5.2. Centrifugation 19
1.6. Environmental Assessments of Biofuel Processes 19
1.6.1. Life Cycle Assessment (LCA) 19
1.6.2. LCA Development: Lessons from Previous Studies 21
1.6.3. Investigating the Applicability of LCA in Biorefineries 22
1.7. Objectives and Key Questions 23
1.8. Thesis Structure 24
2. A Review of Life Cycle Assessments (LCA) of Algae to Biodiesel Processes 25
2.1. Introduction 25
2.2. Algal biodiesel LCAs published during this project 26
2.3. Production system overview 29
2.3.1. Reactors 31
2.3.2. Dewatering 35
2.3.3. Oil extraction and biodiesel production 36
2.3.4. Biogas as a co-product 36
2.4. LCA Methodology and Approach 38
2.4.1. Scope, Allocation and Methodology 38
2.4.2. LCI and data sources 39
2.5. Key issues, findings and recommendations 40
2.5.1. CO_2 provision 40
2.5.2. Fertiliser/Nutrient provision and recycle 41
2.5.3. Climate and Location Considerations 42
2.5.4. Water use 43

2.5.5. Comparison to fossil fuels and 1st generation biofuels 43
2.6. Conclusions 44
3. Methodology 45
3.1. Model development 45
3.2. Base case process details 46
3.2.1. System overview 46
3.2.2. Biomass Growth Characteristics and Media Composition 46
3.2.3. Cultivation in Laboratory Vertical Airlift Reactors 49
3.2.4. Dewatering 51
3.2.5. Oil extraction 54
3.2.6. Biodiesel production 55
3.2.7. Anaerobic digestion 56
3.3. Species comparison/Growth study 57
3.4. Reactor Study 58
3.4.1. Raceway ponds 59
3.4.2. Horizontal Tubular Reactor 61
3.4.3. Vertical tubular reactor 64
3.5. Life Cycle Assessment 65
3.5.1. Goal and Scope Definition 65
3.5.2. Life Cycle Inventory Analysis (LCI) 66
3.5.3. Life Cycle Impact Assessment (LCIA) and Interpretation 67
4. Life-Cycle Comparison between Species of Microalgae 68
4.1. Introduction 68
4.2. Methodology 69
4.3. Material and Energy Inventory Data 71
4.4. Energy Assessment 72
4.4.1. The relationship between lipid productivity and energy requirement 72
4.4.2. System Energy Overview 74

4.5. Sensitivity study 77
4.5.1. CO_2 gas-liquid mass transfer 77
4.5.2. Riser residence time 79
4.5.3. Dissolved oxygen levels 79
4.5.4. Reactor energy 81
4.6. Life cycle Analysis 82
4.6.1. Methodology 82
4.6.2. Neutral energy scenario 82
4.6.3. Digestate from anaerobic digestion used as a soil conditioner 85
4.7. Conclusions 86
5. Life-cycle comparison of reactor design 88
5.1. Introduction 88
5.2. Methodology 89
5.3. Material and Energy Inventory Data 90
5.4. Energy Analysis 92
5.5. Life Cycle Assessment 93
5.5.1. Methodology 93
5.5.2. Life Cycle Impact Assessment 93
5.6. Sensitivity study 95
5.6.1. Reactor configuration and specifications 95
5.6.2. Algal growth parameters 97
5.7. Conclusions 103
6. Conclusions 105
6.1. Major findings 105
6.2. Findings related to key questions 107
6.3. Future work 109
7. References 110
A. Appendix 117

A.1. Data for Algal Process model 117
A.1.1. Biodiesel and Lipase production 117
A.1.2. Experimental Growth and Composition Data 118
A.2. Material and Energy Inventory Data 120
A.3. Determination of the Additional Pipe Length in Horizontal Tubular Airlift Reactor Due to Bends in the Solar Collector 133
A.4. Laboratory Airlift Reactor Sensitivity Calculations 134
A.4.1. Liquid Circulation in Airlift Bioreactors 134
A.4.2. Gas-liquid mass transfer 135

List of Figures

Figure 1-1 A conceptual process for producing biodiesel from microalgae Chisti (2008). 3
Figure 1-2 Aerial schematic of a raceway (Chisti, 2007) 11
Figure 1-3 Schematic of an airlift reactor system (Najafpour, 2007). 13
Figure 1-4 Typical Oscillatory flow reactor configuration (Harvey *et al.*, 2001) 14
Figure 1-5 Typical arrangement of a horizontal tubular reactor system (Chisti, 2007) 15
Figure 1-6 Systematic representation of a helical tubular reactor. Flow through a coiled array tubes in an open circular framework is driven by a centrifugal pump to a degasser and heat exchanger. 16
Figure 1-7 The phases of Life Cycle Assessment (LCA) (Uihlein & Schebek, 2009) 20
Figure 2-1 Diagram of system with boundaries from different LCA studies, where all inputs and outputs to the unit processes shown are included. 29
Figure 2-2 Contributions of cultivation to the Fossil energy requirement and GWP burden in (a) raceways and (b) tubular photobioreactors (Stephenson *et al.*, 2010). 34
Figure 2-3 Water footprint (kg-water/kg-biodiesel) of C. vulgaris-based biodiesel production under different climatic conditions (Yang *et al.*, 2011) 43
Figure 3-1 Process Flow-sheet for the system investigated. Annotations 1-24 refer to flows and A-I to energy inputs. 46
Figure 3-2 Schematic diagram of CeBER laboratory airlift reactor (Langley, 2010) 48
Figure 3-3 Airlift driven tubular photobioreactor (Molina *et al.*, 2001) 61
Figure 3-4 Schematic diagram of concentric draft tube ALRs showing vessel dimensions and air sparger details (Mirón *et al.*, 2000) 64
Figure 4-1 Flow-diagram illustrating the procedure followed to achieve the results of Chapter 4 70
Figure 4-2 Total fossil energy requirements for the production of 1000 kg of biodiesel from *Scenedesmus* sp. at various simultaneously occurring reactor biomass concentration and productivities according to the flow-sheet in Figure 3-1. 73
Figure 4-3 Reactor fossil energy requirements (kWh) as a function of lipid productivity (g/L/day) for the production of 1000 kg of biodiesel from *Chlorella vulgaris*, *Scenedesmus* sp. and *Tetraselmis suecica.* Base case scenario using flow-sheet given in Figure 3.1. 74
Figure 4-4 (a) Total and (b) downstream fossil energy requirements for the production of 1000 kg biodiesel from *Chlorella vulgaris*, *Scenedesmus* sp. and *Tetraselmis suecica* at the point of

highest instantaneous lipid productivity. Base case scenario for flow-sheet given in Figure 3.1.. 75
Figure 4-5 Total fossil energy requirements for the production of 1000 kg of biodiesel from *Chlorella vulgaris*, *Scenedesmus* sp. and *Tetraselmis suecica* at the point of highest instantaneous lipid productivity shown against the energy value of the biodiesel produced, assuming a calorific value of 37.2 MJ/kg. Base case scenario. 76
Figure 4-6 k_La capability of the system according to gas flow rate and k_La required to support the algal growth rate. The simulation was stopped when the system became CO_2 limited and would no longer be able to support the required growth rate for each respective (a) reactor in series at 2 L/min airflow rate and (b) inlet airflow rate to a single reactor. Growth of *Scenedesmus* sp. at maximum lipid productivity for the base case CO_2 concentration of 12.5%. 78
Figure 4-7 Riser residence time for each respective gas flow rate to a single reactor. According to Merchuk et al. (2000), a riser residence time of less than 6 seconds is required so as not to negatively affect the growth rate. 79
Figure 4-8 Dissolved oxygen concentrations calculated in the media and the maximum tolerable level of dissolved oxygen, taken as 300% of air saturation, for each respective (a) reactor in series at 2 L/min airflow rate and (b) inlet airflow rate to a single reactor. Growth of *Scenedesmus* sp. at maximum lipid productivity for the base case CO_2 concentration of 12.5%. 80
Figure 4-9 Reactor energy (per reactor in series) and corresponding air compression requirement for each respective reactor in series at an airflow rate of 2 L/min. 81
Figure 4-10 Reactor energy (kWh) for varying number of reactors in series and inlet gas flow rates within a reduced range. 82
Figure 4-11 Fossil energy requirements for the production of biodiesel from *Chlorella vulgaris*, *Scenedesmus* sp. and *Tetraselmis suecica* at the point of highest instantaneous lipid productivity. Reactor efficiency of 16 W/m^3. 84
Figure 4-12 Life cycle impacts for the production of biodiesel from *Chlorella vulgaris*, *Scenedesmus* sp. and *Tetraselmis suecica* at the point of highest instantaneous lipid productivity. Reactor efficiency of 16 W/m^3. 84
Figure 4-13 Global Warming potential for the production of biodiesel from *Chlorella vulgaris*, *Scenedesmus* sp. and *Tetraselmis suecica* at the point of highest instantaneous lipid productivity. Reactor efficiency of 16 W/m^3. 85
Figure 4-14 Life cycle impacts for the production of biodiesel from *Chlorella vulgaris*, *Scenedesmus* sp. and *Tetraselmis suecica* at the point of highest instantaneous lipid productivity where the

digestate from anaerobic digestion is used as a soil conditioner. Reactor efficiency of 16 W/m^3. 86
Figure 5-1 Flow-diagram illustrating the procedure followed to achieve the results of Chapter 5 90
Figure 5-2 Total Fossil Energy requirements for the production of 1000 kg of biodiesel from *Phaedodactylum tricornutum* in raceway ponds, and horizontal tubular and draft tube airlift photobioreactors. Base case. 92
Figure 5-3 Fossil Energy requirements of the process units involved in the production of 1000 kg of biodiesel from *Phaedodactylum tricornutum* in raceway ponds, horizontal tubular and draft tube airlift photobioreactors. Base case scenario for flow-sheet given in Figure 3.1. 93
Figure 5-4 Normalised life cycle impacts for the production of biodiesel from *Phaedodactylum tricornutum*, cultivated in raceway and hortzontal tubular reactors for the production of 1000 kg of biodiesel. Base case scenario. 94
Figure 5-5 Contributions to the global warming potential impact category for raceway and horizontal tubular reactor systems. 95
Figure 5-6 Reactor energy and corresponding air compression requirement for each respective vertical tubular reactor in series. 96
Figure 5-7 Total, pumping and flocculation energy requirements of biodiesel produced from *P. tricornutum* cultivated in raceway ponds over varying biomass concentrations. Base case scenario: 21% lipid content, 0.07 g/L/day. 98
Figure 5-8 Total and reactor energy requirements over various values of aerial and biomass productivity in (a) a raceway pond (b) horizontal tubular reactors and (c) vertical tubular reactors. Base case scenario: 21% lipid content, biomass concentration 0.5 g/L in raceways, 3.96 g/L in horizontal tubular reactors and 1 g/L in vertical tubular reactors. 99
Figure 5-9 Total reactor and pumping energy requirements and energy payback through anaerobic digestion over various lipid contents in (a) raceway ponds (b) horizontal tubular reactors and (c) vertical tubular reactors. Base case scenario: productivities of 0.07 g/L/day at 0.5 g/L in raceways, 1.9 g/L/day at 3.96 g/L in horizontal tubular reactors and 0.3 g/L/day at 1 g/L in vertical tubular reactors. 101
Figure 5-10 Total energy requirements various biomass productivities for lipid contents of 20, 40 and 60% in (a) raceway ponds (b) horizontal tubular reactors and (c) vertical tubular reactors. Base case scenario: biomass concentration 0.5 g/L in raceways, 3.96 g/L in horizontal tubular reactors and 1 g/L in vertical tubular reactors. 102
Figure A-1 Process Flow-sheet for the system investigated in Chapters 4 and 5. Annotations 1-24 refer to flows and A-I to energy inputs 120

List of Tables

Table 1-1 Comparison of biomass productivities in enclosed photobioreactors (Lee, 2001) 12
Table 2-1 Table showing the scope, method and allocation used in algal bio-energy LCA studies 30
Table 2-2 Reactor types, species and assumed data for resultant biomass growth characteristics and the energy requirement of the reactor. Some papers did not disclose certain parameters. 32
Table 2-3 Modes of dewatering employed and concentrations achieved 35
Table 2-4 Impact categories chosen in LCA studies. 39
Table 3-1 Base case biomass growth characteristics and composition for *Scenedesmus sp.* (Griffiths, 2011) 47
Table 3-2 Elemental compostions of the major biochemical classes found in algae and cyanobacteria (Geider & La Roche, 2002) 47
Table 3-3 Selected design parameters for Laboratory Vertical Airlift Reactors descibed 51
Table 3-4 Comparison of centrifugal methods for the concentration of microalgal biomass (Molina Grima *et al.*, 2003; Richmond, 2004b) 53
Table 3-5 COD destruction relative to volatile solids concentration for 20 days retention time (Samson, 1986). 57
Table 3-6 Design parameters for raceway ponds assumed in this study 59
Table 3-7 Design parameters for horizontal tubular photobioreactors assumed in this study 61
Table 3-8 Selected design parameters for concentric draft tube ALRs assumed in this study 65
Table 4-1 Material and energy inventory data for the three species at the point of maximum lipid productivity 71
Table 4-2 Total energy requirements and material flows through each process unit shown in Figure 3-1 for the three species at the point of maximum lipid productivity 72
Table 4-3 Growth characteristics for the point of highest instantaneous lipid productivity achieved during batch culture of each species and resultant energy requirements if these conditions were held in continuous culture for the production of 1000 kg of biodiesel. Base case scenario for flow-sheet given in Figure 3.1. 74
Table 5-1 Base case composition and culture parameters for the three reactor types investigated .. 89
Table 5-2 Material and energy inventory data for *P. tricornutum* grown in raceway ponds, vertical and horizontal tubular reactors 91

Table 5-3 Total energy requirements and material flows through each process unit shown in Figure 3-1 for *P. tricornutum* grown in raceway ponds, vertical and horizontal tubular reactors..... 92
Table A-1 Mass, energy and utility flows obtained by Harding (2009) for the production of 1 000 kg of biodiesel..... 117
Table A-2 Material, energy and utility flows for the production of lipase from *Candida antarctica* (Harding, 2009)..... 117
Table A-3 Daily growth data and biomass composition for *Chlorella vulgaris* grown under low nitrogen conditions..... 118
Table A-4 Daily growth data and biomass composition for *Scenedesmus* sp. grown under low nitrogen conditions..... 119
Table A-5 Daily growth data and biomass composition for *Tetraselmis suecica* grown under low nitrogen conditions..... 119
Table A-6 Composition of the streams in the process flow diagram, Figure A-1, for the production of 1000 kg of biodiesel from *Scenedesmus* sp. grown at the point of highest instantaneous lipid productivity in the laboratory airlift reactors described in Section 3.4.2 121
Table A-7 Composition of the streams in the process flow diagram, Figure A-1, for the production of 1000 kg of biodiesel from *Phaedodactylum tricornutum* grown in the raceway ponds described in Section 3.4.1. 124
Table A-8 Composition of the streams in the process flow diagram, Figure A-1, for the production of 1000 kg of biodiesel from *Phaedodactylum tricornutum* grown in the vertical tubular airlift reactors described in Section 3.4.3 127
Table A-9 Composition of the streams in the process flow diagram, Figure A-1, for the production of 1000 kg of biodiesel from *Phaedodactylum tricornutum* grown in the horizontal tubular airlift reactors described in Section 3.4.2 130

Nomenclature

Symbol	Description	Units
A_b	free area below draft tube	m^2
A_d	cross-sectional areas of the downcomer	m^2
A_r	cross-sectional areas of the riser	m^2
A_s	cross-sectional area of sump	m^2
B_0	specific yield of methane	L/g VS
C	volumetric fraction in settling pondfeed	-
C*	liquid saturation concentration of CO_2 in the media	g/L
C_L	actual liquid concentration of CO_2 in the media	g/L
C_u	volumetric solids fraction in settling pond outflow	-
C_α	ratio of superficial gas velocity to total superficial velocity in riser	-
C_β	characteristic parameter, taken as 1.1	-
D_i	impeller diameter	m
D_s	distance from sparger level to liquid outflow	m
D_v	vessel diameter	m
g	acceleration due to gravity	m/s^2
h	head loss	m
h_D	sparged liquid height	m
h_r	height of riser	m
j_G	superficial gas velocity	m/s
j_l	superficial liquid velocity	m/s
j_{Lr}	superficial liquid velocity in the riser	m/s
K_B	frictional loss coefficient in the downcomer zone of the airlift loop	-
k_La	overall mass transfer coefficient	s^{-1}

K_T	frictional loss coefficient in the riser zone of the airlift loop	-
L_c	channel length	m
L_{eq}	equivalent length of horizontal tubular reactor loop	m
L_{max}	maximum length of continuous tubing for a given culture velocity	m
L/S	Mass liquids/mass solids	-
M	molar mass of gas	kg/kmol
N	impeller rotational speed	Hz
n	average carbon oxidation state in the substrate	-
n	Manning's roughness coefficient	-
N_{min}	minimum speed of impeller rotation	Hz
P	required compression	Pa
P_b	pressure at the bottom of the fluid in the vessel	Pa
P_G	power input	W
P_h	headspace pressure (usually atmospheric)	Pa
P_M	mixer power	W
P_o	power number	-
Q_0	settling pond inlet flow rate	m^3/h
Q_G	volumetric gas flow rate	m^3/s
Q_L	volumetric liquid flow rate	m^3/day
Q_M	molar flow rate of gas	kmol/s
R	universal gas constant	J/mol.K
Re	Reynolds number	-
r_G	ratio of methane to carbon dioxide in the gas	-
R_h	mean hydraulic diameter	m
R_{O2}	volumetric rate of oxygen generation in the tube	$kg/m^3/day$
T	temperature	K

U	L/S mass ratio in underflow	-
U_0	gas velocity at orifice of sparger	m/s
$U_{b,\infty}$	average bubble rise velocity	m/s
u_c	particle settling speed	m/h
v_L	liquid velocity	m/s
V_m	molar volume of methane	m^3/mol
V_m	Molar volume	m^3/mol
W	work done	W
Y	L/S mass ratio in feed	-
y	ratio of heat capacities	-

Greek Letters

ρ_M	density of 2 phase mixture	kg/m^3
ε	overall gas hold-up	-
ε_d	gas hold-up in downcomer	-
ε_r	gas hold-up in riser	-
η_{PW}	paddle wheel efficiency	-
μ_d	viscosity of dispersed phase	Pa.s
μ_M	viscosity of 2 phase mixture	Pa.s
ρ_d	density of dispersed phase	kg/m^3
ρ_L	density liquid	kg/m^3
ρ_s	density solid	kg/m^3
σ	interfacial tension between phases	J/m^2

Abbreviations

AD	Anaerobic Digestion
ALR	Airlift Reactor
ASP	Aquatic Species Program
ASP	Aquatic Species Programme
BNR	Biological Nitrogen Removal
CAS	Conventional Activated Sludge
CeBER	Centre for Bioprocess Engineering Research
COD	Chemical Oxygen Demand
DAF	Dissolved Air Flotation
DO	Dissolved Oxygen
DSP	Downstream Process
ECPT	Ecosystem Carbon Payback Time
GHG	Greenhouse Gas
GMP	Good Manufacturing Practice
GWP	Global Warming Potential (kg CO_2 eq.)
HeTR	Helical Tubular Reactors
HRT	Hydraulic Retention Time
HTR	Horizontal Tubular Reactors
LCA	Life Cycle Assessment
LCF	Lignocellulose Feedstock
LCI	Life Cycle Inventory Analysis
LCIA	Life Cycle Impact Assessment
NER	Net Energy Ratio (energy in biodiesel produced: fossil energy required)
OLR	Organic Load Rate

PFD	Photon Flux Density
SSU	Source Separated Urine
TAG	Triacylglycerides
ULS	Ultra-Low Sulphur
VS	Volatile Solids
VTR	Vertical Tubular Reactors
WWT	Wastewater Treatment

1. Introduction

1.1. Microalgal Biodiesel in Context

1.1.1. First Generation Biofuels

In an age where fossil fuels are now widely recognised as unsustainable, both due to limited supply and emissions of harmful greenhouse gases, biofuels have gained popularity in the search for clean, renewable fuel sources (Chisti, 2008).

Biodiesel is a proven fuel, derived from plant and animal oils. It is produced in a transesterification reaction, where short-chain alcohols are reacted with triglycerides to produce fatty acid alkyl esters, with glycerol as a by-product (Vasudevan & Briggs, 2008). Low in sulphur, polycyclic aromatic hydrocarbons and metals, it is considered to be a clean burning fuel. While CO_2 is emitted during combustion of biodiesel, it is also taken up by growth of feedstock, resulting in a more favourable carbon balance than that of petroleum diesel (Schenk, 2008).

While some studies have investigated the use of waste cooking oil and animal fats for biodiesel, the majority of biofuels studied are produced from higher plants (Vasudevan & Briggs, 2008). These plants convert sunlight into chemical energy in the process of photosynthesis. Current plant sources for biofuel production include sugarcane, soybean, corn, sunflower, canola, jatropha and oil palm. Biodiesel from oil crops and bioethanol from sugarcane are produced in increasing amounts. Despite their attraction, there are serious economic, environmental and social limitations associated with these first generation biofuel processes (Schenk, 2008).

The main shortcoming of crop-based first generation biofuels regards their unrealistic land requirement. While solar energy is abundant, the low quantum efficiency and oil content of oil crops severely limits their energy productivity (Vasudevan & Briggs, 2008). Even if all the arable land in the world were dedicated to the cultivation of oil producing crops, the biofuel produced would not be enough to meet even half the global energy requirement (Schenk, 2008). Such production would result in competition with food and other agricultural products for arable land, causing food prices to rise. Developing countries, which are already suffering from food shortages, would be the worst hit.

The large land requirement also translates into an unsustainable requirement for both fertilizers and water. Increased production of fertilizer unfavourably impacts both the overall carbon and energy

balance. The use of machinery for cultivation, refining and transport requires energy and results in emissions. The photosynthetic nature of the crops contributes to an improvement in the overall carbon balance through CO_2 sequestration and cycling, but not enough to make the process sustainable. It is also necessary to consider unsustainable practices emerging from the increased demand for arable land, where large areas of natural vegetation are being cleared to make room for fuel crop plantations. The clearance alone not only results in greenhouse gas (GHG) emissions, but also the removal of CO_2 sequestering plants (Fargione, 2008; Larson, 2006; Schenk, 2008; Searchinger, 2008).

All of these factors need to be carefully considered in the development and implementation of second generation biofuel processes.

1.1.2. Biodiesel from Microalgae: a 2nd Generation Biofuel

Biodiesel from microalgae presents a promising alternative. Analogous to higher plants, microalgae are photosynthetic micro-organisms that utilize the sun's energy and water to convert carbon dioxide to algal biomass (Chisti, 2007). Algal strains have been shown to exhibit 15-300 times more oil than higher plants on an area basis. Commonly doubling their biomass within 24 hours, a fast growing alga can lead to a much shorter harvesting cycle and as a result a much higher yield per hectare (Schenk, 2008). The average photosynthetic efficiency may also be better for microalgae, lowering nutrient and fertiliser inputs and hence reducing waste (Vasudevan & Briggs, 2008). Microalgae have been cultivated successfully in wastewater and sea water. Growth in such media and in bioreactors means that they do not compete with food crops for arable land. Microalgal growth may also be combined with direct biofixation of waste CO_2 from power plants (Rodolfi *et al.*, 2009).

Although microalgal biodiesel has the potential to compete with fossil fuels, there are several factors which currently limit large-scale production (Chisti, 2007). These factors include low biomass concentrations achieved in algal cultures. This, in combination with the small size of algal cells, contributes to high downstream processing costs as cheaper harvesting methods such as filtration are effectively eliminated in such large volumes. In addition, large water content translates into a high energy requirement for drying the biomass (Li, 2008).

1.1.3. Environmental Considerations and the Concept of a Biorefinery

There is some disagreement in the literature concerning the environmental feasibility of algal biofuels. Several authors have suggested that microalgal biofuels may do better than terrestrial biofuels particularly regarding the reduction of greenhouse gas emissions (Chisti, 2007; Huntley &

Redalje, 2007). In opposition to this, it has been stated that the energetic input for microalgal growth in bioreactors is likely to be greater than that of the output. Open pond systems may not be favourable both as CO_2 sequestration is not as good and N_2O emissions are possible (Wijffels, 2008). This incongruity necessitates further study into the environmental impacts of algal culture systems in the context of biodiesel production.

The production of microalgal biomass within a biorefinery has been proposed (Chisti, 2007; Griffiths & Harrison, 2009; Li, 2008). This involves the production of a range of products and biofuels through the integration of bioprocessing and low environmental impact technologies in a cost effective and environmentally sustainable manner (Li, 2008). A conceptual process proposed by Chisti (2008) is depicted in Figure 1-1 to produce biodiesel, animal feed, fertiliser, irrigation water and biogas, which could be used for power generation. While irrigation water is not a product of particular value, it is not harmful and thus an acceptable waste product. Nutrients and excess water could theoretically be recycled following biomass recovery. The recycling of nutrients is critical to avoid eutrophication, minimising environmental burden.

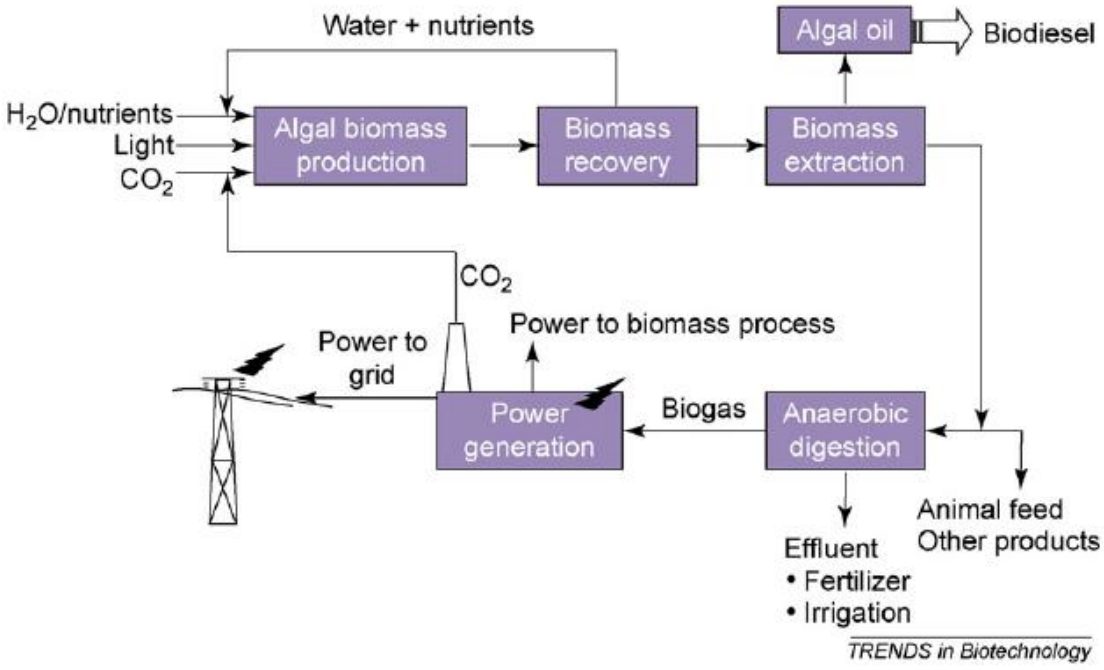

Figure 1-1 A conceptual process for producing biodiesel from microalgae (Chisti, 2008).

The biorefinery seeks to prioritise efficient management of process inputs in the form of water, CO_2, nutrients and energy as well as full utilisation of by-products and waste, thereby enhancing environmental sustainability. Water and nutrients provided during the biomass production phase are recycled following biomass recovery. Lipids are extracted to produce biodiesel in a separate process. Following extraction, there are several options for the use of residual biomass. These include use as an animal feed, the recovery of high value products or anaerobic digestion to produce

biogas for power generation, which is of particular interest. Effluents from the anaerobic digester could be used as fertiliser and irrigation water.

As mentioned in Section 1.1.2, fresh water is not needed for microalgal culture, light is freely available outdoors and CO_2 can be obtained at little or negative cost from power plant flue gas. CO_2 emitted from power generation could theoretically be pumped back into the biomass production phase (Chisti, 2008), using closed photobioreactors, but these are more costly to construct and operate, both energetically and financially (Section 1.4.2).

Power generation from biogas could be used to drive biomass production and downstream processes with the excess being sold to grid. The process' energy demand depends on the specific photobioreactor requirements with respect to aeration, mixing and downstream processing needs, dependent on the nature of the biomass produced (Sialve *et al.*, 2009).

A recent Life Cycle Assessment (LCA) study at the Centre for Bioprocess Engineering Research (CeBER) at the University of Cape Town (UCT) focussed on identifying areas in bioprocesses that dominate contribution to LCA scores or 'hotspots'. Reduced reactor volume and thus increased biomass concentration was shown to improve overall environmental impacts through LCA scores (Harding, 2009). Its applicability to algal systems has not yet been tested explicitly.

1.2. Previous Work: Large-Scale, Low-Value, Low Concentration Processes

In the study conducted by Harding (2009), material and energy balances and LCAs were conducted over several bioprocess case studies. Results showed that certain areas contribute more to LCA scores than others. Often this is due to the biomass concentration of the operating system, which defines the overall system volume required and affects the electrical requirements through agitation and aeration. These areas were then analysed further by extending the range through which relevant variables may change to determine trends in reactor biomass concentrations, electrical requirements, purities and resulting LCA single scores.

The variables identified by Harding (2009) relevant to photosynthetic algal growth are discussed in this section. These include final biomass concentration and downstream processing (DSP) separation efficiencies. Small changes to these variables can cause significant changes in the material and energy requirements of the process. These changes, particularly with respect to energy requirements, ultimately affect LCA scores for overall process.

In analysing the effect of variations in biomass concentration it was found that while increasing biomass concentration resulted in decreased electrical requirements for agitation, aeration and

sterilisation, the electrical requirement for bioreactor temperature control increases. The energy required to maintain the bioreactor temperature is directly related to the amount of biomass present. There is thus an optimal value for biomass concentration. In addition, waste removal from the product stream both increased purity and decreased the total volume entering subsequent DSP units. Accordingly, decreased volumes result in decreased energetic and chemical inputs in such DSP units. Purifying the product early in the DSP chain prevents the transport of unwanted large volumes through the process.

Harding (2009) investigated several scenarios for each case study to compare the effect of optimising the reactor process or downstream process on environmental impact. In all case studies analysed, improved bioreactor performance gave more favourable results than optimising downstream processing. This may be due to the degree of optimisation of the DSP while there is still much scope for improvement in the bioreactor setups. Moreover, an efficient bioreactor phase may lead to more favourable material and energy balances and an improved starting material for the DSP.

In bioprocesses, production in the bioreactor phase is constrained by the metabolic limits of the micro-organism. Furthermore, improvements in reactor productivity must be kept within economic limits. This is especially true in the context of algal biodiesel where success is strongly dependent on economic viability.

1.3. Considerations for the Production of Algal Biomass

Several factors need to be considered in the cultivation of algal biomass. These include the provision of light, adequate mixing, nutrients, CO_2 and removal of O_2, control of temperature and pH, selection of algal species and optimisation of these for the production of a desired product. These factors are integrated with bioreactor design and configuration, which is discussed in Section 1.4.

1.3.1. Light for Photosynthesis

As photoautotrophs, microalgae are able to convert light energy to chemical energy, which is transferred to the Calvin cycle to fix CO_2. Algal photosynthesis is limited by too little light, while excessive light can damage the photosynthetic apparatus through photoinhibition (Janssen, 2003). At high light intensities, microalgae have developed a photoprotective mechanism whereby excess energy is depleted as heat and fluorescence (Schenk, 2008). In the context of biofuel production, this is wasteful. Optimal photosynthetic efficiency occurs at moderate light intensities. Through efficient circulation of the cells through high and low light environments, this waste can be avoided as the

low light phase allows the algal cells to channel the excess energy into downstream metabolic processes (Schenk, 2008).

The density of the culture directly affects the provision of light energy to and thus photosynthetic efficiency of the algal cells. This is mainly due to mutual shading (Rosello Sastre *et al.*, 2007). For example, in *Nannochloropsis* sp. cultures of 2 g/L, light was able to penetrate to a depth at which light energy was 10% of incident light at 9.4 cm. In 10 g/L culture, this light limitation was reached at a depth of only 1.9 cm. In outdoor culture, where the photon flux density (PFD) is much higher than that required for optimum photosynthesis, photoinhibition is also an issue. This can be remedied by increasing the culture density and thus reducing the PFD for individual cells (Richmond, 2004a).

Since the main object of mass culture is the output of biomass or other products, the optimal cell concentration is that at which optimal output can be achieved per unit reactor volume or illuminated area. Thus optimal production rate is a function of both cell concentration and growth rate and is species specific (Richmond, 2004a).

Furthermore, it is important to note that even in optically thin cultures; light only penetrates a short distance into the liquid (Janssen, 2003). Thus, at any given moment, the majority of the cells are not exposed to light. The photic volume (that exposed to light) is a function of the intensity of the light source and the density of the culture. The frequency of light/dark cycling, as determined by the movement of cells in and out of the photic volume in an optimally mixed culture, is strongly related to the depth of penetration and mixing regime (Richmond, 2004a). It has been shown that high frequency light/dark cycles resulting from an optimally dense culture, where cells are subjected to short flashes of light followed by a relatively long dark period, result in considerably higher photosynthetic efficiencies (Janssen, 2003).

1.3.2. Gas Exchange

In order to maintain a high photosynthetic rate, the CO_2/O_2 balance in the reactor has to be tightly controlled so that Rubisco, the principal carboxylating enzyme, fixes CO_2 and not O_2. Fixation of O_2 results in photorespiration and decreased photosynthetic productivity (Pulz, 2001). High levels of dissolved oxygen (DO) in combination with intense sunlight can cause photooxidative damage to algal cells. The maximum tolerable DO level should not exceed 400% of the air saturation value (Molina Grima *et al.*, 1999). Furthermore, in studies with *Chlorella vulgaris*, the rate of photosynthesis has been observed to increase by 14% at low levels of DO, while saturation of the medium with pure oxygen resulted in a 35% rate reduction (Sánchez Mirón *et al.*, 1999).

The 0.03% CO_2 content of air is suboptimal for photosynthesis (Pulz, 2001). Hence, CO_2 is usually provided as a CO_2 enriched air stream, leaving light as the limiting factor (Carvalho, 2006). As the addition of CO_2 acidifies the medium, care must be taken not to adversely decrease the pH (Anderson, 2005).

Thus, in high density algal cultures it must be ensured that sufficient CO_2 is available, while O_2 is removed before reaching inhibitory levels. This is particularly pronounced in large scale horizontal tubular bioreactors, where along the increased tube length, CO_2 concentration may become limiting while O_2 concentration increases to toxic levels. As CO_2 concentration along the tube decreases due to consumption, pH rises. CO_2 can thus be fed in response to a pH controller (Rosello Sastre *et al.*, 2007).

Transfer of CO_2 from the gas phase to the cell occurs through a series of sequential steps according to two-film theory. Most of the resistance to this process occurs in transport across the liquid film adjacent to the gas/liquid interface. The rate of mass transfer is determined by the resistance to mass transfer and the driving force i.e. the CO_2 concentration gradient. This rate can be represented by Equation 1-1 (Bailey & Ollis, 1977; Welty *et al.*, 2001).

1-1

1-2

where: k_La = the overall mass transfer coefficient (s^{-1})

C^* = the saturation concentration of CO_2 in the media (g/l)

C_L = the actual liquid concentration of CO_2 in the media (g/l)

K_La represents the volumetric mass transfer coefficient and can used to compare reactors in small and large scale. It can be determined by measuring the CO_2 uptake rate of the system through the change in dissolved CO_2 concentration. Integration of Equation 1-1, gives Equation 1-2, which can be plotted as a straight line graph to give $-k_La$ as the slope (Bailey & Ollis, 1977; Welty *et al.*, 2001).

The CO_2 saturation concentration in the liquid is directly proportional to the partial pressure of CO_2 in the gas stream (P_{CO2}) and can be calculated using Henry's law, as shown in Equation **Error! eference source not found.** (Chisti, 2002).

1-3

where: H = Henry's law constant (l.Pa/g)

Thus, use of a CO_2 enriched gas and thus a larger P_{CO2}, increases the concentration driving force and therefore the CO_2 gas-liquid mass transfer rate. Thus, even in systems with inherently low k_La values, gas-liquid mass transfer limitations can be overcome.

1.3.3. Mixing

Good mixing affects the distribution of light energy to the cells as well as the frequency of light/dark cycles. An example of inefficient mixing can be seen in raceways (Section 1.4.1) where increasingly laminar flow results in reduced utilisation of light energy and thus reduced solar efficiency. Good mixing aids gas-liquid mass transfer and can also reduce the occurrence of nutrient, CO_2, O_2, pH and temperature gradients as well as preventing cell aggregation (Carvalho, 2006).

Mixing can be achieved through the use of paddle wheels in raceways, impellers in stirred tank reactors and sparged gas in tubular reactors as well as the former. Light/dark circulation can be aided by installing baffles or static mixers (Ugwu *et al.*, 2008).

Sparger design affects, among other things, the size of bubbles produced and thus overall CO_2 mass transfer. Small bubbles are desirable as they increase mass transfer due to their larger surface area to volume ratio (Waites, 2001). While increased flow rate provides better mixing, it may also result in increased bubble diameter. Here, the presence of baffles or static mixers cause the resultant circulation to be interrupted and bubbles to be broken up, hence improving the mass transfer rate (Ugwu *et al.*, 2008).

In considering the mode and level of mixing, it is important to take shear stress into account. A critical shear stress point has been illustrated, beyond which, cell growth is shown to decrease exponentially, resulting in cell death at extreme levels (Wu & Merchuk, 2004). In these sparged cultures, the greatest cause of shear stress is bubble break-up at the gas-liquid interface (Camacho *et al.*, 2000).

1.3.4. Temperature Control

Temperature influences photorespiration more strongly than photosynthesis. Thus, with an increase in temperature, the rate of photorespiration increases significantly while CO_2 uptake and flux through the Calvin cycle only improves slightly. This is inconsequential when light or CO_2 is limiting (Pulz, 2001). Optimal growth temperatures range between 16 and 62°C (Bouterfas *et al.*, 2002).

Due to the inefficiency of photosynthesis, photosynthetic systems generate heat. Theoretically, of the total light absorbed, only 31% is converted to chemical energy for the Calvin cycle while the remaining 69% is dissipated as heat; hence heat generated is proportional to the light received and

cell concentration (Anderson, 2005). Appropriate cooling is required to maintain an optimal photosynthetic rate, usually at temperatures between 20 and 30°C. This can be effectively provided by the use of heat exchangers. Evaporative cooling has also been employed in some systems by spraying tubes with water. In outdoor cultures, care must also be taken to ensure that the temperature does not fall too low at night as this can cause damage to algal cells (Chisti, 2008).

1.3.5. Salinity, Nutrients and pH control

Exact requirements of osmolarity, nutrients and pH are species dependent. Deviations from optimal levels can cause changes in production of photosynthetic intermediates and metabolism. This can result in a decline in photosynthetic rate and thus slower growth (Anderson, 2005; Pulz, 2001). Following the growth phase, modification of growth conditions to promote lipid accumulation is favourable. Studies have shown nutrient deprivation (particularly nitrogen and silicate) to be one of the most efficient approaches to lipid accumulation in algal culture (Rodolfi *et al.*, 2009).

1.3.6. Strain Selection

The choice of algal species is one of the most important decisions governing the success of a microalgal biodiesel production facility. Factors affecting this choice include the lipid content, biomass concentration, productivity and ease of downstream processing. Lipid productivity has been shown to be the desirable characteristic over growth rate and lipid content alone (Griffiths & Harrison, 2009). During the US Department of Energy's Aquatic Species Programme (ASP), over 3000 stains of oil producing organisms were collected. It was suggested that site specific adaption of a species was key to microalgal biomass production as an algae that has been exposed to the prevailing environmental conditions has a distinct advantage over imported strains (Sheehan *et al.*, 1998).

Species is an area of contention in the literature at present as while data is available across most species, much of this data is not comparable due to inconsistencies in scale, reactor type and environmental conditions (Griffiths & Harrison, 2009).

1.4. Photobioreactors

One of the major setbacks of mass cultivation of algae for biodiesel is the lack of efficient photobioreactors. The high productivity, low cost process required is currently limited, primarily by issues around hydrodynamics, mass transfer and scale up (Ugwu *et al.*, 2008). Photobioreactors can be divided into two broad categories; open ponds and closed photobioreactors. Open pond systems are simpler and cheaper to build and operate and thus favoured by many, given the low cost

requirements associated with fuel production (Sheehan *et al.*, 1998). On the other hand, much higher productivities have been achieved in the comparatively expensive closed photobioreactor systems, which offer many advantages over open ponds (Ugwu *et al.*, 2008). A thorough examination of the potential of various systems for mass algal culture is required.

1.4.1. Open Pond Systems

Microalgal growth in open ponds most closely resembles natural growth conditions (Pulz, 2001). Natural water bodies, such as lakes or ponds as well as man-made ponds and containers are all examples of open ponds. Artificial examples include large shallow ponds, tanks, circular ponds and raceways. The major advantage of open pond systems is their ease of construction and operation (Ugwu *et al.*, 2008). Raceway ponds, the most common form of open pond, consist of a closed-loop recirculation channel, typically 0.3 m deep. Mixing and circulation are provided using a paddlewheel and flow guided by baffles. During daylight hours, culture is fed continuously in front of the paddlewheel and broth harvested behind the paddlewheel on completion of the loop. Cooling is achieved by evaporation (Chisti, 2007).

There are several disadvantages associated with the open pond system. There is a large associated land requirement, evaporative water loss can be significant, CO_2 usage is inefficient (particularly if enriched gas streams are used) as much is lost to the atmosphere and cells experience poor light utilization. There is also the constant threat of contamination by unwanted algae, micro-organisms that feed on algae and pollution (Pulz, 2001). Monoculture can only be achieved by maintaining an extreme culture environment, in which only a desired species survives, thus limiting the potential use of open ponds to a few strains. Successful examples of extreme culture include high salinity (*Dunaliella*), high alkalinity (*Spirulina*) and high nutrition (*Chlorella*). These measures do not necessarily exclude biological contaminants and bacteria, leaving contamination as a major failing of open pond systems (Lee, 2001).

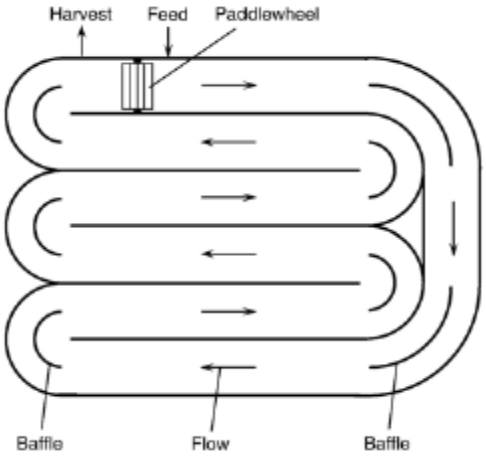

Figure 1-2 Aerial schematic of a raceway (Chisti, 2007)

Poor mass transfer due to inefficient mixing also plays a major role in the low productivities of these systems (Chen, 1996). The resultant low cell densities are a major shortcoming of open ponds greatly increasing the downstream processing costs (Carvalho, 2006).

1.4.2. Enclosed Photobioreactors

The desire for high biomass productivity and for monoculture have led to the development of closed photobioreactor systems (Lee, 2001). These systems offer the advantage of increased control over many of the necessary cultivation conditions mentioned in Section 1.3. This greatly reduces risk of opportunistic contamination, provides control over temperature and hydrodynamics and reduced CO_2 losses (Pulz, 2001). The narrow light path in both tubular and flat plate photobioreactors allows for increased cell concentrations and thus biomass productivities. It is also possible to achieve greater turbulence. Better mixing results in enhanced light availability to the cells, increased light cycles and improved gas-liquid mass transfer and transfer of essential nutrients (Lee, 2001). Better biomass productivity translates into a lower footprint on a yield basis, reduced water footprint and reduced use of fossil energy compared to open ponds. The goal here is to maximise the use of solar energy on any given piece of land, while maintaining a reasonable working volume, mixing pattern and carbon dioxide level (Carvalho, 2006; Schenk, 2008).

Bacterial contamination remains an issue. This is due to the large surface area to volume ratio, which hinders effective sterilisation, both heat and chemical. As a result, many closed photobioreactors may not satisfy Good Manufacturing Practice (GMP) for pharmaceutical products (Lee, 2001).

The main parameter influencing reactor design is light penetration, crucial for high photosynthetic efficiency. This requires a high surface to volume ratio. Successful outdoor photobioreactor configurations can be grouped into two basic shapes: tubular and flat plate. Examples are provided

in Table 1-1. Both systems include a light harvesting unit, designed to optimise photosynthetic efficiency, and a gas exchange unit for CO_2 exchange and biomass harvesting. (Carvalho, 2006).

Table 1-1 Comparison of biomass productivities in enclosed photobioreactors (Lee, 2001)

Bioreactor	ID cm	Location	Alga	Highest productivity	
				$g/m^2/day$	g/L/day
Horizontal tubular	12.3	Italy	*Spirulina maxima*	25.0	0.25
	2.5	Israel	*Spirulina platensis*	27.0	1.60
	6.0	France	*Porphyridium cruentum*	25.0	0.36
Helical tubular	2.4	Australia	*Tetraselmis chuii*	-	1.20
Vertical tubular	20.0	Spain	*Phaeodactylum*	-	0.69
	2.6	Israel	*Isochrysis galbana*	-	1.60
Flat plate	10.4	Israel	*Spirulina platensis*	33.0	0.30
	3.2	Italy	*Spirulina platensis*	24.0	0.80

1.4.2.1. Vertical Tubular Reactors (VTR)

VTRs offer the advantage of being relatively low-cost, compact and easy to operate monoseptically. Air is sparged from the bottom of the reactor, ensuring good mixing and efficient mass transfer (Ugwu *et al.*, 2008). While both bubble columns and airlift designs are employed, the latter have been found to be more efficient in algal culture. Airlift designs differ only in the presence of a draft tube, providing defined circulation of cells through the riser and downcomer zones of the reactor (Figure 1-3). High gas hold-up is achieved through turbulent flow in the riser, where the culture receives little to no illuminace. At the top of the draft tube, effluent gas escapes, controlling dissolved oxygen concentrations. Culture is then circulated through the external downcomer loop, where cells are illuminated (Vunjak-Novakovic *et al.*, 2005).

While VTRs are conventionally constructed from glass or plastic, successful use of polyethylene bags with associated capital cost reduction has been achieved (Ugwu *et al.*, 2008).

Difficulty in scale-up is one of the major shortcomings of these systems. Decrease in productivity and inefficient mass transfer rates with increasing culture volumes have been reported. In addition, VTRs by definition result in a large angle relative to the direction of sunlight. Consequentially, much incident energy is reflected and thus lost in terms of biomass production (Carvalho, 2006).

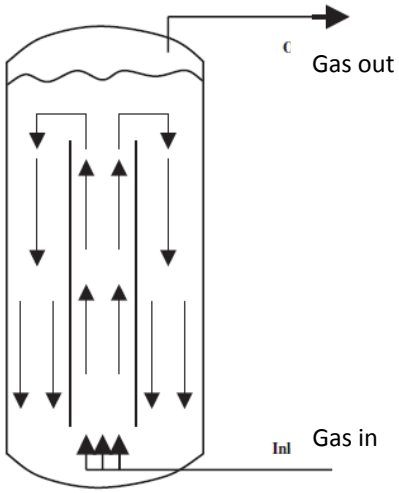

Figure 1-3 Schematic of an airlift reactor system (Najafpour, 2007).

1.4.2.2. Case Study: Oscillatory Flow Reactor

Oscillatory flow reactors are tubular reactors containing equally spaced orifice plate baffles which function to enforce a sinusoidal oscillation over the length of the tube. The fractional baffle open area, *S*, is usually between 0.2-0.5 of the tube diameter and baffles are spaced 1 to 2 times the tube diameter apart. Mixing is characterised by the net flow Reynolds number, Re_n and the oscillatory Reynolds number, Re_o (Harvey *et al.*, 2001).

1-4

1-5

For a sinusoidal oscillation, x_o represents the centre-to-peak amplitude, ω the frequency of oscillation, d the tube diameter, ρ the density, and μ the viscosity. The net flow Reynolds number, Re_n depicts the externally imposed net flow. The superficial fluid flow velocity corresponding to the throughput is represented here by *u* (Harvey *et al.*, 2001).

Oscillatory flow reactors offer the advantage of long residence times with low length/diameter ratios, while maintaining plug flow residence time distribution characteristics, effective mixing and high heat and mass transfer rates (Harvey *et al.*, 2001).

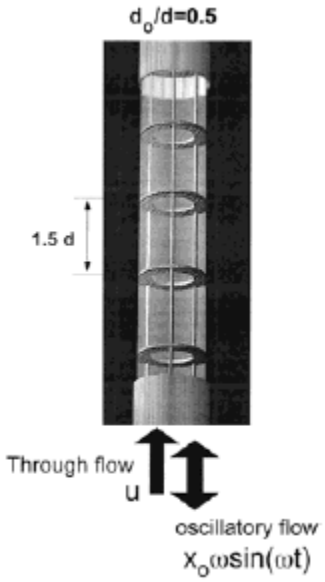

Figure 1-4 Typical oscillatory flow reactor configuration (Harvey *et al.*, 2001)

1.4.2.3. Horizontal Tubular Reactors (HTR)

HTRs are growing increasingly popular for outdoor culture. They generally consist of an array of semitransparent tubes or 'solar array', made of plastic or glass, where sunlight is captured (Ugwu *et al.*, 2008). Tubes rarely exceed 0.1 m in diameter to ensure light penetration through dense cultures. Generally, tubes are placed parallel, either on the ground or in a horizontal fence-like manner, oriented north-south. Flow is provided by a pump or airlift system and culture circulated from the array to a degassing zone and back (Chisti, 2007).

Light harvesting efficiency is much higher than for VTRs due to an improved angle relative to the sun (Carvalho, 2006). However, this also makes these systems more susceptible to photoinhibition (Ugwu *et al.*, 2008).

Control of temperature is a major problem in these systems due to the large amount of heat generated. Temperature control systems can be costly and while cooling by spraying water on the tubes has proved effective, this requires large volumes of water and is thus unsustainable (Carvalho, 2006). Dissolved oxygen levels can also prove problematic, particularly on scale up. Tube length must thus be limited to allow for timely removal of oxygen at the degassing zone. Furthermore, it has been found that pH increases along the length of the tube as CO_2 is consumed. To prevent this, CO_2 is fed into the degassing zone in response to a pH controller. The possible introduction of CO_2 injection points along the length of the tube may also be considered (Chisti, 2007).

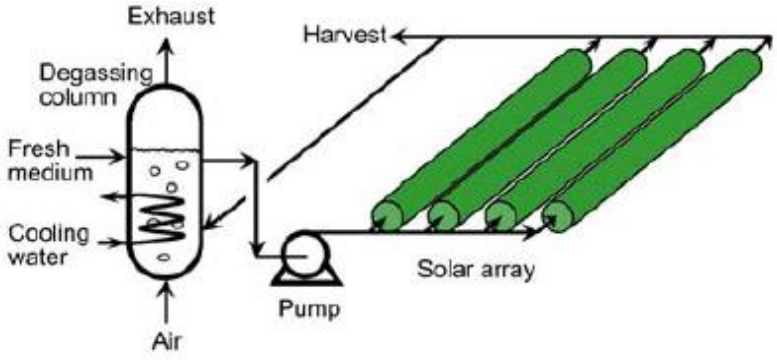

Figure 1-5 Typical arrangement of a horizontal tubular reactor system (Chisti, 2007).

Scale up is relatively simple as it merely requires the addition of more tubes. While the relatively large land area required has been cited as a problem, tubes are thin and industrial scale can be achieved with a very large number of tubes. This may achieve a high productivity, but may not be economically feasible (Carvalho, 2006).

1.4.2.4. Helical Tubular Reactors (HeTR)

In HeTRs, the light harvesting units consist of an array of polyethylene tubes coiled in an open circular framework. This is connected to a degassing zone and heat exchange system. Culture is driven through the long tube to the degassing zone by a centrifugal pump. Experimentation and improvement of this design have resulted in an efficient system, which boasts a high surface area to volume ratio and a relatively small land requirement per unit volume (Carvalho, 2006).

Scale up is simple and can be achieved by increasing the number of parallel layers of tubing. The main weakness of this system is that only a few algal strains can be accommodated due to the increased shear stress associated with the centrifugal pump. This would limit biomass productivity (Carvalho, 2006).

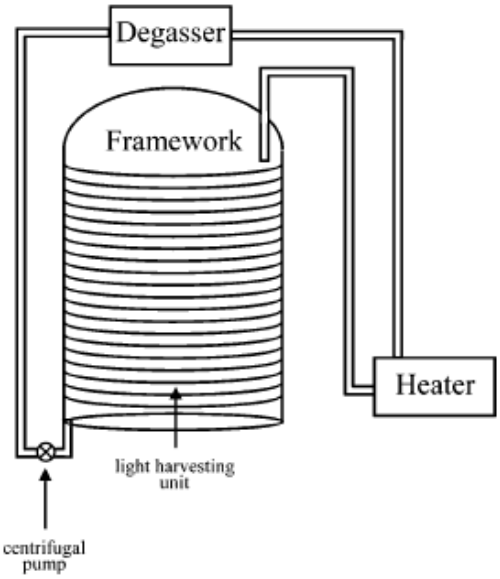

Figure 1-6 Systematic representation of a helical tubular reactor. Flow through a coiled array tubes in an open circular framework is driven by a centrifugal pump to a degasser and heat exchanger.

1.4.2.5. Flat Plate Bioreactors

The attraction of flat plate photobioreactors lies in their large illumination surface area. Transparent materials allow for maximum utilisation of solar energy and very high photosynthetic yields have been achieved (Ugwu *et al.*, 2008). This efficiency can be further exploited in that these reactors can be oriented towards the sun. A variety of mixing systems and configurations has been proposed, each with its own advantages and disadvantages (Carvalho, 2006).

1.4.3. Hybrid Systems

It is clear that while efficient and cost effective, open ponds are at huge risk of contamination. Conversely, closed systems are much better for achieving monoculture, but are vastly more expensive than open ponds (Schenk, 2008). The combination of these two systems is thus logical and has been tested on a small commercial scale in Hawaii, USA. Here, an algal species capable of both rapid growth and high oil content was cultivated in a large closed photobioreactor in conditions favouring cell division. Following the growth phase, a portion of the bioreactor was transferred to a raceway, where cells were subjected to nutrient limitations and other stressors. This functioned both to promote lipid accumulation and discourage contaminant strains which would require the limited nutrients for growth. As carotenoid synthesis increases with lipid production, astaxanthin was sold to aid the process economically. Average oil yield was reported as 422 GJ/ha/yr, resulting in 1200 gal/acre/yr biodiesel, figures much higher than those achieved with crop biofuels (Huntley & Redalje, 2007).

1.4.4. Scale Up

Scale up is a major issue in algal culturing, particularly in closed photobioreactors. Maintaining high mass transfer rates and ensuring good light regimes are both major challenges (Molina Grima *et al.*, 1999).

In tubular reactors, scale up is achieved by increasing either the length or diameter of the tube. Increased length can result in gradients of CO_2 and O_2 along the tube and can affect the pH gradient. Increased diameter, on the other hand, works well as long as care is taken to circulate cells between the illuminated and dark sections of the reactor. Increasing the mixing rate can aid this purpose, but can result in increased energy input and capital cost and imposes hydrodynamic stress which can damage the algal cells (Ugwu, 2005).

Flat plate reactors have been successfully scaled up through compartmentalisation of reactors, but this presents difficulties similar to tubular reactors with regard to mixing and hydrodynamic stress. In addition, wall growth can become a problem, restricting light supply to the reactor (Ugwu *et al.*, 2008).

In contrast, scale up of open systems, particularly raceways, has been largely successfully employed, the largest occupying an area of 440 000 m^2 (Chisti, 2007). Another notable large-scale raceway facility spans 11 000 m^2 and is located at Melbourne's Werribee waste water treatment plant. The major shortcoming here remains the same as in small scale, regarding the large land requirement and low productivity (Schenk, 2008).

Rosello Sastre *et al.* (2007) suggest that poor scale-up of algal bioreactors from laboratory to industrial scale is due to both inadequate management of technical parameters upon scale-up and a gap in our knowledge of the kinetics of the physiological reactions taking place. Scale down was suggested to combat this issue by addressing light transfer, fluid dynamics and cellular metabolic reactions in a manner mimicking large scale conditions.

1.4.5. Capital Cost

The capital and energy costs of building and maintaining closed photobioreactor systems are far higher than that of open ponds. While productivity in the closed systems is superior, this is required to compensate for the high capital costs (Lee, 2001). This highlights the crucial gap between technologically advanced reactors which meet requirements of algal growth and simple reactors which improve the economic viability of the process (Schenk, 2008).

1.5. Harvesting

Harvesting of algal biomass is highly significant as it is directly affected by the reactor choice, which dictates the biomass concentration entering the dewatering process and thus the amount of liquid to be removed.

There are four general methods for harvesting microalgal biomass: sedimentation, filtration, flotation and centrifugation. Pre-treatment of the biomass may also be necessary (e.g. flocculation) to improve harvesting yield. The aim of harvesting is to obtain slurry with a concentration suitable for efficient downstream processing. The choice of harvesting method is dependent on the biomass use, properties and concentration following the reactor phase. For example, filtration is only suitable for relatively large microalgal species (e.g. Spirulina platensis) and is ineffective in separating unicellular species (*Chlorella* and *Scenedesmus* sp.). Energetic and economic expenses also play a role in this decision as the microscopic nature and low concentration of microalgal culture make harvesting a major contributor (Benemann & Oswald, 1996).

1.5.1. Initial Concentration Methods

Increased particle size leads to faster sedimentation according to Stokes' law. Hence, flocculation by the addition of polymers or coagulation through pH adjustment or the addition of electrolytes are used to increase particle size and so, improve sedimentation speed. Similarly, particle size affects flotation bubbles, allowing for concentration of the biomass. Chemical flocculation has become the method of choice in wastewater treatment plants as it allows for the treatment of large volumes. The chemicals are expensive, and only marginally cheaper than centrifugation (Molina Grima *et al.*, 2003; Richmond, 2004b; Schenk, 2008)

The main disadvantage of flocculation is the addition of chemicals. Inorganic chemicals such as alum, ferric chloride and lime have been found to be effective but are relatively expensive for large scale operations of such a low value commodity. The presence of such chemicals, which are not easily removed, in algal sludge can inhibit certain downstream applications, such as animal feed supply or anaerobic digestion (Levin *et al.*, 1962; Schenk, 2008). Further, the low solids content of the algal sludge produced means that additional concentration is required (Levin *et al*. 1962).

Algal cell surface charge is highly negative, which is desirable to maintain dispersed cells for high productivity. However under longer reactor residence times, growth rates are low and relatively few cells are dividing at the time of harvest; hence mean cell surface charge decreases and cells tend to clump, a phenomenon known as autoflocculation (Borowitzka, 1997). This phenomenon has been

noted in some nitrogen limited cultures, but is largely observational and lacks theoretical foundation (Benemann & Oswald, 1996).

1.5.2. Centrifugation

In a centrifuge, the sedimentation rate is accelerated under the enhanced centrifugal force replacing gravitational acceleration. Capable of separating almost all types of microalgae, easy cleaning and availability of sterilisable machines, centrifugation is considered by many to be the preferred mode of harvesting (Richmond, 2004b). However centrifuges have a high capital cost and are energetically expensive and thus only feasible for high value products or for processing of smaller volumes following an initial concentration step (Molina Grima *et al.*, 2003).

Recovery of biomass in a centrifuge depends on the (a) settling rate of the biomass, (b) residence time in centrifugal field and (c) settling depth. Residence time can be increased by reducing the flow rate and settling depth reduced through centrifuge design to enhance biomass recovery (Richardson *et al.*, 2002).

Despite the high energy requirement, centrifugation is still considered a preferred method for the recovery of microalgal cells (Borowitzka, 1988; Richmond, 2004b).

1.6. Environmental Assessments of Biofuel Processes by Life Cycle Assessment (LCA)

The driving force behind biofuels and other forms of renewable energy comes largely from concerns regarding the environmental impact of current energy processes. It is therefore necessary to consider these potential impacts in the design of a biofuels process, particularly with regard to global warming, climate change and depletion of fossil reserves. Additionally, as an energy product, it is important that the energy gained from the biofuel produced is greater than that consumed in the overall fuel production process. In this thesis, a cradle-to-gate Life Cycle Assessment (LCA) will be used to quantify the environmental impact of the algal biodiesel production.

1.6.1. Life Cycle Assessment (LCA)

LCA is an analytical tool that systematically identifies and evaluates opportunities for minimizing the environmental impact of an overall process (Curran, 2000). LCA is chosen as it has a good literature base, clear definition and has been widely used in the environmental assessment of biofuel processes (Evans *et al.*, 2009; Harding *et al.*, 2008; Kaltschmitt *et al.*, 1997; Kim & Dale, 2005; Larson, 2006; Lechón, 2005; Poitrat, 1999). Additionally, LCA offers the benefit of including the entire life cycle and thus accounting for shifting of burdens. Thus, it overcomes the shortcomings of other, site

specific environmental assessment tools where improvements in one part of the life cycle (e.g. production) may lead to higher impacts in other parts of the same life cycle and be unaccounted for. It is important to note that this tool is not without fault and careful considerations need to be made in using life cycle methods. Shortcomings and misconceptions are discussed below.

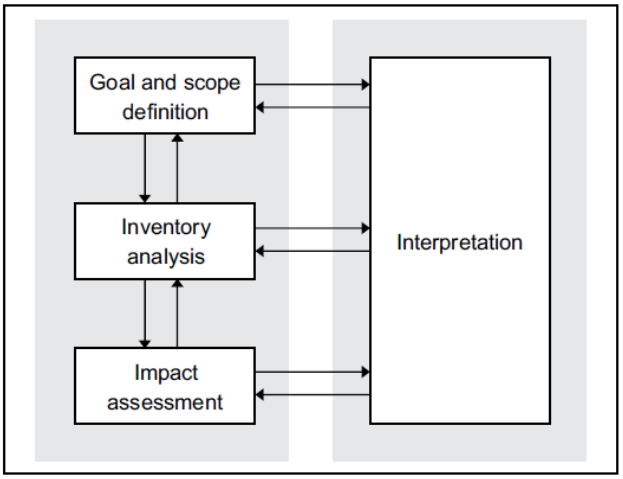

Figure 1-7 The phases of Life Cycle Assessment (LCA) (Uihlein & Schebek, 2009)

In terms of the ISO 14040 standards (ISO 14040: 2006, ISO 14044: 2006), LCA methodology consists of four phases; Goal and scope definition, inventory analysis (LCI), impact assessment (LCIA) and interpretation (Figure 1-7). These are outlined below and further discussed in the context of this thesis in Section 3.5.

1.6.1.1. Goal and Scope Definition

To allow for meaningful comparison, it is necessary to define the goal and scope of the study, including the identification of the functional unit to be evaluated in each process and setting appropriate system boundaries. In this study, there are multiple products and thus, a suitable allocation method was required to allocate environmental burdens across products by mass, volume, economic value or other measures. According to the ISO guidelines, where possible, substitution is preferred to allocation (Guinée, 2002).

1.6.1.2. Life Cycle Inventory Analysis (LCI)

Data collection is necessary to quantify all inputs to the process in terms of energy and resources (solid, liquid and gaseous) as well as all products and waste. Data can be gained experimentally and from literature or from a flow-sheet model. This data must be validated through mass and energy balances and reported in terms of the functional unit. The list of inputs and outputs generated forms the LCI and is then input to the chosen LCA software.

1.6.1.3. Life Cycle Impact Assessment (LCIA) and Interpretation

The LCI results are used in a Life Cycle Impact Assessment (LCIA) to assess the environmental impacts of the data, condensing the LCI data into a more manageable set of impact categories. These are known as mid-point categories and include categories such as global warming, abiotic depletion and eutrophication. These categories are sometimes further grouped into endpoint categories such as human health, climate change and ecosystem quality.

1.6.2. LCA Development: Lessons from Previous Studies

Searchinger *et al.* (2008) highlighted that while most life cycle studies have found displacement of fossil fuels with ethanol to be favourable and result in a net reduction of GHGs, this is an inadequately informed conclusion. It results from counting the carbon benefits of land use for biofuels, but negating the emissions resulting from the land use change. A study by Fargione *et al.* (2008) estimated that the direct impacts of the conversion of natural habitats for use in biofuel crop production could result in GHG release several times greater than biofuels provide through displacing fossil fuels. This emphasizes the importance of accounting for carbon storage in natural ecosystems. Thus, the use of the metric of ecosystem 'carbon payback time' (ECPT) of different biofuels is used in order to ascertain how many years it would take for the biofuel carbon savings from avoided fossil fuel combustion to offset the losses in ecosystem carbon from clearing land to grow new feedstock (Gibbs *et al.*, 2008).

In reviewing LCA studies pertaining to liquid biofuels, several factors can be noted. Firstly, the literature is still dominated by analysis of systems located in Europe or North America (although studies from as far afield as Brazil, China, Thailand, South Africa and Australia have been reported). Such studies exhibit a large range of net energy balance results, for the same and different biofuels. Furthermore, a wide range of GHG impacts are reported, few of which pertain to impact per unit area. This variability may be due to several parameters contributing to uncertainty and variability in results. Significant parameters include (1) the effect of climate specific algal species, (2) assumptions regarding N_2O emissions and (3) allocation of by-product and co-product credits. It is also reasonable to conclude that greater GHG savings can be achieved for biofuel systems where biomass yields are high, biomass to fuel conversion is efficient and biofuel consumption is efficient. Thus, analysis is largely case-specific (Larson, 2006).

To avoid the mistakes of first generation biofuels, it is necessary to consider the evolution of environmental assessment methods and their results, and use them as guidelines in the evaluation of potential environmental impact of biodiesel from microalgae.

1.6.3. Investigating the Applicability of LCA in Biorefineries

The biorefinery approach, mentioned in Section 1.1.3, is of particular interest as it is thought to contribute to more sustainable resource use through the production of multiple products, reduced waste resources and reduced GHG emissions.

Case Study 1: Multiple Product Production from Wheat Straw

Kaparaju *et al.* (2009) investigated wheat straw as a source of biomass within an integrated biorefinery framework. A thermal pre-treatment resulted in cellulose (used to produce bioethanol) and hemicelluloses (used to produce biohydrogen). The residues from these two processes were used to produce biogas through anaerobic fermentation and residual effluents used as fertilisers. All experimental procedures were performed at lab scale.

Various wheat straw-to-biofuel production scenarios were evaluated in terms of energy produced. Experimental data were compiled into mass and energy balances. It was envisioned that the data would be used in a later in-depth LCA study. The overall results showed that biogas production and multi-fuel production were more energetically efficient compared to production of a single fuel such as bioethanol from C6 sugar fermentation. Thus, production of multiple biofuels was shown to increase the material and energy efficiency and process economics for biomass utilization.

Case Study 2: A Lignocellulose Feedstock

Uihlein and Schebek (2009) conducted an LCA study on a lignocellulose feedstock (LCF) biorefinery system producing ethanol, xylite and lignin. The LCA was performed in order to analyse whether such a biorefinery would be more environmentally friendly than conventional fossil fuel alternatives. In addition, the study aimed to identify the environmental issues associated with biorefineries of this type and the steps in the life cycle associated with these impacts.

A biorefinery system was defined and paralleled to a conventional fossil fuel alternative for the production of equivalent quantities of equivalent products. Since there are currently no LCF biorefineries in commercial operation, several variations were designed including a basic setup, three systems with varying heat and material recoveries and two systems where lignin was used to provide heating and electricity respectively. As it was not known which of the products should be considered the main output, impacts were calculated for a reference feed of 100 kg straw. The energy requirements and efficiencies of each step in the fossil and LCF systems were then obtained from relevant sources and appropriate assumptions made. Outputs and yields were then calculated.

The LCIA was performed using Eco-Indicator methodology. Results were assigned first to midpoints, areas where they create environmental problems (soil, air, water) and then to endpoint impact

categories (climate change, ecotoxicity). Following this, results were translated into damages in three endpoint categories, namely resources, ecosystem quality and human health. Finally, a single score indicator was obtained.

Results allowed for the selection of a preferred system variant and showed that the production of biorefinery based products and fuels may be associated with environmental disadvantages due to issues involving land use or eutrophication of water. The greatest impacts were found to take place in the categories of fossil fuel use, respiratory effects and carcinogens, accounting for 37.0%, 25.4%, and 17.3% of the total environmental impact, respectively. These impacts were largely due to the provision of hydrochloric acid and to a lesser extent, process heat. Optimum yields however, resulted in favourable comparison with fossil counterparts with total environmental impacts approximately 41% lower (Uihlein & Schebek, 2009).

1.7. Objectives and Key Questions

There has been much written about the potential of algal biofuels (Chisti, 2008; Li, 2008; Rodolfi *et al.*, 2009; Schenk, 2008; Ugwu *et al.*, 2008). In terms of making commercial production a reality, an integrated biorefinery approach for the production of multiple products has been seen to improve the overall efficiency of biomass utilization, contributing to both economic success and environmental sustainability (Chisti, 2007; Kaparaju *et al.*, 2009). In view of the disagreement discussed in Section 1.1.3 around the environmental and energetic feasibility of algal systems, it is necessary to further explore the sustainability of an algal biorefinery in the context of biodiesel production.

A recent Life Cycle Assessment (LCA) study within CeBER focussed on identifying areas in bioprocesses that dominate in contribution to LCA scores (Harding, 2009). Knowledge gained from this study (Section 1.2) shifted focus to the bioreactor as a key phase in bioprocesses. Variation in biomass and specific product concentration leads to variation in volume which affects overall environmental impacts through LCA scores, particularly with regards to resultant energy requirements in both the cultivation phase and DSP. Several case studies were performed on heterotrophic microbial systems, but algal systems were not investigated. A range of bioreactors for algal culture have been reviewed in this study (Section 1.4), capable of varying degrees of productivity and biomass concentrations linked to varying degrees of sophistication and input requirements. Biomass concentration impacts reaction volume required, while productivity is also of interest as it impacts the overall energy balance of the biorefinery due to shortened cultivation cycles for a standard input.

The objectives of this study are thus as follows:

- To select, design and model a process flow-sheet representing a suitable biorefinery for the production of microalgal biodiesel and suitable co-products
- To collect appropriate data to inform the material and energy inventory of this flow-sheet
- To use the process simulation model to investigate several microalgal species and bioreactor configurations and generate material and energy inventories for the production of a functional unit of microalgal biodiesel
- To assess the system dependence on bioreactor design in terms of fossil energy requirement and overall environmental impact using Life Cycle Analysis (LCA)

Key Questions:

1. Is the production of algal biodiesel environmentally feasible?
2. How does the reactor unit contribute to the energetic and environmental burden relative to the remainder of the process?
3. How does the environmental impact of biofuel production differ depending on the microalgal species used?
4. How does the environmental impact of biofuel production differ depending on the bioreactor used for algal growth?
5. What are the key contributors to the environmental impact of algal biodiesel production?
6. What operating variables most influence changes to the energetic and environmental impact of the overall process?

1.8. Thesis Structure

Chapter 2 provides a review of recent LCA studies of microalgal biodiesel, published during the course of this study. Chapter 3 describes the process simulation model and presents the methods and calculations used to generate material and energy data. A description of the research approach taken in Chapters 4 and 5 is also given here. Chapter 4 then uses the model to investigate the effect of species choice on the energetic and environmental impact of the production of microalgal biodiesel. This is done by comparing several species of microalgae grown in laboratory airlift reactors through energy and life cycle analysis. Similarly, Chapter 5 investigates the effect of reactor choice, considering three reactor configurations. The effect of changes to algal growth parameters in these reactors is also analysed. This is followed by overall conclusions in Chapter 6.

2.A Review of Life Cycle Assessments (LCA) of Algae to Biodiesel Processes

2.1. Introduction

While there is much published literature on algal bio-energy, the first algal biodiesel LCA was published by Lardon *et al*. in 2009. Prior to that, relevant work included a LCA study on comparing electricity production using coal and microalgae co-firing (Kadam, 2002) and a study by Sazdanoff *et al* (2006), which presented a model of the algal to biodiesel fuel cycle and its use, with climatic data to simulate production at four different locations in the United States. Both formed a significant contribution to the field.

Kadam (2002) used a functional unit of 1 MW electricity to investigate the potential benefit of recycling the CO_2 produced by power plants to microalgal production. System boundaries included the power plant only in Scenario 1 and the power plant and microalgal production unit in Scenario 2. The requirement for flat land adjacent to a power plant was acknowledged. Following cultivation in open ponds, algae were initially concentrated in microstrainers prior to centrifugation. Notably, solar drying was assumed to be feasible for algae, based on agricultural experience with crop drying and dehydration practices and a zero energy input assumed for this step. Additional scenarios investigated varied the mode of CO_2 provision to the ponds and the degree of CO_2 recycled. The study showed significantly lower greenhouse gas (GHG) and air pollution burdens in Scenario 2 due to the reduced use of coal and thus reduced CO_2 emissions. However, energy and fertiliser inputs required for microalgal production were shown to contribute to positive environmental burdens for the resource depletion and eutrophication impact categories respectively.

Following this, in a study by Sazdanoff *et al.* (2006), a model was developed to predict the algal production, energy use and emissions of potential algal biodiesel production facilities at various locations in the United States. Algae were assumed to be grown in open raceway ponds and harvested by free settling, followed by centrifugation. Data generated during the Aquatic Species Program (ASP) was used in conjunction with communication with key members of the ASP. Oil extraction, biodiesel production and emissions were modelled using the GREET model (Wang, 1999). This pioneering work to model algal biodiesel production and use includes prediction of algal growth from climatic variables, a noteworthy feature.

2.2. Algal Biodiesel LCAs Published during this Project

The two studies described in Section 2.1 laid a solid initial foundation for the subsequent LCAs, which are outlined below. This development of the life cycle assessment of algal biodiesel has been described in eight papers that were all published during the present study. They thus serve to inform the direction taken by the present study and provide useful basis for comparison of approaches and findings; however they do not provide a basis for it. This chapter aims to review these papers by assessing the systems, methodology, conclusions made and the extent to which these studies are comparable. It must be noted that while economic feasibility is an important issue that is central to the future of algal biodiesel, it lies outside the scope of this thesis.

The algal biodiesel LCAs published to date are summarised in the following paragraphs. In the remainder of the chapter these studies are discussed in terms of their production system (Section 2.3), LCA methodology (Section 2.4) and key findings (Section 2.5).

Lardon *et al. (07-2009)*

Objectives: To assess the environmental impacts of biodiesel from microalgae as a technologically immature process and to identify the barriers to large scale process environmental sustainability. Cultivation in nitrogen sufficient and deplete conditions was investigated as well as wet and dry extraction.

Functional unit: Combustion of 1 MJ of fuel in a diesel engine.

System: Reactor to combustion, plant construction

Findings: Lardon *et al.* found that while microalgae show promise as a potential biodiesel feedstock, there is a need to decrease energy and fertiliser use, which emerged as the most impacting flows. To this end, the use of nitrogen-starved culture conditions and optimisation of wet extraction were shown to be good options. Anaerobic digestion of the non-lipid biomass was shown to have potential both to reduce the process energy demand and recycle part of the mineral fertilisers. LCA was found to be an appropriate tool for the analysis of a technologically immature process and efficient in identifying the bottlenecks to large scale production.

Jorquera *et al.* (10-2009)

Objectives: To investigate of the production of algal biomass in raceway ponds, tubular and flat-plate photobioreactors to evaluate their feasibility through comparative life cycle and energy analysis.

Functional unit: Biomass production of 100 000 kg/year

System: Cultivation and plant construction

Findings: The use of horizontal tubular photobioreactors (PBRs) was shown have an NER<1, while both flat plate PBRs and raceways ponds had positive NERs. The latter NERs were shown to be significantly higher should the biomass lipid content be increased to 60% dw/cdw (dry weight/cell dry weight). Neither system was shown to be competitive with petroleum on an economic basis.

Clarens *et al.* (12-2009)

Objectives: To compare algae to other switchgrass, canola and corn as a bio-energy feedstock. The use of flue gas and wastewater to offset the dominant environmental burdens of algal cultivation were investigated.

Functional unit: 317 GJ of biomass-derived energy

System: Reactor, dewatering and plant construction

Findings: The conventional land crops displayed lower environmental impacts in the categories of energy use, GHG emissions and water, regardless of cultivation location. Algae only performed favourably in land use and eutrophication. The demand for CO_2 and fertiliser were the dominant contributors to the overall algal environmental footprint, in addition to energy. Use of flue gas and, to a greater extent, wastewater was found to significantly reduce these respective burdens.

Stephenson *et al.* (05-2010)

Objectives: To compare open raceways and tubular photobioreactors for the production of biomass in a 2-stage cultivation approach of high growth followed by nitrogen starvation for lipid accumulation. Different methods of downstream processing were also investigated.

Functional unit: 1 ton of biodiesel, blended and combusted in a diesel engine

System: Reactor to combustion, AD and plant construction

Findings: Cultivation in raceways was shown to be significantly more sustainable than that in tubular photobioreactors, with raceways showing a GWP ~80% lower than fossil derived diesel. Fossil energy requirements and GWP were found to be particularly sensitive to the oil yield during cultivation, linear culture velocity in raceways, recycle of culture media and the concentration of CO_2 in the flue gas. The study further reinforced the necessity of using LCA in the development of microalgal biodiesel as a technologically immature process.

Campbell *et al.* (06-2010)

Objectives: To investigate the environmental impacts and economic feasibility of biodiesel production from microalgae grown in open ponds in Australia, looking at cost and GHG emissions. Three different scenarios for CO_2 provision to the ponds and two different growth rates were considered.

Functional unit: A ton-kilometre of diesel fuel combusted (the weight in tons of material transported multiplied by the number of kilometres driven)

System: Reactor to combustion and AD

Findings: The GHG emissions resulting from algal biodiesel production compared favourably with biodiesel from canola and ULS diesel. On a cost basis, however, this study emphasised the importance of a higher algal production rate to make algal biodiesel economically feasible.

Collet *et al.* (06-2010)

Objectives: To assess the environmental impacts of anaerobic digestion of microalgae to produce methane and recycle N, P and K nutrients. The study aimed to identify the barriers to large scale process environmental sustainability compared to microalgal biodiesel.

Functional unit: Combustion of 1 MJ of fuel in an internal combustion engine

System: Reactor to conversion, AD and plant construction

Findings: Like microalgal biodiesel production, results were dominated by electricity requirements. Improvements in the reactor phase to decrease mixing costs and lower pumping energy between phases and improved efficiency of anaerobic digestion were suggested as a means reduce this burden. The system was deemed competitive with other bio-energy generation processes.

Yang *et al.* (07-2010)

Objectives: To quantify the water footprint and nutrient usage during microalgae biodiesel production. The use of fresh, sea and wastewater were analysed with and without recycling. Geographic and species variation were also investigated.

Functional unit: Production of 1 kg of microalgal biodiesel

System: Reactor to conversion and distribution

Findings: Yang *et al.* showed that 3726 kg water, 0.33 kg nitrogen, and 0.71 kg phosphate are required per kg microalgal biodiesel. Recycle of harvest water reduced both the water and nutrient usage and use of sea/wastewater decreased the overall fresh water requirement by 90% and removed the need for all nutrients apart from phosphate.

Batan *et al.* (09- 2010)

Objectives: To evaluate an industrial scale model for biodiesel production from algae grown in photobioreactors using a life cycle net energy ratio and greenhouse gas emissions analysis. The model was used to compare microalgal biodiesel to soybean-based biodiesel and petroleum diesel.

Functional unit: 1 MJ of produced energy

System: Reactor to fuel conversion and distribution

Findings: Both microalgal and soy-based biodiesel production showed a net reduction in GHG emissions, with microalgal biodiesel showing a 5% advantage due to its net avoidance of N_2O emissions. The NER of microalgal biodiesel was given as 1.1 MJ produced per MJ energy consumed, superior to soy-based biodiesel, which gave an NER of 0.61. Both were inferior to that of petroleum diesel (5.3).

These studies are summarised in Table 2-1 and discussed more fully in the following sections of this chapter in terms of their production systems, LCA methodology and key findings.

2.3. Production system overview

In the studies presented in Section 2.2, LCA is used as a tool to assess the potential adverse environmental impacts of material and energy flows across the system boundaries. Thus, selection of a meaningful functional unit and system boundary is of great importance, particularly when comparing and compiling lessons from previous studies. Within the defined system boundaries, the production system is disaggregated into a number of unit processes, shown in Figure 2-1. Depending on the objective and functional unit of a particular study, the system boundaries may include or exclude a portion of the process chain. Even when the boundaries of two or more studies are identical, any unit process may be performed by a different method or use different data or assumptions. This may affect the results of the studies or make them incomparable. This is particularly pertinent to LCA of algal biodiesel production as a technologically immature process where a lack of large scale data and disagreement on appropriate unit processes make analysis difficult. Most LCA studies published to date aim to analyse the viability of a particular process option or assess barriers to large scale production.

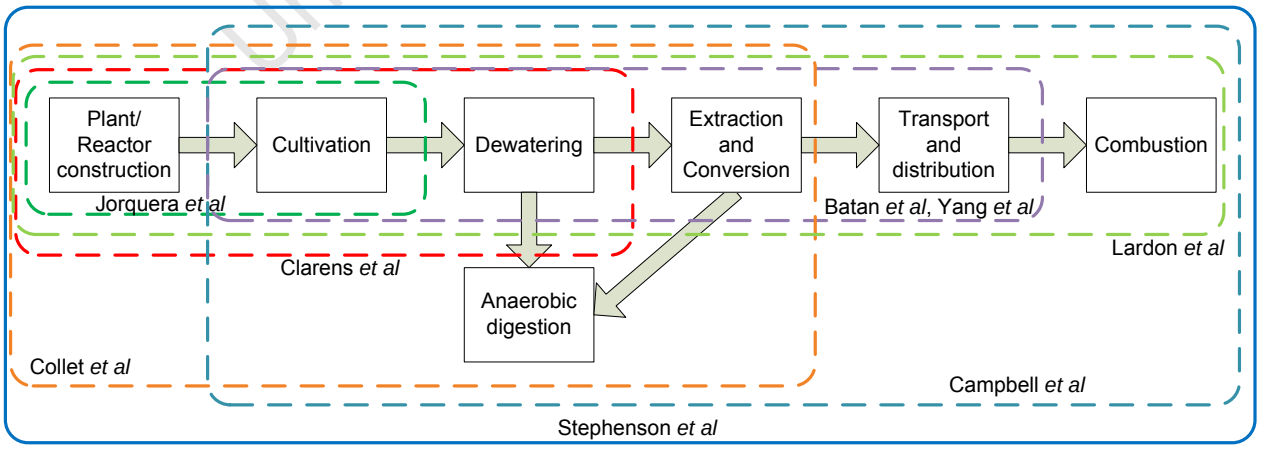

Figure 2-1 Diagram of system with boundaries from different LCA studies, where all inputs and outputs to the unit processes shown are included.

Table 2-1 Table showing the scope, method and allocation used in algal bio-energy LCA studies

Study	System boundaries							Method	Allocation
	Infrastructure	Cultivation	Dewatering	Anaerobic digestion	Extraction & Conversion	Transportation & distribution	Combustion		
Lardon *et al.* (2009)	✓	✓	✓		✓	✓	✓	CML	energetic
Jorquera *et al.*(2010)	✓	✓						NER	none
Clarens *et al.*(2010)	✓	✓	✓					-	none
Campbell *et al.*(2010)		✓	✓	✓	✓	✓	✓	GHG	none
Stephenson *et al.*(2010)	✓	✓	✓	✓	✓	✓	✓	EDIP	Market value & substitution
Collet *et al.*(2010)	✓	✓	✓	✓				CML	substitution
Yang *et al.* (2011)		✓	✓	✓	✓	✓		Water	none
Batan *et al.*(2010)		✓	✓	✓	✓	✓		NER, GHG	substitution

Various unit processes analysed in the previous studies are presented in Section 0 - 2.3.4. Discussion of the data and unit process selected and assumptions made follow.

2.3.1. Reactors

The role of the reactor phase in algal biodiesel production is central to this thesis. As seen in Table 2-2, raceways are the most common mode of microalgal culture investigated. This is largely justified by their lower energy (Lardon *et al.*, 2009) and economic requirements (Jorquera *et al.*, 2010). Also notable in Table 2-2 are the varying biomass concentrations, productivities and oil contents assumed in each respective reactor type. The effect of varying these and other parameters on the energetic and environmental impact of algal biodiesel production will be dealt with in Chapters 4 and 5. Data source are further discussed in Section 2.4.2. Despite the differing assumptions however, these papers have contributed considerably to the knowledge gap. Their approaches and findings are given below and will be later discussed in more rigour in conjunction with the findings of this thesis.

In the first published LCA of algal biodiesel, Lardon *et al.* (2009) investigated culture in raceways under nitrogen sufficient conditions to allow high biomass concentrations and under nitrogen limited conditions to allow lipid accumulation. Results showed a low nitrogen condition to be most favourable for biodiesel production, as expected. This high sensitivity to lipid content was further confirmed by Stephenson *et al* (2010).

Jorquera *et al* (2010) then compared open ponds to flat plate and horizontal tubular photobioreactors. This study aimed to calculate the net energy ratio (NER) of each system and thus evaluate feasibility. The NER was defined as the total energy content of the produced biomass divided by the energy requirement for air pumping and materials and construction of the reactors. The photobioreactors were found to exhibit significantly higher volumetric and areal productivities as well as much higher biomass concentrations than the ponds. Consequently, ponds were shown to require twice the available land and consume sixteen times the amount of water as photobioreactors. However, the energetic requirement for mixing was shown to be significantly higher in both photobioreactor systems and render horizontal tubular photobioreactors unfeasible. Flat plate photobioreactors and raceways ponds demonstrated biomass NERs of 4.33 and 7.01 respectively. While this study represented a valid comment on the different reactor types, the authors did acknowledge that these results were limited as they do not take downstream processing into account. The lower concentrations achieved in raceways could significantly affect the relative NERs following the inclusion of a dewatering step in particular.

Table 2-2 Reactor types, species and assumed data for resultant biomass growth characteristics and the energy requirement of the reactor. Some papers did not disclose certain parameters.

Study	Reactor	Species	Biomass conc., X (kg/m^3)	Oil content (%)	Productivity ($g/m^2/day$)	Energy[i] (W/m^3)
Lardon *et al.* (2009)	Raceway	*Chlorella vulgaris*	0.5	17.5 38.5	24.75 (reg N) 19.25 (low N)	-
Jorquera *et al.* (2010)	Raceway Tubular Flat plate	*Nannochloropsis*	0.35 1.02 2.7	29.6	11 25 27	3.72 2500 53
Clarens *et al.* (2010)	Raceway	$C_{106}H_{181}O_{45}N_{15}P$	1	-	10-20	-
Campbell *et al.* (2010)	Raceway	-	-	-	15 30	-
Stephenson *et al.* (2010)	Raceway Tubular	*Chlorella vulgaris*	1, 1.7 5, 8.3[ii]	40[iii]	10 1 ($kg/m^3/day$)	~2.8 ~144
Collet *et al.* (2010)	Raceway	*Chlorella vulgaris*	0.5	-	25	-
Yang *et al.* (2011)	Raceway	*Chlorella vulgaris*	1	35	35	n/a
Batan *et al.* (2010)	Plastic bag photobioreactor	*Nannochloropsis*	-	50	25	0.4 (W/m^2)

i. Included energy for mixing and CO_2 provision

ii. Successive cell concentrations for the nutrient sufficient and deprived reactor stages

iii. Following nutrient deprivation

The raceway versus photobioreactor debate was further added to by Stephenson *et al.* (2010). In this study, the entire life cycle from cradle to combustion was taken into account. In the process flow-sheet, algae were cultivated by a two-stage method of cultivation in either raceways or tubular photobioreactors. In each case, an initial growth reactor allowed for a high concentration of biomass to be reached under nitrogen sufficient conditions. Following this, culture was transferred to a second reactor, where nitrogen provision ceased to allow for lipid accumulation. Upon entering the second reactor, the culture was diluted 2 fold to increase light availability. The raceways and bioreactor systems were assumed to be operated continuously during photosynthetically active periods (assumed as 8 hours a day) and as batch systems for the remaining time. For the sake of consistency, the raceway and tubular photobioreactor designs used by Stephenson are again employed in this thesis and are detailed in Sections 3.4.1 and 3.4.2.

Results showed the reactor phase to be a dominant contributor to the total process energy requirement. The particular design of the tubular airlift photobioreactor investigated (Figure 3-3) was shown to result in process energy requirements an order of magnitude higher than the raceway system. This translated into a higher fossil energy requirement and global warming potential (GWP), which was also significantly higher than that of fossil derived diesel on an equivalent energy basis. On the other hand, the fossil energy requirement and GWP of biodiesel produced where microalgae were grown in raceways showed values ~85 and ~78% lower than that of fossil derived diesel respectively. A closer look at the fossil energy requirement and GWP of cultivation in tubular bioreactors (Figure 2-2) showed the electrical energy requirement of cultivation and manufacture of the tubing to be the only significant burden contributors. While the contribution of electrical energy of ~85% was considerably higher than that of tubing manufacture, the manufacturing associated burden was still considered noteworthy as its GWP was roughly equal to the entire of the raceway cultivation phase. In raceway cultivation, the electricity required to drive the paddle wheel was found to be dominant, followed by significant contributions by manufacture of nitrogen fertiliser. The burden associated with fertiliser use was found to be lower than that reported by Clarens *et al.* (2010) for nitrogen sufficient growth due to the dual stage cultivation mode employed. PVC was the only material of construction that contributed significantly to the manufacturing burden. Reactor related sensitivity analysis showed a notable sensitivity to the concentration of CO_2 in the flue gas supplied and the liquid circulation velocity of the culture.

Contrasting to the finding of Jorquera *et al.* (2010), the water requirements of the raceway cultivation system were found to be lower than that of the photobioreactor system, showing respective values of 3.8 and 13.7 m^3/ton biodiesel, where Jorquera *et al.* had found the water consumption of raceways to be 16 times higher than that of photobioreactors. This was because annual rainfall in the U.K. was considered as greater than evaporation. It was further discussed that were the facility located in the Mediterranean, while the increased evaporation-rainfall balance would increase the water requirement to 101 m^3/ton for raceways, the required cooling water for tubular bioreactors would increase by an additional 362 m^3/ton.

Largely, microalgal growth in raceways is deemed more sustainable than that in photobioreactors, principally due to the significantly higher requirement for electrical energy to drive liquid circulation in photobioreactors and the cost of reactor construction. Batan *et al.* (2010) however, considers these drawbacks to have been overcome by technological advances and model their system assuming growth in sparged polyethylene photobioreactor bags. While the raceway versus enclosed photobioreactor debate appears to be more heavily weighted in the direction of raceways from an LCA perspective, it is still unresolved.

(a)

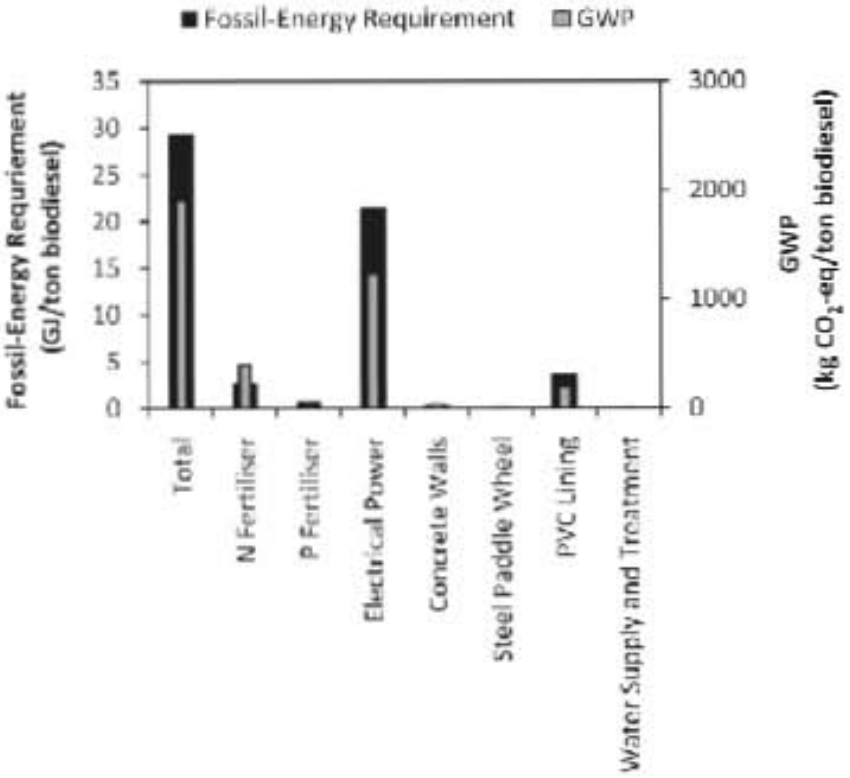

(b)

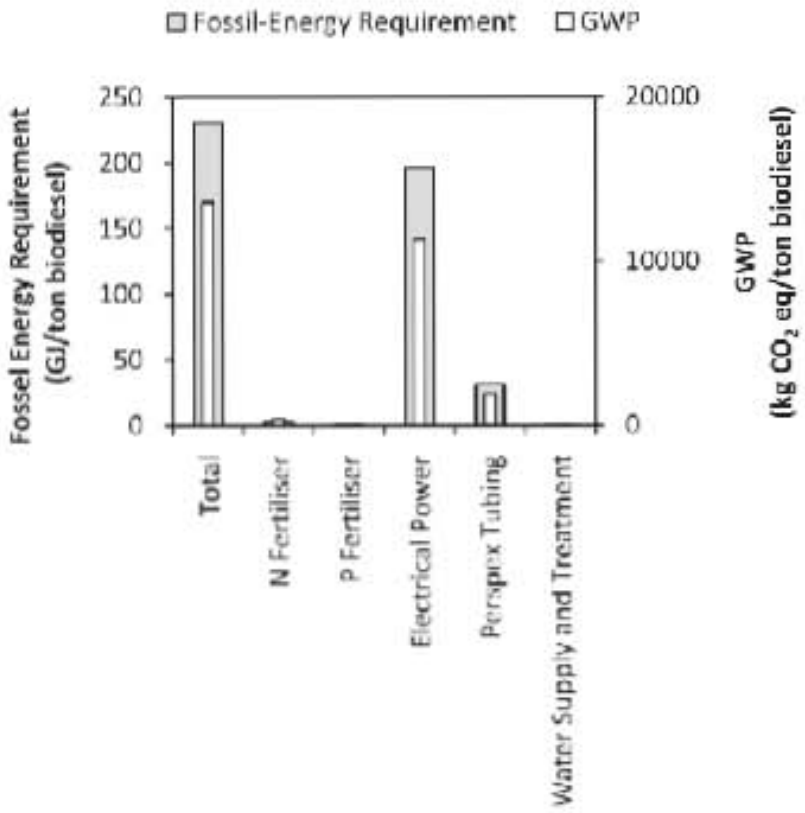

Figure 2-2 Contributions of cultivation to the Fossil energy requirement and GWP burden in (a) raceways and (b) tubular photobioreactors (Stephenson *et al.*, 2010).

The present work further addresses the role of reactor design, firstly by assessing three microalgal species grown in identical reactors and culture conditions (Chapter 4). The effect of improving the power input per unit volume for these reactors on the environmental and energetic burden of the process is then investigated. Chapter 5 looks at a single species in three different reactor configurations and probes the effect of changing growth characteristics in these reactors.

Table 2-3 Modes of dewatering employed and concentrations achieved

Paper	Species	Dewatering step 1		Dewatering step 2	
		Method	kg/m^3 (% recovery)	Method	kg/m^3
Lardon *et al.* (2009)	*Chlorella vulgaris*	Flocculation, settling	20 (90)	Rotary press [a]	200
Jorquera *et al.* (2010)	*Nannochloropsis*	-	-	-	-
Clarens *et al.* (2010)	$C_{106}H_{181}O_{45}N_{15}P$	Flocculation	none	Decanter centrifuge	100
Campbell *et al.* (2010)	-	Flocculation, DAF [b]	-	Centrifuge	-
Stephenson *et al.* (2010)	*Chlorella vulgaris*	Flocculation, settling	25 x [c] (100)	Decanter centrifuge	220
Collet *et al.* (2010)	*Chlorella vulgaris*	Natural settling	10 (65)	Spiral plate centrifuge	50
Yang *et al.* (2011)	*Chlorella vulgaris*	Flocculation, filtration	15 (85)	Drying	900
Batan *et al.* (2010)	*Nannochloropsis*	-	-	Continuous clarifier [c]	-

a. Following this step, biomass was dried (using a belt drier) to reach 900 kg/m^3 as required for soybean oil extraction.
b. Dissolved air flotation
c. 25x initial concentration.

2.3.2. Dewatering

Dewatering is considered one of the barriers to large scale algal cultivation and no well accepted pathway currently exists. As shown in Table 2-3, dewatering has been modelled largely assuming an initial concentration step followed by centrifugation (Campbell *et al.*, 2010; Clarens *et al.*, 2010; Collet *et al.*, 2010; Lardon *et al.*, 2009; Stephenson *et al.*, 2010). Centrifugation is considered a mature technology and is used industrially. This is in line with the recommendations of Benemann and Oswald (1996), who advocated that while centrifugation is not a viable method for primary harvesting, it could be considered as a secondary harvest method. Dewatering is required to reduce

the algal slurry concentration to 15 to 20% solids, as required for lipid extraction (Benemann & Oswald, 1996).

2.3.3. Oil Extraction and Biodiesel Production

Stephenson *et al.* (2010) investigated two different methods of oil extraction: extraction decanters and a counter-current cascade of mixer settlers. However it was found that there was no significant difference between these methods in terms of fossil energy requirement and GWP. In both cases, hexane was used as the extraction solvent in a 2:1 ratio of algal slurry to solvent. Extraction was assumed to recover 99% of the TAG. Cells were broken to aid solvent extraction. Solvent recover and transesterification are modelled as for oil-seed rape in the U.K.

The notional biodiesel production system described by Campbell *et al.* (2010) employs a system whereby, following the initial dewatering step, the algal stream is heated and centrifuged to further concentrate the algae and extract the lipids. Transesterification using a methanol catalyst follows, modelled as for canola oil, the only other potential biodiesel feedstock grown in Australia.

A number of studies follow the example of Sazdanoff *et al.* (2006) in assuming that biodiesel production from microalgae is similar to that of producing soybean biodiesel when the algal slurry content is greater than 90% wet weight (Batan *et al.*, 2010; Lardon *et al.*, 2009; Yang *et al.*, 2011; Zhang *et al.*, 2010). This requires the biomass to be dried to this level by belt or drum drying, which makes up a large portion of the process energy requirements. In other cases, the slurry is rarely concentrated above 22%. Considering the high cost of drying to this concentration, this assumption should be revisited.

Where modelled as for the soybean to biodiesel process, extraction yields of about 70% are achieved with hexane as the solvent (Batan *et al.*, 2010; Lardon *et al.*, 2009; Yang *et al.*, 2011). Solvent recovery and esterification with methanol or ethanol and a catalyst follow the extraction process.

Oil extraction and fuel conversion are generally found to form a significant portion (2-27%) of the process energy burden (Batan *et al.*, 2010; Lardon *et al.*, 2009; Stephenson *et al.*, 2010).

2.3.4. Biogas as a Co-Product

In several papers, the flow-sheet allows the biomass remaining after lipid extraction to undergo anaerobic digestion, where methane is produced for further processing by combustion to produce electricity (Campbell *et al.*, 2010; Stephenson *et al.*, 2010). Campbell *et al.* (2010) assume that the biomass is readily digested, but acknowledge that an additional carbon source such as waste paper

may be required for optimal yields. Stephenson *et al* (2010), who investigated two different modes of cell disruption, assume that only disrupted cells are digested.

In response to the dominant contributions of fertiliser consumption, harvesting and oil extraction to the high energy debt of algal biodiesel, Collet *et al* (2010) investigated anaerobic digestion (AD) of *Chlorella vulgaris* to produce methane as a sole energy product. This approach avoids the concentration and oil extraction steps and thereby significant energetic and economic cost. In addition, recycling the liquid fraction of the digestate could significantly reduce the need for fertiliser. A portion of the methane produced (30%) was burned directly to provide process heat for the AD plant, while the remainder was processed in a purification plant to enrich the biogas and recover CO_2. This CO_2 could then be dissolved in water and re-injected into the growth phase. Notably, the anaerobic digester in this study offered a retention time of 46 days, based on experimental data from the same laboratory which showed that a hydraulic retention time (HRT) higher than 40 days was required to achieve a methanisation yield of greater than 75% (Ras *et al.*, 2010). This experimental data, published concurrently with the LCA study, also led to the estimate of a 90% mineralisation rate, which in application as a soil conditioner, could replace the equivalent amounts of mineral fertilisers for N, P and K. The liquid portion of the digestate, also containing mineralised matter, was recycled back to the growth unit in the flow-sheet to partially supply fertiliser needs. This was not validated experimentally.

Results of the life cycle impact assessment (LCIA) showed the life cycle burdens of the entire process to be largely due to energy consumption, which were dominated by digester energy requirements, which was in turn directly linked to HRT. If the concentration of the input stream to the digesters were higher, this would increase the organic load rate (OLR) and thus increase plant productivity. Alternatively, maintaining a constant OLR could reduce HRT for the same result. It was thus suggested that an optimisation between the HRT and concentration of the microalgal stream from the reactors be performed in future work in order to increase methane yield. Other recommendations for improving digester performance included exploring various pre-treatment options, co-digestion, controlling the C/N ratio through nitrogen addition and screening of different microalgal species. Given that the majority of the process burden comes from electricity usage, hosting other alternate energy producers such as wind turbines or solar panels on site could provide a more efficient path to biogas production.

2.4. LCA Methodology and Approach

2.4.1. Scope, Allocation and Methodology

The scope of each study is shown in Figure 2-1 and Table 2-1. Both Jorquera *et al* (2010) and Clarens *et al.* (2010) investigated the reactor phase, excluding all downstream processes. This approach was largely justified by Stephenson *et al.* (2010) who showed the majority of the process burdens to come from the cultivation of algal biomass.

One significant system boundary consideration is that of facilities and reactor construction, a part of the life cycle excluded by several studies. This exclusion is justified by Campbell *et al*. (2010) in that the comparison being made is to fossil fuels and in the literature, embodied environmental impacts of the construction of infrastructure required for the initial exploration and production of fossil fuels is rarely, if ever, mentioned. Further, Lardon *et al.* (2009) showed that the life cycle impacts attributed to the building and recycling of the facility were minimal in all categories except for land use, an area where algal biodiesel offers a clear advantage over conventional feedstocks (Clarens *et al.*, 2010).

When choosing an impact assessment methodology, the impact categories of interest must first be chosen. The impact categories investigated in the various LCA studies are shown in Table 2-4, while impact assessment methods are shown in Table 2-1. Not surprisingly, as most biofuels strategies are driven in response to global warming, climate change and a desire for independence from fossil fuels, GWP and GHG emissions and the (fossil) energy linked fossil energy consumption and NER are the most frequently used modes of analysis.

According to the ISO guidelines, where possible, substitution is preferred to allocation (Guinée, 2002). Batan *et al.* (2010) employed co-product substitution for both glycerol and the residual non-lipid biomass. The latter was considered to displace microalgal biomass used as an ingredient in aquaculture as fish feed. Stephenson *et al.* (2010), while using substitution to account for energetic and heat by-products, argued that as glycerol was generally manufactured as a by-product of soap production, substitution was difficult. Allocation for glycerol and potassium sulphate was thus done by market value. Lardon *et al.* (2009) allocated energy consumption to the co-products, which made comparison to the results of the algal biogas production LCA of Collet *et al*. (2010) difficult.

Table 2-4 Impact categories chosen in LCA studies.

		Lardon *et al.* (2009)	Jorquera *et al.* (2010)	Clarens *et al.* (2010)	Campbell *et al.* (2010)	Stephenson *et al.* (2010)	Collet *et al.* (2010)	Yang *et al.* (2011)	Batan *et al.* (2010)
Abiotic depletion	kg Sb eq.	X					X		
Acidification	kg SO_2 eq.	X					X		
Ozone layer depletion	kg CFC^{-11} eq	X					X		
Human toxicity	kg 1,4-DB eq.	X					X		
Marine toxicity	kg 1,4-DB eq.	X							
Ionising radiation	DALYs	X					X		
Photochemical oxidation	kg C_2H_4	X					X		
Net energy ratio	-		X						X
Fossil energy consumption	MJ			X		X			
Global warming potential [i]	kg CO_2 eq.	X		X	X	X	X		X
Eutrophication	kg PO_4^- eq.	X		X			X		
Water use	m^3			X				X	
Land use	ha	X		X			X		

i. Or GHG emissions

2.4.2. LCI and Data Sources

Data sources were first raised as an issue of contention by Collet *et al.* (2010), who considered values for paddle wheels and water pumping of 0.2 kWh and 0.153 kWh per kg algae respectively. In contrast, Clarens *et al.* (2010) considered values of 0.035 kWh and 0.029 kWh per kg algae. It was found that substitution of the lower values assumed by Clarens *et al.* resulted in a 44% reduction in total energy demand.

In general, authors made use of their own data (Batan *et al.*, 2010; Collet *et al.*, 2010; Stephenson *et al.*, 2010), literature studies (Jorquera *et al.*, 2010; Lardon *et al.*, 2009; Yang *et al.*, 2011) and/or pilot studies (Campbell *et al.*, 2010; Clarens *et al.*, 2010). Pilot scale data was mostly associated with the

US Department of Energy (Benemann & Oswald, 1996; Weissman & Goebel, 1987; Weissman & Tillet, 1989).

As discussed in Section 1.3.6, a key concern in choosing an appropriate species for algal biodiesel production is that of lipid productivity, which is the product of lipid content and biomass productivity. High algal lipid contents often occur at the expense of lower biomass productivity under conditions of nitrogen or other environmental stress. The trade off between these variables is accounted for in lipid productivity and is vital in determining an algal species' suitability for biodiesel production. However, some studies to date use assumed or literature values for biomass productivities and lipid contents that were not or could not be achieved simultaneously (Campbell *et al.*, 2010; Jorquera *et al.*, 2010; Yang *et al.*, 2011).

There is a need both for more accurate large scale data for simultaneous occurring biomass productivities and lipid contents and to assess the system sensitivity to these variables. The present study attempts to further address this issue.

2.5. Key issues, findings and recommendations

2.5.1. CO_2 provision

Part of the appeal of algal production lies in the potential for CO_2 cycling and the utilisation of flue gas as a source of CO_2. It has been shown that use of liquefied compressed CO_2 in fact contributes roughly 40% of the energy consumption and 30% of GHG emissions during algal cultivation on a life cycle basis (Clarens *et al.*, 2010). Further investigation into co-location of algal ponds next to power stations showed that while some burden reduction is achieved, the principal burden driver of fertiliser production is still significant such that algal production would not be sustainable until this burden was reduced or a suitable alternative found.

CO_2 provision was defined in Stephenson *et al.* (2010) as coming from flue gas at 12.5% CO_2 that would otherwise have been released to atmosphere. Batan *et al.* (2010) assumed that the microalgal production facility was located adjacent to an amine plant, implying no transportation, pre-processing or energy costs to deliver CO_2.

A later study investigated three different modes of CO_2 supplementation (Campbell *et al.*, 2010);

1. Delivery of pure CO_2 from an adjacent ammonia plant
2. Delivery via flue gas at 15% concentration from an adjacent power station
3. Delivery of liquefied, compressed CO_2 from local storage.

All of the above scenarios for algal biodiesel production were shown to have lower GHG emissions than that of both biodiesel from canola and ultra-low sulphur (ULS) diesel from fossil reserves. CO_2 supplied from both the ammonia plant and power plant flue gas showed net negative GHG emissions due to the payback achieved through AD of the residual biomass left after lipid extraction. CO_2 delivery from the ammonia plant was shown to be slightly favourable.

As world industry moves towards cleaner energy production, a sizeable move toward technologies that generate electricity without CO_2 emissions is expected. This will reduce the number of locations where algae could be economically and sustainably produced. This, in conjunction with the expected move towards electrification in the transport sector, suggests that algal biodiesel may be useful mainly as a transition fuel (Campbell *et al.*, 2010). However, its potential role in distributed energy supply in remote areas remains interesting beyond the transition.

2.5.2. Fertiliser/Nutrient Provision and Recycle

Given that a notable portion of the environmental and energetic burden of algal biodiesel comes from the provision of fertiliser and the synergies between algal biomass production and wastewater treatment, Clarens *et al.* (2010) investigated three types of wastewater effluent for their usefulness as nutrient sources. Namely, effluents from conventional activated sludge (CAS) and biological nitrogen removal (BNR) wastewater treatment (WWT) plants and source separated urine (SSU) were considered. The data showed that use of wastewater in place of chemical fertiliser indeed contributed to reduction in the life cycle burdens of the process. The extent of improvement was proportional to the relative nutrient concentrations in each wastewater, with SSU showing the most dramatic offset. Improvements were shown to be 30-50% due to the avoided use of chemical fertilisers and 50-70% due to the energy intensive nature of municipal WWT. This is a particularly positive result as it shows incentives for both algal production and WWT for potential partnerships and industrial ecology. The water burden was shown to be reduced to almost zero using CAS or BNR, but showed little improvement for SSU, which would need to be significantly diluted prior to addition to the ponds. Yang *et al.* (2011) further showed that recycling of harvest water reduced nutrient usage by 55%.

Another way to reduce the requirement for chemical fertilisers is to recycle the nitrogen and phosphorous present in the residual biomass following AD. This is feasible as AD mineralises the biomass waste, producing ammonium and phosphate ions (Sialve *et al.*, 2009). Stephenson *et al.* showed that if 80% of the N and P present in the residual biomass could be recycled, significant burden reduction could be achieved. However, this was only the case for cultivation in raceways as, due to the dominant energy burden associated with liquid circulation in airlift tubular bioreactors,

the benefit achieved by nutrient recycle was negligible. Conversely, Batan *et al.* (2010) recycle the growth media, but do not attempt to recover nitrogen from the residual biomass. This is done in response to a lack of data regarding the energy and material costs associated.

2.5.3. Climate and Location Considerations

In Sazdanoff's (2006) study of the algae to biodiesel fuel cycle, a first attempt was made to link solar radiation and day length to algal productivity and thus CO_2, nutrient and electricity requirements. Various locations in the United States were compared on the basis of solar radiation received. Clarens *et al.* (2010) took this further, analysing the potential of three locations on the basis of both solar radiation and the evaporation-precipitation balance. It was shown that, apart from the land use burden, there was no significant difference in burden between locations. This was explained by the large fraction of each burden which is derived from upstream processes, such as the offsite production of CO_2, electricity and fertilisers. It was thus concluded that should any of these requirements be reduced or provided by an alternate source, geographic differences would play a larger role.

Location was further considered by Campbell *et al.* (2010) who considered a potential production facility on the coast of Australia. It was stated that the abundance of sunlight, temperatures favourable for algal growth and large areas of available land were a benefit not necessarily available in other locations. The lack of available fresh water on this relatively dry continent however dictates the requirement for a salt water species. In drier areas, evaporation could cause salt concentration and disposal to be an issue. Overall, it was concluded that it was economically viable to reduce GHG emissions by producing biodiesel from algae in Australia.

Yang *et al.* (2011) noted that, in general, solar radiation and temperature, which vary geographically, contribute positively to microalgal growth, which thus lowers the water footprint. However, these factors also result in an increased evaporation rate, which increases the water footprint. This trade-off was further investigated in various US states and is shown in Figure 2-3. The figure shows the overall water footprint of microalgae-based biodiesel production to decreases as solar radiation and temperature increase. Notably however, this analysis was undertaken assuming microalgal growth in enclosed photobioreactors and may show a stronger sensitivity to evaporation and thus different results for raceway cultivation.

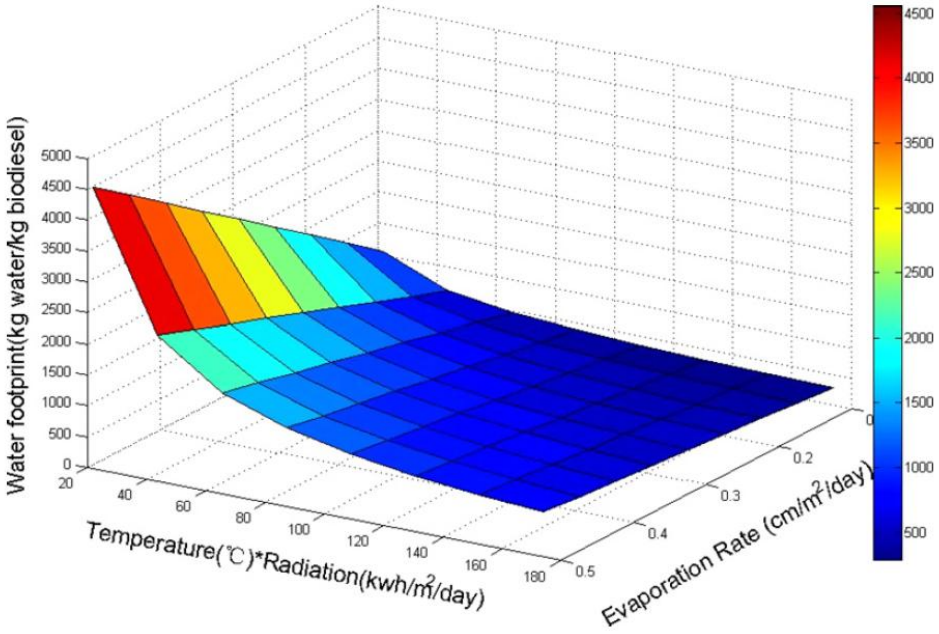

Figure 2-3 Water footprint (kg-water/kg-biodiesel) of C. vulgaris-based biodiesel production under different climatic conditions (Yang *et al.*, 2011)**.**

2.5.4. Water Use

Water use is linked to a number of different areas (reactor type, dewatering, recycle and climate considerations) and has thus been mentioned a number of times already in this review. Yang *et al.* (2011) undertook a quantitative examination of the water footprint of algal biodiesel. Process options investigated included the use of freshwater, seawater and waste water, with and without recycle of harvested water. It was found that using seawater or wastewater, as considered by Clarens *et al.* (2010), the demand for fresh water could be reduced by as much as 90%. Sensitivity analysis showed the water burden to be most sensitive to evaporation rate, algal growth rate and lipid content and the slurry concentration following harvesting. Further analysis showed algal growth rate to be the most sensitive parameter. Increases in the growth rate and lipid content were both found to reduce the water footprint, further motivating continued research into the trade-off between these two parameters. An investigation into the water footprints of eleven other microalgal species justified the choice of *Chlorella vulgaris* as a base case species and showed *Chaetoceros gracilis*, *Cyclotella cryptic* and *Nannochloropsis* sp. to have comparably favourable footprints.

2.5.5. Comparison to Fossil Fuels and 1st Generation Biofuels

In their comparison between algae, corn, canola and switchgrass (excluding oil extraction and fuel conversion processes), Clarens *et al.* (2010) found the production of terrestrial crops to have significantly lower energy requirements, GWP and water use than algae. Notably, algal cultivation was found to emit more GHG than it sequestered, a finding in contrast to that of Lardon *et al.*

(2009). In the areas of land use and eutrophication however, algae were shown to perform significantly better. Favourable eutrophication potential was attributed to the use of engineered ponds, which allowed for better runoff control than in terrestrial crop systems.

Yang *et al.* (2011) showed algal biodiesel to be very competitive with biodiesel produced by other conventional feedstocks in terms of its water footprint.

In Batan's (2010) comparison to soybean based biodiesel, while microalgal oil extraction required less energy, it required 2.1 times more energy during the growth phase in photobioreactors and an energy intensive dewatering step. Overall however, it was found to possess a more favourable NER than soybean biodiesel. This was largely due to the superior energy content of algae of 50% lipid as opposed to soybeans' 18%. In terms of GHG emissions, both soybean and microalgal biodiesel showed set negative emissions, with microalgae showing slightly superior.

In most studies, it is accepted that algal biodiesel is still a relatively immature process, with much potential for improvement (Lardon *et al.*, 2009). In contrast, it is unlikely that major improvements will be achieved in corn, canola or switchgrass cultivation (Clarens *et al.*, 2010). This should be kept in mind in comparisons and evaluations of algal bio-energy.

2.6. Conclusions

At the end of 2009, the following was evident from the literature according to the findings of Lardon *et al.* (2009), Jorquera *et al.* (2010) and Clarens *et al.* (2010):

- Process burdens are highly sensitive to changes in algal growth rate parameters
- The dominant contributors to the environmental burden of algal biodiesel are energy and fertiliser use and CO_2, if liquefied compressed CO_2 was used.
- Anaerobic digestion of the non-lipid biomass was shown to have the potential to both reduce the process energy demand and recycle mineral nutrients, thereby reducing the fertiliser requirements
- The use of wastewater in place of chemical fertiliser contributed significantly to reduction in the life cycle burdens of the process. Recycling the process water and biomass waste following AD was also effective in reducing fertiliser use and thus associated burden.
- Data quality was an issue of contention and there is a need both for more accurate data for simultaneous occurring biomass productivities and lipid contents and to assess the system sensitivity to these variables

In general, LCA was shown to be an effective tool in assessing algal biodiesel production as an immature process and to identify obstacles to large scale production.

3.Methodology

3.1. Model development

In order to investigate the production of microalgal biodiesel on an energetic and environmental level, an appropriate process model is required. This model is needed to generate material and energy inputs and outputs, including emissions. The inventory resulting is required for both a net energy analysis and environmental assessment. For the latter, life cycle assessment (LCA) has been selected to inform this study, as justified in Section 1.6.1 and following the suitability demonstrated in the studies described in Chapter 2. To ensure maximum value is derived from the study, the model should:

1. Allow for scenario analysis
2. Allow for the assessment of different process options
3. Be easy to adapt and introduce new or increased complexity
4. Provide the requisite inventory for LCA and allow for easy transfer to SimaPro for LCA study
5. Be scalable to a defined functional unit.

The biorefinery approach selected for production of microalgal biodiesel involves the following general processes: algal cultivation, concentration of the algal suspension and dewatering, oil extraction and its transesterification for biodiesel production and anaerobic digestion of residual biomass. These processes can each consist of one or more steps. This basic flow-sheet was used to investigate the environmental burden of algal biodiesel *per se*. In addition, this thesis extends this to consider in detail the reactor used and species dependence. To accommodate this, unit processes downstream of the reactor were largely maintained as constant inputs, while species and reactor configuration were varied to achieve the goals of the study. Small changes to DSP were mediated in response to algal concentration and the solid-liquid separation characteristics of the algal species. The process model of the flow-sheet was created using MATLAB and data output to Excel to allow easy input into SimaPro v7.2 (Pré Consultants B.V. 2010) for LCA purposes.

In Section 3.2, the basic flow-sheet model is detailed. Details of the input growth data, laboratory tubular airlift reactor, used in the base case and all downstream operations follow. Section 3.3 provides an outline of further methodology for the species study presented in Chapter 4. This involves an investigation into the effect of growth characteristics (biomass concentration, productivity and associated compositions) on the overall production process. The methodology used

in the reactor study presented in Chapter 5 is detailed in Section 3.4. Here, the effect of reactor configuration on a large scale is investigated, analysing horizontal tubular reactors and raceway ponds, as well as a larger vertical tubular airlift reactors. In Section 3.5, details of the methodology for the LCA are given.

3.2. Base Case Process Details

3.2.1. System Overview

The process flow-sheet investigated in this study is shown in Figure 3-1. Algae are grown continuously in airlift reactors and harvested in settling tanks with or without flocculation. The resultant slurry is concentrated by centrifugation. Oil extraction is done with hexane and biodiesel production via transesterification using lipase as a biological catalyst (Harding *et al.*, 2008). Waste streams from the oil extraction and refining phases were digested anaerobically to produce methane and carbon dioxide. The latter was utilised for biomass growth. Methane gas produced was used to produce electricity to offset the power requirements of the process facility partially. Digestate from anaerobic digestion was given free of charge to the farmers for use as a soil conditioner (environmentally neutral). All pumps were assumed to operate at an average efficiency of 70% with a total dynamic head of 10 m. Chemicals were assumed to be transported an average of 100 km by truck. The technical details and associated calculations of the various unit processes are described below.

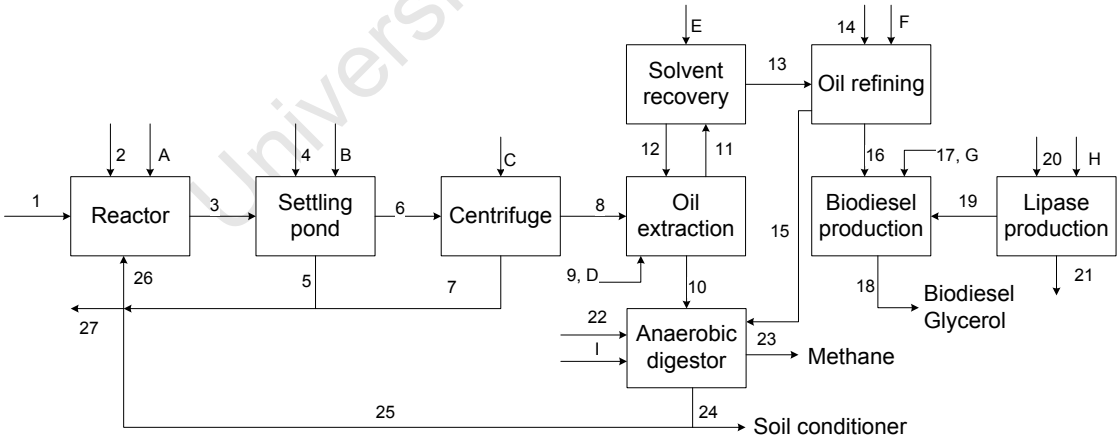

Figure 3-1 Process Flow-sheet for the system investigated. Annotations 1-24 refer to flows and A-I to energy inputs.

3.2.2. Biomass Growth Characteristics and Media Composition

The base case was developed for *Scenedesmus sp.* grown in the CeBER Laboratory Vertical Airlift Reactors shown in Figure 3-3, under conditions of maximum lipid productivity generated in a concurrent laboratory study reported in Griffiths *et al.* (2011). For any given study model inputs for

growth characteristics and biochemical composition of the chosen algal species are required. This is shown in Table 3-1 for *Scenedesmus* sp., as for the base case. The elemental composition was then extrapolated from the biochemical composition. This was done according to the gross elemental compostion of the biochemical classes for algae and cyanobacteria reported by Geider (2002), summarised in Table 3-2 and shown to be in good agreement with experimental data (Griffiths, 2009). Nutrient and CO_2 requirements were then calculated from the biomass elemental composition. Potassium and phosphorus were then estimated based on respective ratios compared to nitrogen of 178 and 216 g/kg N respectively (Borowitzka, 1988). Nitrogen is provided by ammonium nitrate, phosphorous by triple superphosphate and potassium by potassium chloride (Stephenson, 2009). The water removed in both the settling and centrifugation steps is recycled at a 10% purge to prevent the build up of salts and impurities. Nutrients were assumed to be utilised in perfect stoichiometric efficiency. CO_2 was provided through CO_2 enriched air in a bioreactor specific manner. The entire carbon content of the biomass is attributed to CO_2 fixation.

Table 3-1 Base case biomass growth characteristics and composition for *Scenedesmus sp.* (Griffiths, 2011)

	Input parameter	Unit	Value
Growth characteristics:	Biomass concentration	g/L	0.63
	Biomass productivity	g/L/day	0.37
Biochemical composition:	Protein	%	52
	Carbohydrate	%	18
	Lipid	%	18
	Pigment	%	3
Elemental composition:	C	%	60
	H	%	7
	N	%	9

Table 3-2 Elemental compostions of the major biochemical classes found in algae and cyanobacteria (Geider & La Roche, 2002)

fraction	Formula	Molar mass (g/mol)
Protein	$C_{4.43}H_7O_{1.44}N_{1.16}$	99
Lipid	$C_{40}H_{74}O_5$	634
Carbohydrate	$C_6H_{12}O_6$	180
Pigment	$C_{48}H_{57}O_5N_4$	778
Nucleic acids	$C_{9.5}H_{14}O_8N_4$	312

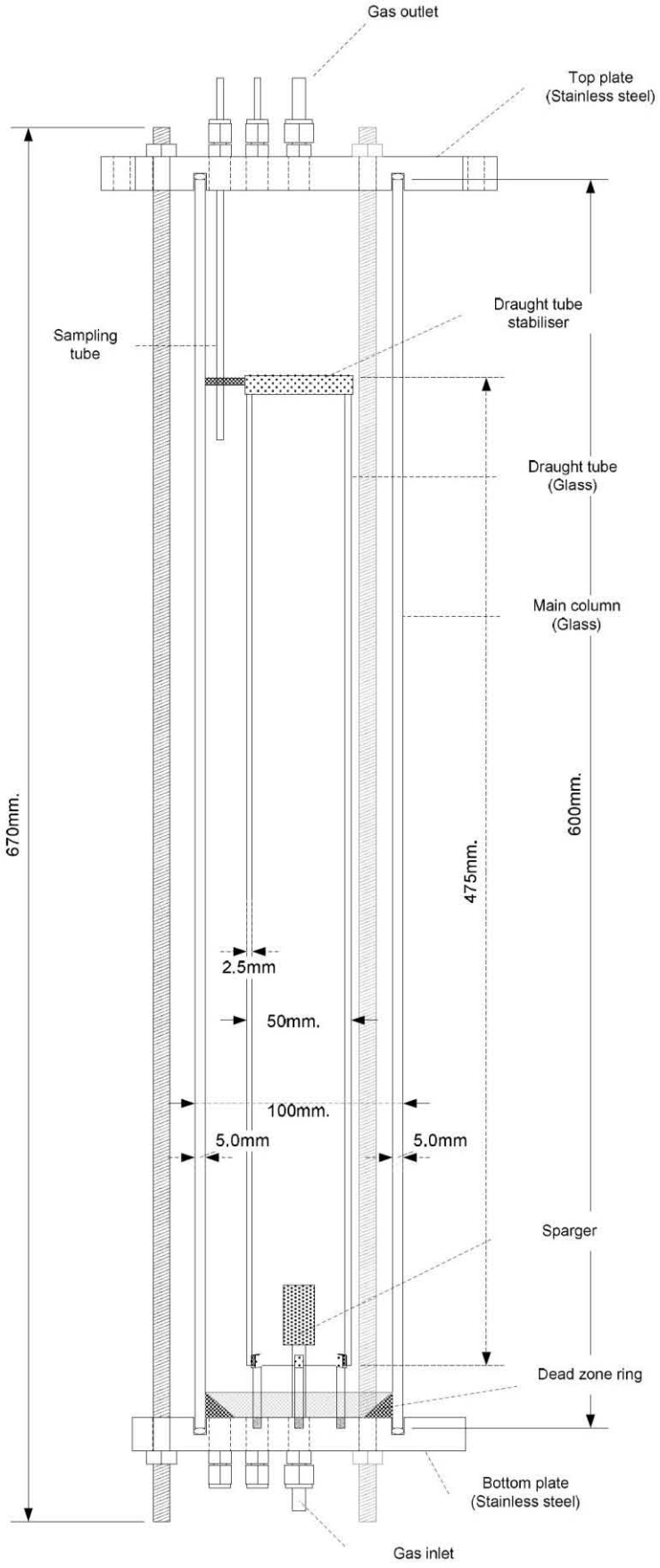

Figure 3-2 Schematic diagram of CeBER laboratory airlift reactor (Langley, 2010)

3.2.3. Cultivation in Laboratory Vertical Airlift Reactors

In Centre for Bioprocess Engineering Research (CeBER) at the University of Cape Town, Langley (2010) designed and constructed the CeBER vertical airlift reactors with a concentric draft tube configuration as detailed in Figure 3-2. These reactors were used to generate pertinent experimental data with respect to the algal species selected. This design was used as the basis for the airlift reactor in the model.

The main column and draft tube were manufactured from glass. The main design parameters pertinent to the calculations to follow are shown in Table 3-3. The gas free liquid height, h_D was 0.536 m, with an overall liquid volume of 3.2 L. Gas was sparged through a 2 µm HPLC solvent inlet filter, at 2 L/min. This resulted in a superficial gas velocity in the riser of 0.021 m/s (Langley, 2010).

In airlift reactors, the power input results exclusively from the gas sparged. Thus, the total power input consists of the work done by the isothermal expansion of the gas and the kinetic energy transferred to the fluid by the gas inflow as shown in Equation 3-1 (Chisti, 1989):

3-1

where:
- P_G = power input (W)
- Q_M = molar flow rate of gas (kmol/s)
- P_b = pressure at the bottom of the fluid in the vessel (Pa)
- P_h = headspace pressure (usually atmospheric) (Pa)
- U_0 = gas velocity at orifice of sparger (m/s)
- M = molar mass of gas (kg/kmol)

The kinetic energy term is generally found to be negligible. The superficial gas velocity, j_G for the airlift reactor can be calculated (Chisti, 1989):

3-2

Combining Equations 3-1 and 3-2 results in the following equation for power input per unit volume for an airlift reactor with uniform cross sectional area:

3-3

It was assumed that a compressor with an isentropic efficiency of 80% would be used. Losses in the distribution system of 0.07 bar and losses over the sparger of 0.07 bar were assumed (Weissman & Goebel, 1987). This resulted in a total power consumption of 229 W/m^3.

The hydrodynamic regime of an algal photobioreactor is an important factor in characterising the reactor's performance. The methods for estimating these parameters are presented by Chisti (1989) and have been developed for a range of airlift reactor configurations. They have proved accurate in predicting hydrodynamic conditions for a range of operating conditions, hence suitable for the purpose of this study. From the known reactor configurations and superficial gas velocity, the following equations can be solved to determine the superficial gas velocity in the riser j_{Lr}, (m/s):

3-4

where: j_{Lr} = superficial liquid velocity in the riser (m/s)

K_B = frictional loss coefficient

h_D = sparged liquid height (m)

A_r & A_d = cross-sectional areas of the riser and downcomer (m^2)

ε_r = gas hold-up in riser

ε_d = gas hold-up in downcomer

The frictional loss coefficient in the downcomer zone of the airlift loop, K_B can be calculated as follows:

3-5

where: A_b = free area below draft tube (m^2)

The gas hold-up in the riser can be estimated using a correlation developed by Hills (1976):

3-6

where: j_{Gr} = superficial gas velocity in the riser (m/s)

Equation 3-7, an empirical correlation developed by Bello *et al.* (1985), relates the gas hold-up in the riser to that in the downcomer.

3-7

As ε_r and j_{Lr} are both dependent on each other, Equations 3-4 and 3-6 need to be solved iteratively from an initial guessed value of j_{Lr}. For the 3.2 L airlift reactors under the operating conditions described, the calculations yielded a superficial liquid velocity in the riser of 0.148 m/s with fractional gas hold-ups in the riser and downcomer of 0.042 and 0.037 respectively.

Table 3-3 Selected design parameters for Laboratory Vertical Airlift Reactors descibed

Draft tube diameter	m	0.045
Draft tube length	m	0.475
Reactor diameter	m	0.09
Total reactor length	m	0.600
Distance from bottom to base of draft tube	m	0.02
Ratio of riser area to downcomer area	-	0.364
Liquid height	m	0.536
Liquid volume	m^3	0.0032
Superficial liquid velocity	m/s	0.148
Reactor power required [i]	W/m^3	67
Total power required [ii]	W/m^3	229

i. Compression power to overcome static head
ii. Compression power to overcome static head as well as losses in the distribution system and over the sparger.

3.2.4. Dewatering

According to Benemann and Ostwald (1996), while centrifugation is not a viable method for primary harvesting, it can be considered as a secondary harvest method. Dewatering and concentration jointly are required to produce an algal slurry or paste of 15 to 20% solids on dry weight basis, the concentration necessary for lipid extraction. Thus, depending on the algal species, either natural settling or chemical flocculation was employed as the primary harvesting method. If necessary, centrifugation was then used to increase the slurry concentration to the appropriate level.

3.2.4.1. Natural Settling

Laboratory settling tests for *Tetraselmis* and *Scenedesmus* showed free settling at 35 cm/h to a maximum concentration of 163 kg dw/m^3 and 41 cm/h to 103 kg dw/m^3 respectively (Griffiths *et al.*, 2011). Thus, following the cultivation step, these species could be dewatered in a circular settling pond, 3 m in depth (Benemann & Oswald, 1996; Stephenson *et al.*, 2010). The settling pond was sized according to the observed settling rate and final concentrations according to Stokes' law as described by Equations 3-8 to 3-13 (Richardson *et al.*, 2002).

3-8

3-9

3-10

3-11

where: Y = Liquid/Solid (L/S) mass ratio in feed

U = L/S mass ratio in underflow

C = fractional volumetric feed concentration

C_u = fractional volumetric outflow concentration

ρ_L = density liquid (kg/m^3)

ρ_s = density solid (1070 kg/m^3 (Henderson *et al.*, 2008))

3-12

3-13

where: A = area of settling pond (m^2)

Q_0 = inlet flow rate (m^3/h)

u_c = settling speed (m/h)

Rotating flight scrapers would be used to transfer algae to a central hopper at 0.8 W/m^2 of pond area (Liu & Liptak, 1997; Stephenson *et al.*, 2010). In the base case, for *Scenedesmus sp.*, the

resultant slurry was then pumped through to centrifugation. For *T. suecica*, the final concentration was considered sufficient for oil extraction without prior centrifugation. The supernatant would then be recycled to the cultivation stage with an assumed 10% purge.

3.2.4.2. Flocculation

In the case of *C. vulgaris*, where free settling was too slow, biomass was flocculated with aluminium sulphate (Molina Grima *et al.*, 2003). It was assumed that the addition of 0.5 g/m^3 of flocculent and 300 g/m^3 of lime (to pH 11) would flocculate 90% of the algal biomass (Lardon *et al.*, 2009). Following mixing at 100 W/m^3 for 1200 s (Sinnott, 1999), the slurry was transferred to a settling tank as described above. A settling rate of 2 m/h to a final concentration of 20 kg/m^3 was assumed (Lardon *et al.*, 2009).

3.2.4.3. Centrifuge

For *C. vulgaris* and Scenedesmus *sp.*, where settling did not achieve the concentration to 15-20% solids as required for oil extraction, centrifugation was employed. Several types of centrifuge employed in algal separations are shown in Table 3-4. Typically, disc-stack centrifuges deliver g-forces in the range of 7000-14000 g and decanter centrifuges in the range of 1000 – 5000 g (Perry & Green, 1997). Each centrifuge was assumed to concentrate the slurry to 200 kg/m^3 at an electrical efficiency of 93% as described by Sánchez Mirón *et al.* (2003) for a continuous centrifuge running at 6300 g. Biomass recovery of 95 % was assumed (Benitez, 2002). The modern equivalent assumed in this study would be a direct drive disc-stack centrifuge, which would treat 10 m^3 algal slurry per hour and require electricity at a rate of 0.78 kWh/m^3 algal slurry entering the centrifuge (Piek, 2010).

Table 3-4 Comparison of centrifugal methods for the concentration of microalgal biomass (Molina Grima *et al.*, 2003; Richmond, 2004b)

Machine and make	Operational mode	Final suspended solids, %	Feed suspended solids, %	Energy, kWh/m^3
Self-cleaning, disc-stack; Westfalia	Suspension continuous; concentrate discontinuous	12	0.2 – 20	1
Nozzle discharge; Westfalia	Continuous	2–15	0.1	0.9
nozzle-disc, Alfa Laval	Intermittent discharge	15	1-30	1.25
Decanter bowl; Westfalia	Continuous	22	5-8	8

3.2.5. Oil extraction

Solvent-based oil extraction was modelled according to Stephenson *et al.* (2010), using a counter-current cascade of mixer-settlers followed by solvent recovery and oil refining steps.

3.2.5.1. Mixer-Settlers

In order to extract the algal oil from the cells into an organic solvent, agitation is required to provide adequate contact between the solvent and aqueous suspension, prior to phase separation. Stephenson *et al.* (2010) showed that using a countercurrent cascade of mixer-settlers is marginally preferable to extraction decanters. Although good results have been achieved using chloroform and methanol as the solvent (Griffiths, 2009), hexane was preferred in this study due to its lower toxicity. It was assumed that hexane supplied at half the volumetric flowrate of algal slurry would remove 80% of the lipids and chlorophyll contained in the biomass. The cell debris and remaining lipid fraction was sent to the anaerobic digester.

Oil extraction was modelled according to Benitez (2002). The algal slurry passes through a countercurrent cascade of five mixer-settlers, each with a residence time of 600 s and a vessel height to diameter ratio of 1. Each vessel contains 4 vertical baffles with a width one twelfth that of the vessel diameter (D_v). Mixing is provided by a flat blade turbine, with diameter (D_i) one third of D_v with 6 blades. As the algal slurry has the greater volumetric flowrate, it is dispersed in the solvent phase so as to create a larger interfacial area. The power requirement of the mixer (P_M) can be calculated by solving Equations 3-14 to 3-17 simultaneously (Benitez, 2002).

3-14

3-15

3-16

3-17

where: N_{min} = minimum speed of impeller rotation (Hz)

N = impeller rotational speed (Hz) (= 1.1 x N_{min})

P_o = Power number (equal to 5.7 for the impeller described above if the impeller Reynolds numbers greater than 10^4)

σ = interfacial tension between phases (J/m^2)

ρ_M = density of 2 phase mixture (kg/m^3)

μ_M = viscosity of 2 phase mixture (Pa.s)

ρ_d and μ_d = density and viscosity of dispersed phase

μ_c and ρ_c = density and viscosity of continuous phase

ε_d and ε_c = holdup in dispersed and continuous phase ($\varepsilon_d/\varepsilon_c = Q_d/Q_c$)

Literature values were taken for σ, ρ_c and μ_c (Sinnott, 1999). The value for μ_d was taken as 0.001 Pa.s (Stephenson *et al.*, 2010; Taylor, 2009). Assuming a motor efficiency of 90%, each mixer was calculated as being agitated at 5.3 Hz and 3.4 kW/m^3 mixer volume. At the end of the mixer-settler cascade, the solvent-rich phase would be sent to a desolventising step and the aqueous phase sent to anaerobic digestion.

3.2.5.2. Solvent Recovery

Following extraction, the solvent stream would be sent to a stripper column for separation. Stephenson *et al.* (2010) modelled this step applying the Peng-Robinson equation of state for vapour-liquid equilibria showing hexane recoveries of > 99.5 %. Here, it was assumed that the tops would be condensed by heat exchange with the inlet stream so as to maximise efficiency and heat the inlet from 25 to 60 °C. Thus, the total heat requirement for the boiler was taken as 1.6 kJ/kg lipid.

3.2.5.3. Oil Refining

The oil refining process was assumed to be identical to that used in the production of first generation biodiesel from oil-seed rape. This involved the addition of phosphoric acid (80 wt% H_3PO_4 in water) and sodium hydroxide (50 wt% in solution). Heat, electricity and water requirements were taken as 540 kJ/kg, 108 kJ/kg and 0.108 m^3/kg unrefined oil respectively. The process was said to remove 98 % chlorophyll, 1 % lipids and 50 % residual hexane (0.25% of hexane input), which would be sent to the anaerobic digester (Stephenson *et al.*, 2010).

3.2.6. Biodiesel Production

For the production of biodiesel, inventory data generated in a previous study was applied (Harding *et al.*, 2008). In this study, an enzyme catalyst was shown to have an environmental advantage over the conventional chemical catalyst, and is used in this investigation. Although the enzyme catalysed

route exhibits lower rates, it is not restricted by the water content or level of free fatty acids in the oil. The ester yield is high and saponification reactions do not occur, while achieving similar conversions to the alkali catalysed option. In addition, chemical catalysts require neutralisation before removing glycerol, which results in salt formation, contaminating the glycerol. With lipase catalysis, this is not required, thus simplifying the recovery and purification of the glycerol byproduct.

Flow-sheets and inventory data for the production of 1000 kg of biodiesel and the required lipase are shown in Appendix A.1.1.

3.2.7. Anaerobic Digestion

Theoretically, the production of methane, ammonia and carbon dioxide via anaerobic digestion can be calculated stoichiometrically as shown in Equation 3-18 (Sialve *et al.*, 2009).

3-18

Thus, the specific yield of methane, B_0 (L/g VS) can be calculated according to Equation 3-19, where V_m is the molar volume of methane. As a simplification, ash content is assumed to be negligible.

3-19

The ratio of methane to carbon dioxide in the gas, r_G is then calculated from n, the average carbon oxidation state in the substrate.

3-20

3-21

Assuming 20 days retention time, efficiency of COD destruction was modelled according to Sampson *et al.* (1986) based on the volatile solids concentration (kg VS/m^3) as shown in Table 3-5.

Table 3-5 COD destruction relative to volatile solids concentration for 20 days retention time (Samson, 1986).

kg VS/m^3	20	40	60	80	100
COD destruction %	49.9	46.3	42.4	37.8	26.3

Phosphoric acid, NaOH and urea were required at 0.9 x 10^{-3} kg/kg, 6 x 10^{-4} kg/kg and 2.7 x 10^{-3} kg/kg COD removed respectively and the digester mixed at 10 W/m^3 (Aden *et al.*, 2002). The reaction is considered sufficiently exothermic that no external heating is required. The digestate from anaerobic digestion is proposed as a useful soil conditioner (Jury *et al.*, 2010). As there is minimal information about the quality of this fertiliser it is considered a neutral product that does not affect the assessment in the base case.

It was assumed that the methane produced would be sent to a gas-fired power station using compressors, with losses in the distribution system of 0.07 bar. The power station was assumed to operate at an electrical efficiency of 60%, based on a 50 Hz combined cycle platform (Stephenson *et al.*, 2010).

3.3. Species Comparison/Growth Study

The algal process model was used to investigate *Chlorella vulgaris*, *Scenedesmus sp.* and *Tetraselmis suecica* grown under identical nitrogen starved cultivation conditions in vertical tubular airlift reactors (ALRs) on a laboratory scale. This study aimed to investigate the effect of microalgal species-specific growth characteristics and composition on the energetic and environmental benefit of algal oil for biodiesel. Particularly of interest is the impact of lipid productivity and the trade-off between reactor biomass concentration and productivity.

These species were chosen following a laboratory investigation of eleven different microalgal species, grown under high and low nitrogen conditions (Griffiths, 2011). The study aimed to assess each species' suitability for the production of microalgal biodiesel. *Chlorella vulgaris* has been widely studied in this regard (Chisti, 2007; Chisti, 2008; Illman *et al.*, 2000; Lardon *et al.*, 2009; Scragg *et al.*, 2002; Sheehan *et al.*, 1998; Stephenson *et al.*, 2010; Ugwu *et al.*, 2005). In the laboratory investigations, it showed promise in its ability to reach relatively high biomass concentrations, productivities and lipid contents. While not as widely mentioned in the literature, *Scenedesmus sp.* was arguably the most promising species of those cultured. Notably, it demonstrated the highest instantaneous lipid productivity (50 mg/L/day), a factor highlighted as a key desirable characteristic for biodiesel production (Griffiths & Harrison, 2009; Rodolfi *et al.*, 2009). Lastly, while only achieving fairly modest lipid productivities, *Tetraselmis suecica* showed high instantaneous biomass concentrations and productivities. Of particular interest, was the superior settling ability of this

species after growth under nitrogen deprivation. These three species were consequently investigated using the algal process model.

Growth rate, biomass concentration, lipid and chlorophyll contents were taken from laboratory data over the full growth cycle (Griffiths, 2011). This study is described and the data presented in Appendix A.1.2. Typical initial biochemical (lipid, protein, carbohydrate and chlorophyll) and CHON compositions of the biomass were taken from Becker (1994). CHON analysis of the final dry biomass was then correlated for the balance of growth cycle. This was done according to conversions based on the gross elemental composition of biochemical classes for algae and cyanobacteria as reported by Geider (2002).

Apart from the differences in growth characteristics and composition, the three species were also dewatered by different methods. *C. vulgaris* was flocculated using aluminium sulphate and settled as described in Section 3.2.4.2. *Scenedesmus* and *T. suecica* both demonstrated acceptable settling rates during laboratory investigations and were thus assumed to be settled naturally as described in Section 3.2.4.1. In the cases of *C. vulgaris* and *Scenedesmus*, the resultant slurry was then further concentrated by centrifugation. In the case of *T. suecica,* an acceptable concentration was achieved following settling, hence centrifugation not required. The results of this study are given in Chapter 4.

3.4. Reactor Study

The algal process model was used to investigate the growth of *Phaeodactylum tricornutum* in raceway ponds, horizontal tubular airlift reactors (HTRs) and vertical tubular airlift reactors (VTRs) on a large scale. This study aimed to investigate the effect of reactor configuration on the energetic and environmental benefit of algal oil for biodiesel. Given that different reactors allow for higher biomass concentrations and productivities, the trade-off between reactor energy input and biomass productivity is of particular interest.

P. tricornutum was studied extensively during the Aquatic Species Programme (ASP) and was noted as having a high overall productivity (Sheehan *et al.*, 1998). Experiments showed that while the species did reach higher lipid contents under N-deficient conditions, the highest lipid productivities were observed under N-replete conditions. Importantly, growth data could be obtained for the growth of this species in the reactor configurations considered in this study. The biomass concentration and productivities for each reactor and the biochemical composition of the biomass are described in Section 5.2.1. Dewatering is done as for *C. vulgaris*, by the addition of lime to pH 11.

Descriptions of the modelled reactor configurations are given below.

3.4.1. Raceway Ponds

Large scale cultivation of microalgae usually takes place in raceway ponds. Typically, these ponds have an area of 0.5 to 1 ha, a depth of 0.2 to 0.3 m and a width of 10 m. Mixing is provided by a paddlewheel to give a mean culture velocity of 0.3 m/s. At 25°C, this corresponds to a Reynolds number of 85000. This turbulent mixing prevents thermal stratification and maintains the algae in suspension (Anderson, 2005). The assumed typical design parameters for the raceway pond considered in this study are thus shown in Table 3-6. CO_2 was assumed to be supplied from a counter current carbonation sump of depth, 3 m as found optimal by Stephenson *et al.* (2010).

Table 3-6 Design parameters for raceway ponds assumed in this study

Depth	m	0.3
Length	m	150 (x2)
Width	m	10
Hydraulic mean diameter	m	0.285
Pond volume	m^3	994
Mean liquid velocity	m/s	0.3
Reynolds number	-	85000
Paddle wheel power	W	1585
Power for gas provision	W	422.3

The power required to operate the paddle wheel, P_{PW} can be determined using Equation 3-22 as described by Anderson (2005).

3-22

where: Q_L = volumetric flow rate (m^3/day)

ρ_L = liquid density (kg/m^3)

h = head loss (m)

η_{PW} = paddle wheel efficiency

For paddlewheels operating over a flat bottom, a typical efficiency of 17% can be assumed. Head loss originates from friction, h_1 and in the carbonation sump, h_2. Head loss due to friction is calculated from Manning's equation (3-23), with n taken as 0.012, an estimated value for flow over smooth plastic on granular earth (Anderson, 2005).

3-23

where: j_l = superficial liquid velocity (m/s)

n = Manning's roughness coefficient, taken as 0.012

L_c = channel length (m)

R_h = mean hydraulic diameter (m)

It was assumed that the countercurrent carbonation sump would only operate during daylight hours and would transfer 70% of the carbon dioxide in the flue gas to the culture. While this is more complex in reality, the results of Wiessman and Goebel (1987) of the Aquatic Species Program support this conservative estimate. The head loss in the carbonation sump is calculated using Equation 3-24, with an additional 1% of the total calculated added to account for minor frictional losses (Weissman & Goebel, 1987).

3-24

where: D_s = distance from sparger level to liquid outflow (m)

The head loss in the carbonation sump is dependent on the gas hold-up, ε_g which can be calculated from Equation 3-25. The width of the sump was set to achieve a liquid velocity in the sump of 0.1 m/s. An average bubble rise velocity of 0.3 m/s and pressure correction factor of 0.89 for subsurface depth of 3 m can be assumed (Weissman & Goebel, 1987).

3-25

where: Q_G = volumetric gas flowrate (m^3/s)

C_{PE} = pressure correction factor

A_s = cross-sectional area of sump (m^2)

$U_{b,\infty}$ = average bubble rise velocity (m/s)

Gas was compressed using an isentropic compressor with an efficiency of 80%, assuming pressure losses in the distribution system of 0.7 bar and pressure losses over the sparger of 0.7 bar. During the culture process, freshwater is added regularly to compensate water loss and avoid salt build-up due to evaporation. The annual balance between rainfall and evaporation was assumed to be 4.4 mm/day water loss, as for the Orange River (Basson *et al.*, 1997).

3.4.2. Horizontal Tubular Reactor

The horizontal tubular photobioreactor in this study was modelled according to that described by Molina *et al.* (2011). As shown in Figure 3-3, the airlift driven tubular photobioreactor consists of an airlift system and solar receiver. An airlift pump circulates the culture from the airlift system to the solar receiver, where the majority of photosynthesis occurs. As the culture circulates, oxygen is accumulated until it reaches the degassing zone at the top of the airlift, where accumulated oxygen can be stripped by air.

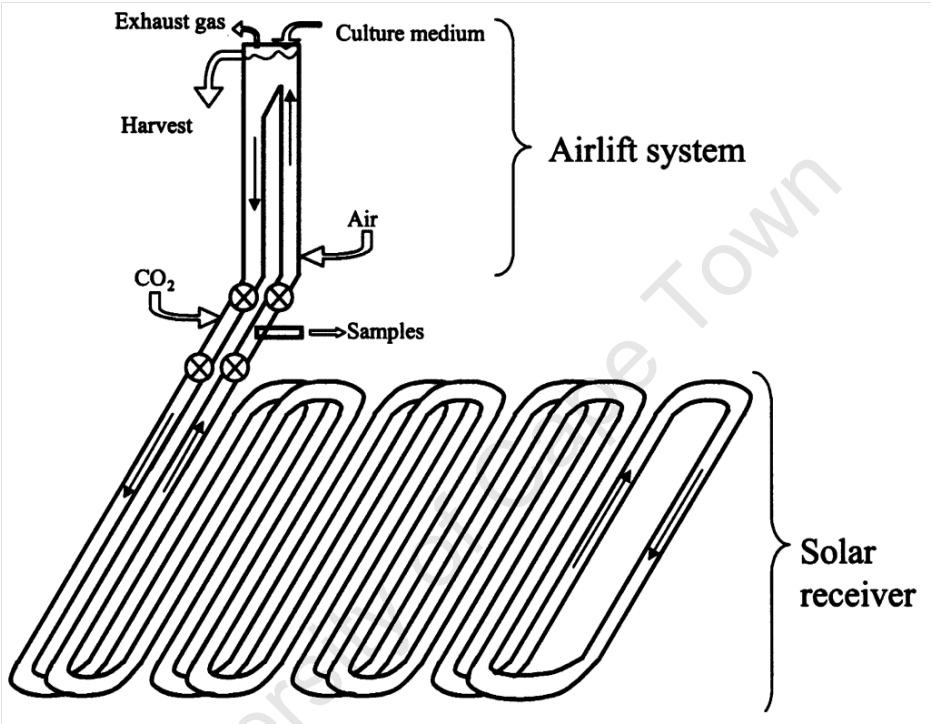

Figure 3-3 Airlift driven tubular photobioreactor (Molina *et al.*, 2001)

The required liquid velocity (v_L) to provide adequate turbulence for optimal cell growth without settling has been reported as 0.5 m/s (Molina *et al.*, 2001). This velocity is thus assumed here, accompanied by a typical Reynolds number of 25000.

Table 3-7 Design parameters for horizontal tubular photobioreactors assumed in this study

Tube internal diameter	m	0.053
Tube length	m	95
Riser height	m	4.4
Reactor volume	m^3	0.23
Mean liquid velocity	m/s	0.5
Reynolds number	-	85000
Power	W	22

The maximum length (L_{max}) of continuous tubing for any given culture velocity is restricted by the upper limit of dissolved oxygen concentration, $[O_2]_{out}$ and can be calculated using Equation 3-26.

3-26

where: j_L = superficial liquid velocity (m/s)

$[O_2]_{out}$ = maximum acceptable concentration of dissolved oxygen in the culture, taken as 300% of air saturation

$[O_2]_{in}$ = concentration of dissolved oxygen at the inlet of the solar receiver, taken as 100% of air saturation

R_{O2} = volumetric rate of oxygen generation in the tube, taken from the biomass productivity

The velocity of the fluid in the tubing is driven by an airlift pump and is largely determined by the geometric configuration of the circulation loops and the difference in gas hold-up in the riser and downcomer. The relationship, as established by Chisti (1989), is represented in the following equations which can be solved simultaneously to determine the superficial gas velocity, j_G, needed to provide the required liquid velocity.

3-27

where: K_T & K_B = frictional loss coefficients in the riser and downcomer zones of the airlift loop

h_r = height of riser (m)

A_r & A_d = cross-sectional areas of the riser and downcomer (m^2)

ε_r = gas hold-up in riser

ε_d = gas hold-up in downcomer (assumed to be 0 as no bubbles recirculate)

Generally in airlift devices, the energy loss in the riser (top), K_T is much smaller than that in the downcomer (bottom), K_B and thus, K_T can be neglected. This is particularly true in the case of the loop configuration, where the bottom zone includes both the downcomer and solar receiver (Molina *et al.*, 2001). K_B was calculated according to the empirical formula for continuous flow in a smooth pipe:

___ **3-28**

where: Re = Reynolds number

L_{eq} = equivalent length of loop (straight length plus additional pump bend length) (Appendix A.2)

As it is assumed that no bubbles recirculate, $\varepsilon_d = 0$. Hence, considering this and neglecting K_T, Equation 3-27 becomes:

_____

_____ **3-29**

___

The gas hold-up in the riser, ε_r depends on the superficial velocities of the gas and liquid in the riser zone and was calculated using the Zuber and Findlay (Richardson *et al.*, 2002) equation (1965):

_____ **3-30**

_____

where: j_G & j_L = superficial velocities of the gas and liquid in the riser

C_α = ratio of superficial gas velocity to total superficial velocity in riser

C_β = characteristic parameter, taken as 1.1

$U_{b,\infty}$ = bubble rise velocity, taken as 0.3 m/s (Molina *et al.*, 2001)

C_β is a function of the radial velocity profile that typically varies from 1.0 to 1.3 as the flow changes from turbulent to laminar (Molina *et al.*, 2001). These equations can then be solved simultaneously to determine flowrate of gas to provide the desired liquid velocity of v_L = 0.5 m/s, given that

3-31

The energy required to compress the gas can then be calculated from Equation 3-32 ():

where: W = work done to compress the gas (W)

P = required compression, considering the static head in the riser and losses of 0.07 bar in the distribution system sparger respectively

y = ratio of heat capacities

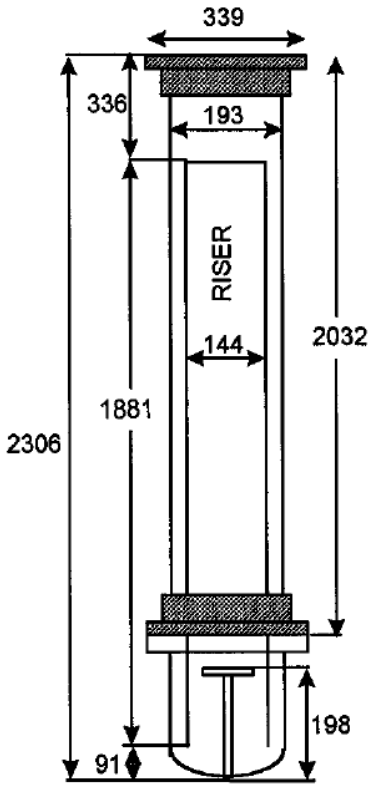

Figure 3-4 Schematic diagram of concentric draft tube ALRs showing vessel dimensions (cm) and air sparger details (Mirón *et al.*, 2000)

3.4.3. Vertical Tubular Reactor

To provide an appropriate scale up to the laboratory concentric draft tube ALRs described in Section 3.2.3, reactors described by Mirón *et al.* (2000; 2003) were modelled and the equations described in Section 3.2.3 used to determine power requirements. Reactor geometry and other specifications are described in Table 3-8. Miron *et al.* found cultures of *Phaeodactylum tricornutum* to reach a steady state concentration of 1 kg/m^3 and a biomass productivity of 0.3 kg/m^3/day when the aeration velocity was 0.01 m/s. At higher superficial aeration velocities, cells were found to be susceptible to aeration associated hydrodynamic stress. Considering an aeration velocity, U_G of 0.01 m/s, the

energy requirements for the reactor can be calculated as for the laboratory tubular reactors described earlier, using Equation 3-3.

Table 3-8 Selected design parameters for concentric draft tube ALRs assumed in this study

Draft tube diameter	m	0.144
Draft tube length	m	1.881
Reactor diameter	m	0.193
Total reactor length	m	2.306
Distance from bottom to base of draft tube	m	0.091
Ratio of riser area to downcomer area	-	1.24
Liquid height	m	2.0
Liquid volume	m^3	0.06
Aeration velocity	m/s	0.01
Superficial liquid velocity	m/s	0.108
Reactor power required [i]	W/m^3	98.6
Total power required [ii]	W/m^3	159.4

i. Compression power to overcome static head
ii. Compression power to overcome static head as well as losses in the distribution system and over the sparger.

3.5. Life Cycle Assessment

Life Cycle Assessment (LCA) was employed as a means of evaluating the environmental burdens associated with the cradle-to-gate life cycle of this process. The first two phases of the LCA were completed prior to the analysis phase of the project and are listed in Sections 3.5.1 and 3.5.2.

3.5.1. Goal and Scope Definition

As stated in Chapter 1, it is one of the goals of this thesis to examine the effect of changes to the reactor phase though two LCA studies, in a South African context. The specific goals of each study are given in Chapters 4 and 5 respectively.

The functional unit is defined as the cradle-to-gate production of 1000 kg of algal biodiesel, having a calorific value of 37.8 MJ/kg. The system was defined as cradle-to-factory-gate production of algal biodiesel as shown in Figure 3-1, including the extraction and production of raw materials. Boundaries exclude facility construction and dismantling. This was done, as a result of the findings of previous algal biodiesel LCAs as discussed in Section 2.4.1, where the building and recycling of the facility were found to only contribute minimally in all impact categories except for land use (Clarens *et al.*, 2010; Lardon *et al.*, 2009).

As shown in Chapter 2, the environmental burden of algal biodiesel production is generally dominated by impacts related to electricity and fertiliser production. As 88% of South African

electricity is coal based, this dominance is particularly pronounced. Accordingly, following impact categories are of interest:

- Abiotic depletion (kg Sb eq.)
- Acidification (kg SO_2 eq.)
- Eutrophication (kg PO_4^{3-} eq.)
- Global warming (kg CO_2 eq.)

The abiotic depletion and global warming impact categories well represent the energy related impacts, through the depletion of fossil reserves and emission of greenhouse gases. Both of these are key drivers in biofuel studies. The acidification and eutrophication impact categories serve to link fertiliser and energy related impacts and are thus of interest. Impact categories omitted in the present study include photochemical oxidation and toxicity impact categories, which largely mirror the energy related impacts. Additionally, at the first order level of mass balances conducted, the accuracy and precision regarding use and environmental emissions of potentially toxic substances (such as solvents and other ancillary materials) was deemed insufficient for impact assessment predictions. Improvements in this regard were deemed to go beyond the scope of this study, but represent a topic that could be taken up in a future study. Ozone layer depletion is irrelevant as there are no refrigeration cycles in the process and is thus omitted.

The foreground system, analysed in the energy study, includes all processes directly used to produce biodiesel, shown in Figure 3-1. The background system, analysed in the LCA, is comprised of the processes that provide the materials and energy used by the foreground system.

Burden allocation is a key issue in LCA. Glycerine is the only by-product of biodiesel production in the present study and was accounted for according to the substitution method, which involves the expansion of system boundaries to account for by-product impacts. This was done in accordance with the ISO guidelines, which recommend substitution over allocation where possible (Guinée, 2002).

3.5.2. Life Cycle Inventory Analysis (LCI)

Data collection was necessary to quantify all inputs to the process in terms of energy and resources (solid, liquid and gaseous) as well as all products and waste. Growth data was gained experimentally (Chapter 4) and from literature (Chapter 5) and used as inputs to flow-sheet model described in Sections 3.1 to 3.4. Outputs were validated through material and energy balances and reported in terms of the functional unit.

The LCA of the different biodiesel production models was performed using the LCA software package Simapro v7.2® (PRé Consultants B.V. 2010). The LCA included all raw materials, agricultural inputs in addition to the process represented in Figure 3.1 towards the final biodiesel product. Electricity production was based on the South African Energy mix (Harding, 2009).

3.5.3. Life Cycle Impact Assessment (LCIA) and Interpretation

The LCI results generated in the flow-sheet model were used as input to the Life Cycle Impact Assessment (LCIA) to assess the environmental impacts of the data. This was done using the CML 2 Baseline 2000 assessment v2.1 methodology. This methodology meets all the mandatory requirements of the ISO standards and has been widely used (Collet *et al.*, 2010; Harding *et al.*, 2008; Lardon *et al.*, 2009; Panichelli, 2009). The impact categories related to energy and fertiliser production, mentioned in Section 3.5.1, are of particular interest and form the basis for the choice of this method.

Wherever possible, the LCA database, Ecoinvent v1.3 (Swiss Centre for Life Cycle Inventories 2007) was used. At each stage of the assessment, an interpretation was conducted.

4. Life-Cycle Comparison between Species of Microalgae

4.1. Introduction

Technically, microalgae have the potential to compete with fossil fuels as a source of biodiesel. However, there are several factors which currently hold back large-scale production (Chisti, 2007). One of the major disadvantages is the low biomass concentrations achieved in algal cultures and the resultant low volumetric oil concentration. This translates into a requirement for large reactor volumes which, in turn, translates into a high power requirement. In combination with the small size of algal cells, the dilute concentration of algae contributes to higher downstream processing costs as cheaper harvesting methods such as filtration are effectively eliminated in such large volumes (Li, 2008).

Lipid productivity has been shown to be a desirable indicator over growth rate and lipid content (Griffiths & Harrison, 2009) and to vary from species to species. Thus, one of the most important decisions informing the design of a microalgal biodiesel production system is the choice of species. Factors affecting this choice include the lipid content, biomass concentration, biomass and lipid productivity and ease of downstream processing. This is a challenging decision to address from the literature at present. While the data are available across most species, much of these data are not comparable due to inconsistencies in scale, reactor type and environmental conditions (Griffiths & Harrison, 2009). Furthermore, the stress conditions reported for algal oil induction are not typically consistent.

To this end, the growth and initial harvesting of *Chlorella vulgaris*, *Scenedesmus* sp. and *Tetraselmis suecica* were investigated under identical nitrogen starved cultivation conditions in airlift reactors on a laboratory scale (Griffiths, 2011). Justification for the choice of these species is given in Section 3.3. A flow-sheet of a virtual biodiesel refinery was then created from reasonable assumptions in line with current large scale production (Figure 3.1). Material and energy balances were generated via the process model described in Sections 3.2 and 3.3 using laboratory data for the growth of all three species and initial concentration steps. The impact of species choice was investigated using both the energetic balance and comparative life cycle assessment (LCA) to determine the overall environmental impact of the production of 1000 kg of biodiesel.

The goal of this LCA is to assess the chosen process flow-sheet (Figure 3-1) for the production of biodiesel from microalgae and to examine the effect of species choice on the environmental impact of the process. While biodiesel is the dominant product of this flow-sheet, biogas from anaerobic digestion of waste algal biomass contributed to the energy requirements of the process.

4.2. Methodology

The three species chosen were investigated experimentally under defined low nitrogen conditions in the airlift reactor over a 10 day period to ensure comparative data. The growth curve and lipid production data are presented in Appendix A.1.2 in terms of instantaneous biomass concentrations, productivities and biochemical and elemental compositions at specific time points. Experimental conditions are also given in Appendix A.1.2. Settling data collected during this study are given in Section 3.2.4.1.

Figure 4-1 outlines the steps taken in order to compare the three species on a life cycle basis. For each set of conditions recorded, a continuous culture algal and lipid production system was simulated and the model used to calculate the material and energy inputs and outputs required for the production of the functional unit of biodiesel. The output of this model, across the range of process conditions informed by the experimental study, was then used in the comparison of energy requirement and productivity. This allowed selection of the conditions for minimum fossil energy input for each species. The simulation model was then used to carry out sensitivity studies on reactor operation and setup to refine operating conditions. Inventory data were generated using the simulation model at the most favourable culture conditions and with a hypothetically optimised reactor setup. This was then used for an LCA comparison of the species.

The use of a low-nitrogen fertiliser mix and wet extraction scenario have been shown to result in lower impacts (Lardon *et al.*, 2009). In accordance with these findings, low nitrogen fertiliser mix and wet extraction have been employed in this flow-sheet and flue gas with a CO_2 content of 12.5% assumed to provide the required carbon.

An additional process scenario whereby soil conditioner from the anaerobic digestion digestate (stream 24 in Figure 3.1) was substituted with the equivalent nitrogen and phosphorous fertilisers was investigated to assess its effect on the process burdens.

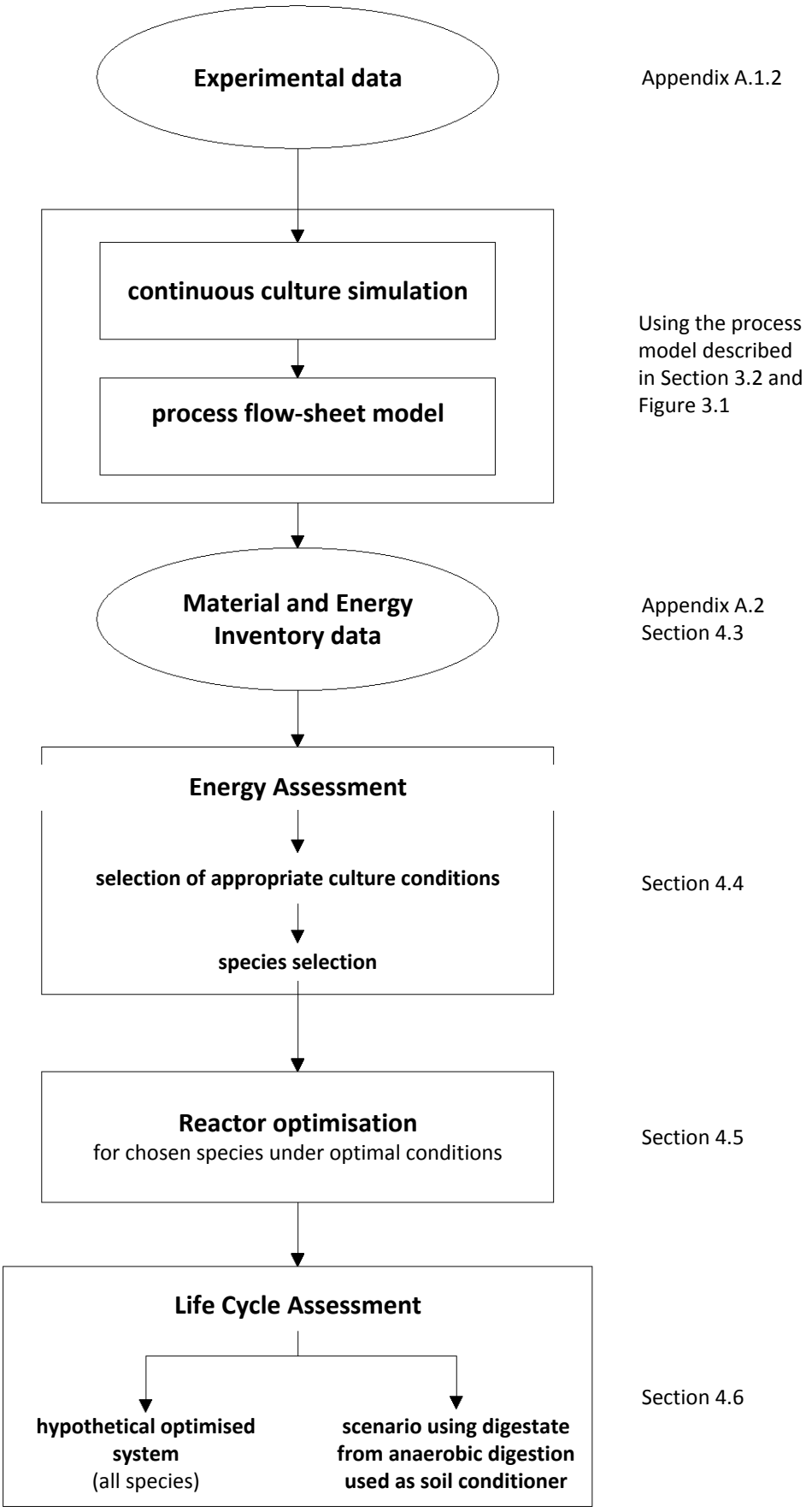

Figure 4-1 Flow-diagram illustrating the procedure followed to achieve the results of Chapter 4

4.3. Material and Energy Inventory Data

For any set of conditions investigated, the process simulation model described in Section 3.2 was used to generate the composition of each of the streams in Figure 3-1. An example of this tabulated is given in Appendix A.2 for *Scenedesmus* sp. Such stream tables were then used to create inventory tables as shown in Table 4-1 for all three species, at the point of maximum lipid productivity. Table 4-2, also generated by the model, shows the contributions of the individual process units. These data are used in the energy analyses in Section 4.4.2 and as input to the LCA in Section 4.6.

Table 4-1 Material and energy inventory data for the three species at the point of maximum lipid productivity

	C. vulgaris		*Scenedesmus sp.*		*T. suecica*	
Biomass Concentration (g/L)	0.103		0.63		0.83	
Biomass Productivity (g/L/day)	0.27		0.37		0.45	
Lipid content (%)	0.22		0.18		0.071	
	Input kg/day	Output kg/day	Input kg/day	Output kg/day	Input kg/day	Output kg/day
Water	12300000	12300000	2620000	2620000	4730000	4730000
Cells	0	123	0	236	0	306
Ammonium nitrate	1640	950	2120	1160	4440	2620
Triple super phosphate	681	393	878	480	1840	1080
Potassium chloride	288	0	372	0	779	0
Aluminium sulphate	30.6	30.6	0	0	0	0
Hexane	46.9	0	57.3	0	178	0
Phosphoric acid	13.9	0	19.5	0	37.2	0
Caustic soda	87.8	0	125	0	244	0
Methanol	111	2.4	111	2.4	111	2.4
Biodiesel	0	1000	0	1000	0	1000
Glycerol	0	106	0	106	0	106
Cooling water	120	120	120	120	120	120
Steam	1540	0	1540	0	1540	0
Glucose	5.76	0.0576	5.76	0.0576	5.76	0.0576
Yeast	3.84	0.192	3.84	0.192	3.84	0.192
Precipitating chemical	2.4	2.4	2.4	2.4	2.4	2.4
CO_2	12400	81.8	17800	134	31400	205
Phosphates	0	1.44	0	1.44	0	1.44
Urea	3.78	0	5.47	0	10.8	0
Methane (STP)	0	32.6	0	53.9	0	74.9
Lime (floc)	18400	18400	0	0	0	0
Total Energy (kwh)	43800	0	37200	0	71900	0

Table 4-2 Total energy requirements and material flows through each process unit shown in Figure 3-1 for the three species at the point of maximum lipid productivity

	C. vulgaris		*Scenedesmus sp.*		*T. suecica*	
Unit	Kwh	kg/day	Kwh	kg/day	Kwh	kg/day
Reactor	37500	61500000	35300	13000000	68400	23200000
Settling	228	61500000	250	13000000	525	23200000
Centrifuge	239	319000	56.8	71500	0	130000
Extraction	137	61900	166	53200	492	165000
Solvent recovery	456	10600	456	12600	456	36700
Oil refining	38.8	1440	36.8	1360	38.8	1440
Biodiesel	34.1	2830	34.1	2830	34.1	2890
Lipase	22.1	66.6	22.1	66.6	22.1	66.6
AD	158	51600	194	40900	614	129000
Pumping	5290	197000000	1120	41700000	2010	74800000
AD biogas generated	0	32.6	-450	53.9	-626	74.9

4.4. Energy Assessment

4.4.1. The Relationship between Lipid Productivity and Energy Requirement

Using the experimental data generated by Griffiths *et al.* (2011) presented in Appendix A.1.2, the relationship between biomass concentration, productivity and energy requirement was explored. The process simulation model was used to generate material and energy inventory data for each species at each set of conditions, as described in Section 4.2, under the conditions given in Appendix A.1.2. This data was used to select the optimal conditions for the continuous culture of each species. The process energy requirements for the production of 1000 kg of biodiesel from *Scenedesmus* sp. at various combinations of reactor biomass concentration and productivity are shown in Figure 4-2.

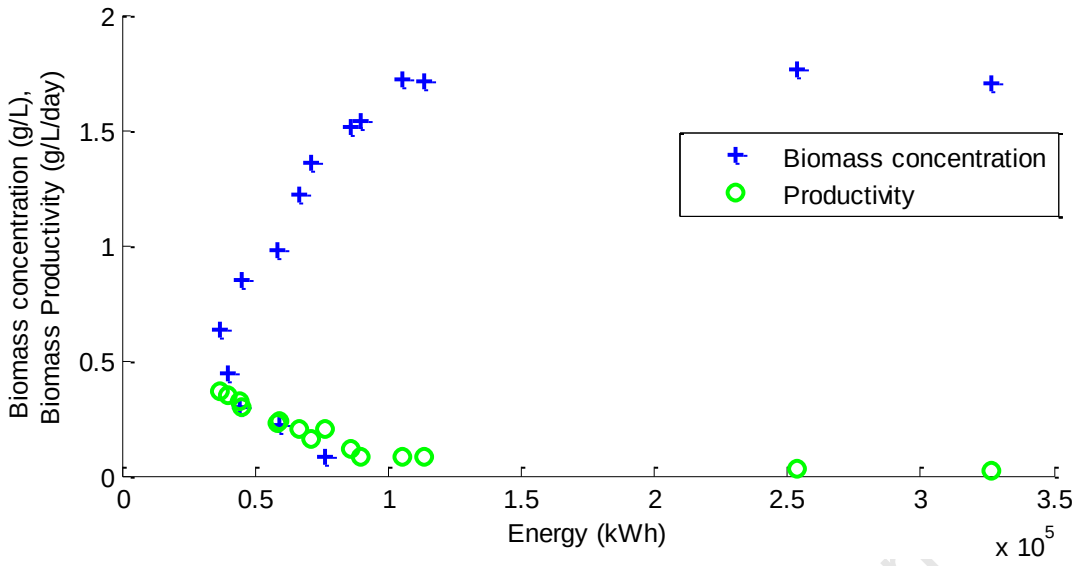

Figure 4-2 Total fossil energy requirements for the production of 1000 kg of biodiesel from *Scenedesmus* sp. at various simultaneously occurring reactor biomass concentration and productivities according to the flow-sheet in Figure 3-1.

In general, the process energy requirement decreases with increasing biomass productivity and decreasing biomass concentration. At higher biomass concentrations, growth rate and thereby productivity is limited by insufficient supply of light to the cells (Richmond, 2004a). At low biomass concentrations, where the productivity is much higher, the process energy is lower as reactors are operated continuously at very low residence times. The low biomass concentration does however result in much greater volumes to be processed downstream. This is discussed further in Section 5.6.2.1.

A correlation can be seen when examining the relationship between lipid productivity and reactor energy in Figure 4-3. The parameters are inversely proportional meaning that the maximum value of lipid productivity observed experimentally corresponded to the lowest overall reactor energy requirement. So, when lipid productivity was higher, a smaller number of reactor volumes were required to produce the same amount of biodiesel. Lipid productivity has been identified as a key variable in the choice of a microalgal species for biodiesel production (Griffiths & Harrison, 2009; Rodolfi *et al.*, 2009). Notably, while the three batch cultures were grown in low nitrogen media, in all cases, the point of maximum lipid productivity occurred early in the growth phase when the culture was relatively dilute and not yet nitrogen deprived. This supports the findings of the Aquatic Species Program, who concluded that lipid accumulation achieved through nitrogen deprivation does not increase lipid productivity, since the higher oil content is more than offset by the lower biomass productivities under nutrient deficiency (Sheehan *et al.*, 1998).

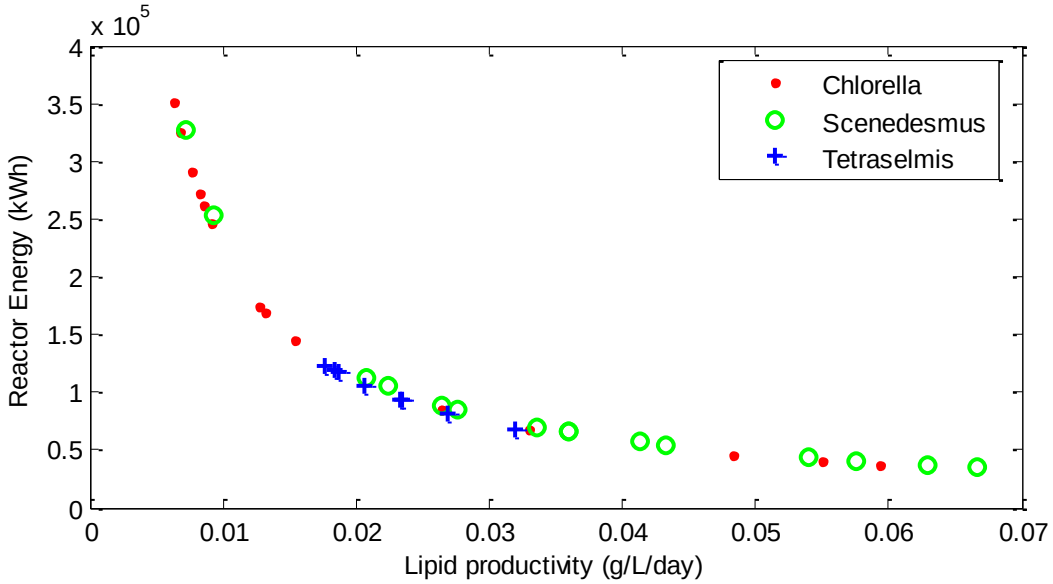

Figure 4-3 Reactor fossil energy requirements (kWh) as a function of lipid productivity (g/L/day) for the production of 1000 kg of biodiesel from *Chlorella vulgaris*, *Scenedesmus* sp. and *Tetraselmis suecica*. Base case scenario using flow-sheet given in Figure 3.1.

4.4.2. System Energy Overview

The growth characteristics and energy requirements for each species at the point of maximum lipid productivity are shown in Table 4-3. Figure 4-4a shows the fossil energy requirements for the various processes involved in the production of biodiesel for these growth characteristics. Figure 4-4b allows for the downstream processes to be viewed more clearly. As all energy generated from biogas is utilised by the system and is not in excess, additional fossil energy is needed. For the success of any renewable energy system, this requirement for non-renewable fuel must be minimised.

Table 4-3 Growth characteristics for the point of highest instantaneous lipid productivity achieved during batch culture of each species and resultant energy requirements if these conditions were held in continuous culture for the production of 1000 kg of biodiesel. Base case scenario for flow-sheet given in Figure 3.1.

	Biomass concentration	Biomass productivity	Lipid content	Lipid productivity	Energy requirements (kWh)		
	g/L	g/L/day	%	g/L/day	Overall	Reactor	DSP
C. vulgaris	0.10	0.27	0.22	0.059	44 000	37 000	6 300
Scenedesmus sp.	0.63	0.37	0.18	0.067	37 000	35 000	1 900
T. suecica	0.83	0.45	0.07	0.032	72 000	68 000	3 600

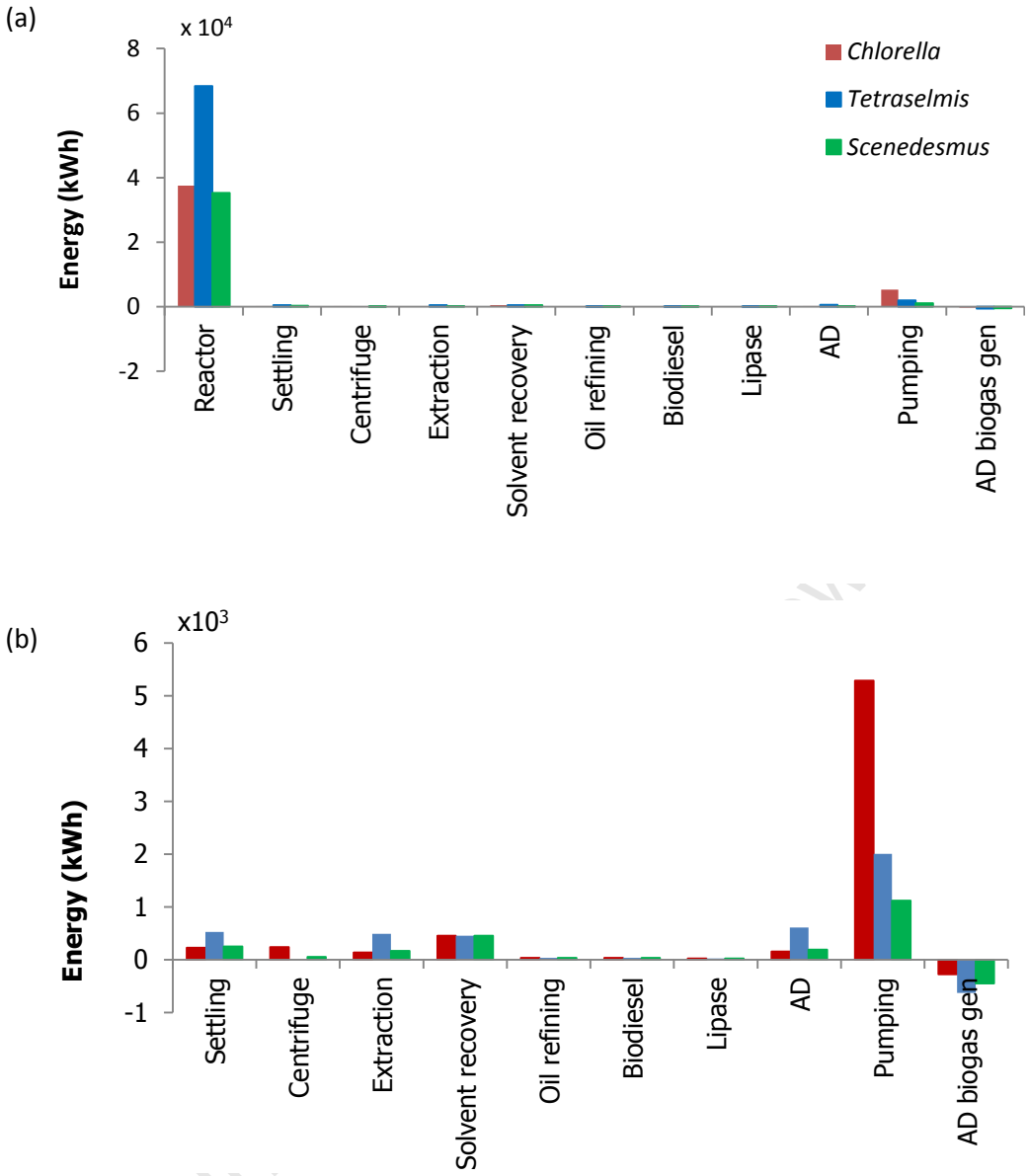

Figure 4-4 (a) Total and (b) downstream fossil energy requirements for the production of 1000 kg biodiesel from *Chlorella vulgaris*, *Scenedesmus* sp. and *Tetraselmis suecica* at the point of highest instantaneous lipid productivity. Base case scenario for flow-sheet given in Figure 3.1..

Figure 4-4a shows clearly that the reactor phase was the dominant contributor to the overall process energy. *T. suecica* had the lowest lipid productivity and thus highest energy requirement in the reactor phase. This is due to its lower lipid content, which implies that a greater amount of biomass is needed to produce 1000 kg of biodiesel. A larger amount of biomass is therefore non-lipid and routed to anaerobic digestion. The increased electricity generated by biogas produced through anaerobic digestion partially offsets the increased energy requirements of the downstream process resulting from processing additional volume. This is observed to a lesser extent with *Scenedesmus* sp., but not with *C. vulgaris* where, due to the low biomass concentration, the energy associated

with pumping was large. Further, *C. vulgaris* presented the highest lipid content; hence a smaller amount of the biomass produced is processed by anaerobic digestion unit.

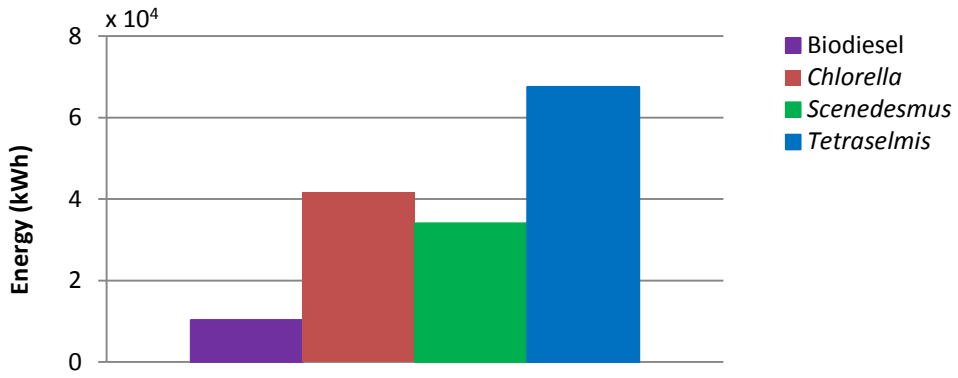

Figure 4-5 Total fossil energy requirements for the production of 1000 kg of biodiesel from *Chlorella vulgaris*, *Scenedesmus* sp. and *Tetraselmis suecica* at the point of highest instantaneous lipid productivity shown against the energy value of the biodiesel produced, assuming a calorific value of 37.2 MJ/kg. Base case scenario.

In Figure 4-5, the relative energy value of the biodiesel product is compared to the fossil energy requirement of the process, using a calorific value of 37.2 MJ/kg for biodiesel. Due to the high reactor energy requirement, none of the species investigated, using the small scale airlift reactor design and supply of compressed CO_2 enriched air, showed a positive energy balance in the base case scenario (Figure 4-5). From Figure 4-5 and Table 4-3, it can be calculated that, in order for *Scenedesmus* sp. to show a positive energy balance, the total reactor energy must be reduced to 8 448 kWh, roughly 23% of the current value. *C. vulgaris* and *T. suecica* would require reactor energies of 4 006 (9.1% of current value) and 6 770 kWh (9.4% of current value) respectively. The required total reactor energy for *C. vulgaris* is lower due its higher downstream energy requirement, largely from pumping due to the dilute concentration of the suspension. To achieve the required reactor energy value for *Scenedesmus* sp. a power input per unit volume of 16.07 W/m^3 would be required. *C. vulgaris* and *T. suecica* would require a power input per unit volumes of 7.17 and 6.65 W/m^3 respectively. This is an order of magnitude less than the current value of 229 W/m^3.

Alternatively, considering Figure 4-3, at the current reactor power input per unit volume, lipid productivities of greater than 0.36, 0.19 and 0.21 g/L/day are estimated to be required by extrapolation for *C. vulgaris*, *Scenedesmus* sp. and *T. suecica* respectively to show positive energy balances at the given biomass concentrations. This extrapolation was done using Figure 4-3, which illustrates the inversely proportional relationship between total reactor energy requirement and lipid productivity. From the 55 species documented in the 2009 review of Griffiths and Harrison, the highest lipid productivity calculated was 0.164 g/L/day with the freshwater species, *Ettlia oleoabundans*. Hence, a balance must be found between increased reactor efficiency and lipid productivity. This is dependent on both the algal species and the reactor configuration. The reactor

configuration is explored more in Chapter 5, where several large scale reactor configurations are investigated.

4.5. Sensitivity study

In this section, two scenarios for reducing the overall reactor energy are investigated using *Scenedesmus* sp. at maximum lipid productivity. Specifically, the effect of connecting an increasing number of reactors in series (at an air flow rate of 2 L/min) is considered to provide a greater reaction volume for the same reactor energy. Secondly, variation in the inlet gas flow rate, and thereby reactor energy input, is investigated. In each case parameters are varied in such a manner that the growth of the algal species is unaffected. Thus, four parameters are observed: mass transfer limitation, dissolved oxygen levels, riser residence time and reactor energy requirements. In Sections 4.5.1 - 4.5.3, the first three parameters are investigated to determine the limits to which airflow rates could be decreased and number of reactors increased before algal growth is affected. The methods of calculation of these parameters are described in Appendix A.3. In Section 4.5.4, the effect on reactor energy within the established limitations is investigated.

It is important to note that the scale of these laboratory reactors is not appropriate for the production of 1000 kg of biodiesel per day. The purpose of this chapter is to compare species grown under identical conditions and to identify key operational variables, not to perform a rigorous design of the reactor. The insights gained by the sensitivity study are then used to give direction to the more in depth reactor study, considering large scale reactor configurations, conducted in Chapter 5.

4.5.1. CO_2 Gas-Liquid Mass Transfer

As explained in Section 1.3.2, the overall mass transfer coefficient, k_La is one of the most important design parameters in an algal photobioreactor. In combination with the partial pressure of CO_2 in the inlet gas, the k_La determines the rate at which CO_2 can be transferred from the gas to the liquid. It is therefore critical that the k_La of the system be able to support the required growth rate. The CO_2 uptake rate required to support the algal growth rate can be calculated from the growth rate on a stoichiometric basis. Equation 1.1 was used to calculate the minimum k_La for this uptake rate, assuming that the residual concentration of CO_2 in the media approached zero. The k_La of a given system is a function of gas hold-up, bubble size, gas flow rate and temperature (Welty *et al.*, 2001). In each case, both the required k_La and the system k_La are plotted. The model was configured to stop the simulation when the system became mass transfer limited and was unable to support the growth rate.

In Figure 4-6 it can be seen that mass transfer limitation set in after ~260 reactors were connected in series. At this point the CO_2 in the inlet gas to the final reactor is no longer sufficient. The gas flow rate of the system remained constant as O_2 is given off at the same rate as CO_2 is taken up during photosynthesis. Thus, the volumetric mass transfer coefficient was unchanged. The system became mass transfer limited when the CO_2 concentration in the inlet gas diminished such that the driving force was insufficient to support the CO_2 transfer rate necessary to satisfy the growth rate. In reality, such a large number of reactors would not be connected in series due to the immense pressure requirement that would result in an unrealistically expensive system. Thus it can be assumed that mass transfer limitation would not be a limiting factor in such a scale up scenario. The energy impact of this pressure requirement is discussed in Section 4.5.4.

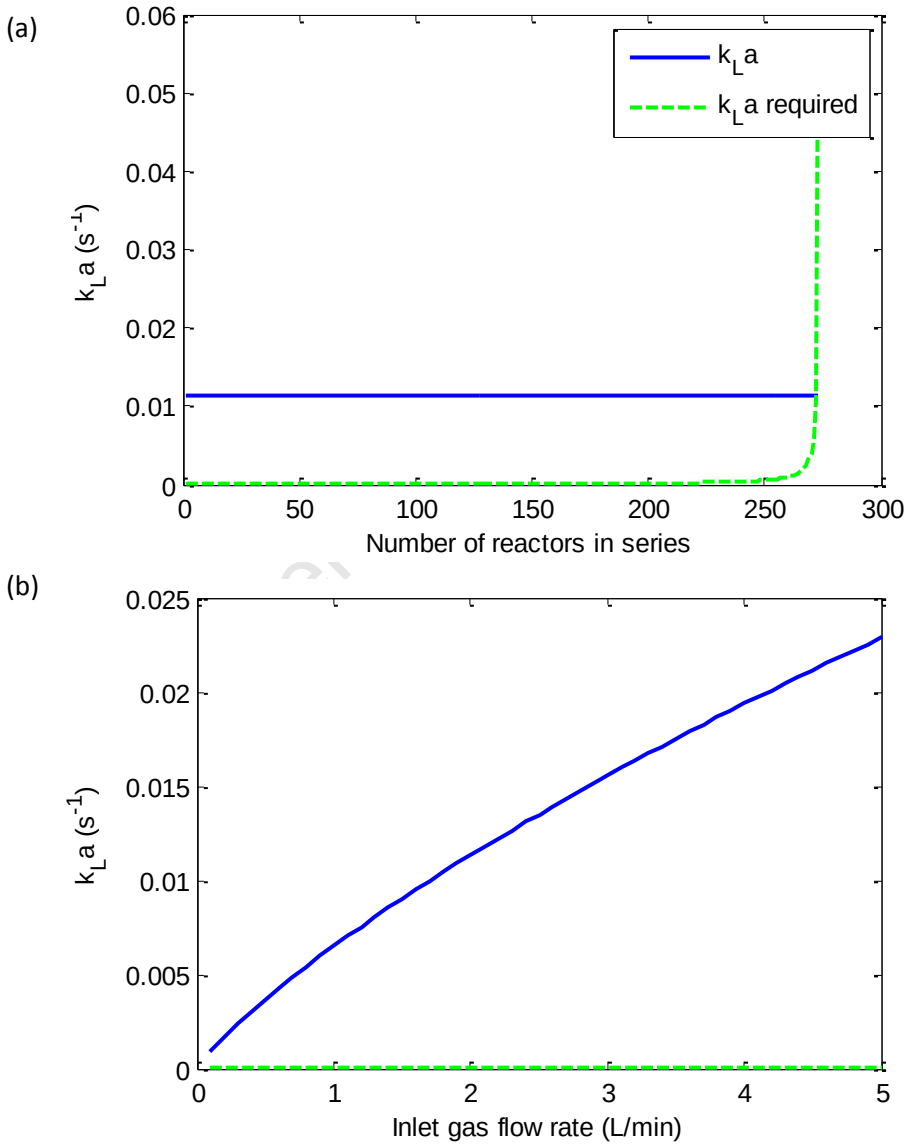

Figure 4-6 k_La capability of the system according to gas flow rate and k_La required to support the algal growth rate. The simulation was stopped when the system became CO_2 limited and would no longer be able to support the required growth rate for each respective (a) reactor in series at 2 L/min airflow rate and (b) inlet airflow rate to a single reactor. Growth of *Scenedesmus* sp. at maximum lipid productivity for the base case CO_2 concentration of 12.5%.

In Figure 4-6b, as expected, the system k_La increased with increasing gas flow rate. It is only at very low gas flow rates that the system k_La is even close to being mass transfer limited. Such low flow rates would not be considered as they would limit the circulation time as discussed in the following section.

4.5.2. Riser Residence Time

As discussed in Section 1.3.1, the frequency of light dark cycles is an important factor in algal photosynthesis. Work by Merchuk *et al*. (2000) showed that dark periods of up to 6 seconds did not have a negative effect on the algal growth rate. Considering that there is no light in the riser, 6 seconds is taken as the maximum allowed residence time for this simulation. The method and basis for the calculation of riser residence times are given in Appendix A.4.1. From Figure 4-7, inlet gas flow rates of above 0.6 L/min would be required for riser residence times of less than 6 seconds in the standard lab airlift. As the inlet gas flow rate to each reactor in series remains constant, there is no notable variation in reactor residence time for an increasing number of reactors, e.g. it remains at ~3.6 seconds for an airflow rate of 2 L/min.

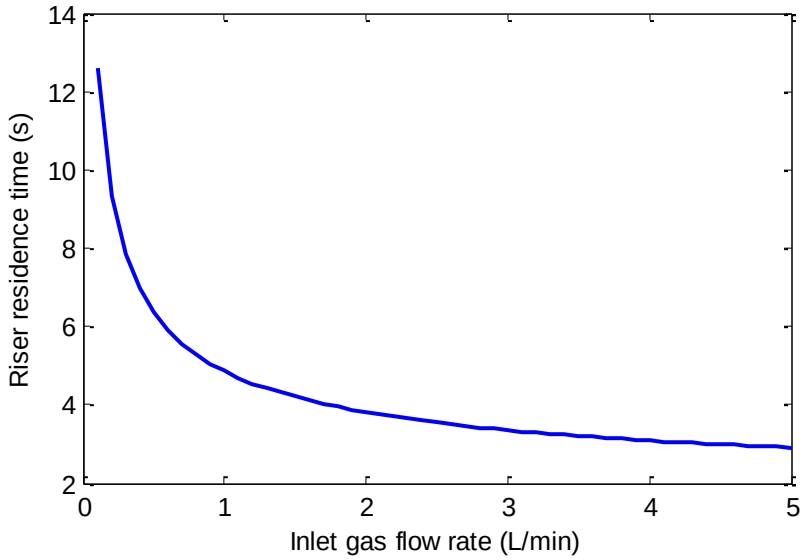

Figure 4-7 Riser residence time for each respective gas flow rate to a single reactor. According to Merchuk et al. (2000), a riser residence time of less than 6 seconds is required so as not to negatively affect the growth rate.

4.5.3. Dissolved Oxygen Levels

High levels of dissolved oxygen can be inhibitory to algal growth, as mentioned in Section 1.3.2. Here, the maximum acceptable level of dissolved oxygen concentration in the media was taken as 300% of air saturation at ambient temperature (Molina *et al.*, 2001). The dissolved oxygen concentration in the media can be calculated from the diffusivity of oxygen in water, Henry's law constant for oxygen, the rate of oxygen generation and the system CO_2 mass transfer coefficient,

which is in turn dependent on the inlet gas flow rate. The necessary calculation is detailed in Appendix A.3.2.

It can be seen in Figure 4-8 that neither scenario presented in Section 4.5.1 is limited by inhibitory levels of dissolved oxygen. As the inlet gas flow rate increased, the mass transfer coefficient increased, which in turn caused the dissolved oxygen concentration to approach equilibrium with the oxygen concentration in the inlet gas feed, according to Equation 1.1. With an increasing number of reactors in series, the dissolved oxygen concentration in the media did increase. As seen in Figure 4-8, the system becomes CO_2 mass transfer limited (causing the simulation to stop) before inhibitory levels can be reached.

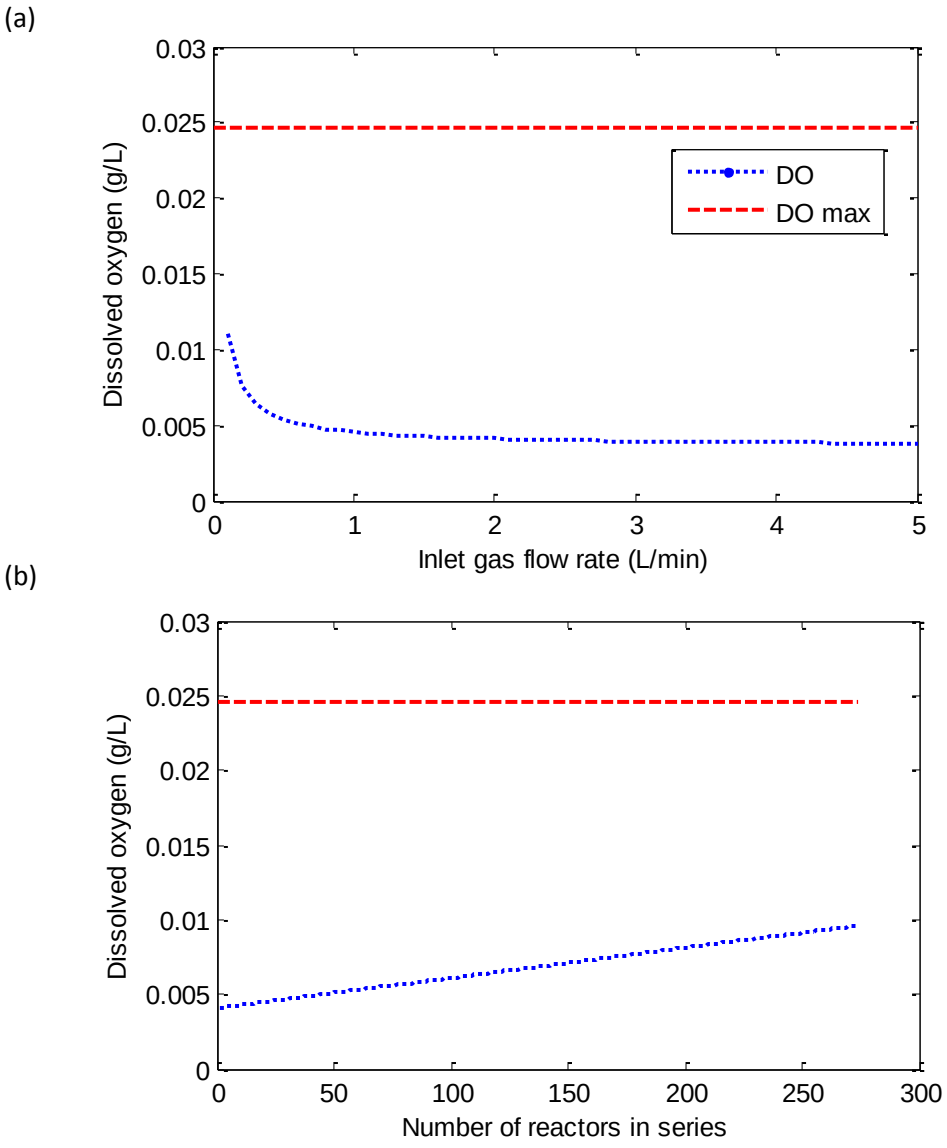

Figure 4-8 Dissolved oxygen concentrations calculated in the media and the maximum tolerable level of dissolved oxygen, taken as 300% of air saturation, for each respective (a) reactor in series at 2 L/min airflow rate and (b) inlet airflow rate to a single reactor. Growth of *Scenedesmus* sp. at maximum lipid productivity for the base case CO_2 concentration of 12.5%.

4.5.4. Reactor Energy

As alluded to in Section 4.5.1, the pressure to which the inlet gas must be compressed is likely to limit the number of reactors that can be operated in series prior to mass transfer limitation. The reactor material and the cells themselves must be able to withstand the pressure required in the first reactor in series, as shown in Figure 4-9. As discussed in Section 3.2.3, for a single reactor, losses in the distribution system of 0.07 bar and losses over the sparger of 0.07 bar were assumed. The total pressure requirement consists of these friction losses, atmospheric pressure and the static head. For each reactor added in series, the total pressure was calculated to increase by that required to overcome the static head and sparger-related losses of the additional reactor. Thus, the power requirement per unit volume decreases for each added reactor, as shown in Figure 4-9.

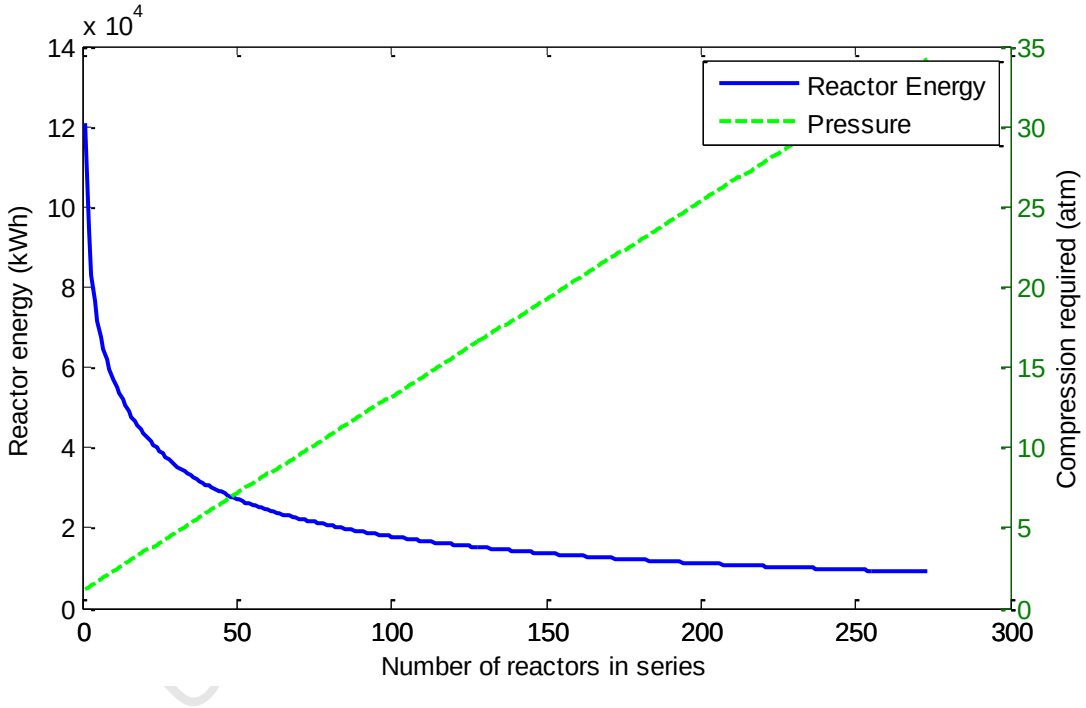

Figure 4-9 Reactor energy (per reactor in series) and corresponding air compression requirement for each respective reactor in series at an airflow rate of 2 L/min.

Given that an airflow rate of at least 0.6 L/min is required to drive liquid circulation, the data used to generate Figure 4-10 showed that for a gas flow rate of 0.6 L/min, at least 26 reactors would need to be connected in series to yield a positive energy balance. This would result in an initial pressure of 4.2 atm. For 1 L/min, 66 reactors would need to be connected in series, resulting in an initial pressure of 7.1 atm. The purpose of this chapter is not to optimise this reactor system. Further the experimental work required to evaluate the feasibility of these scenarios lies outside the scope of this project.

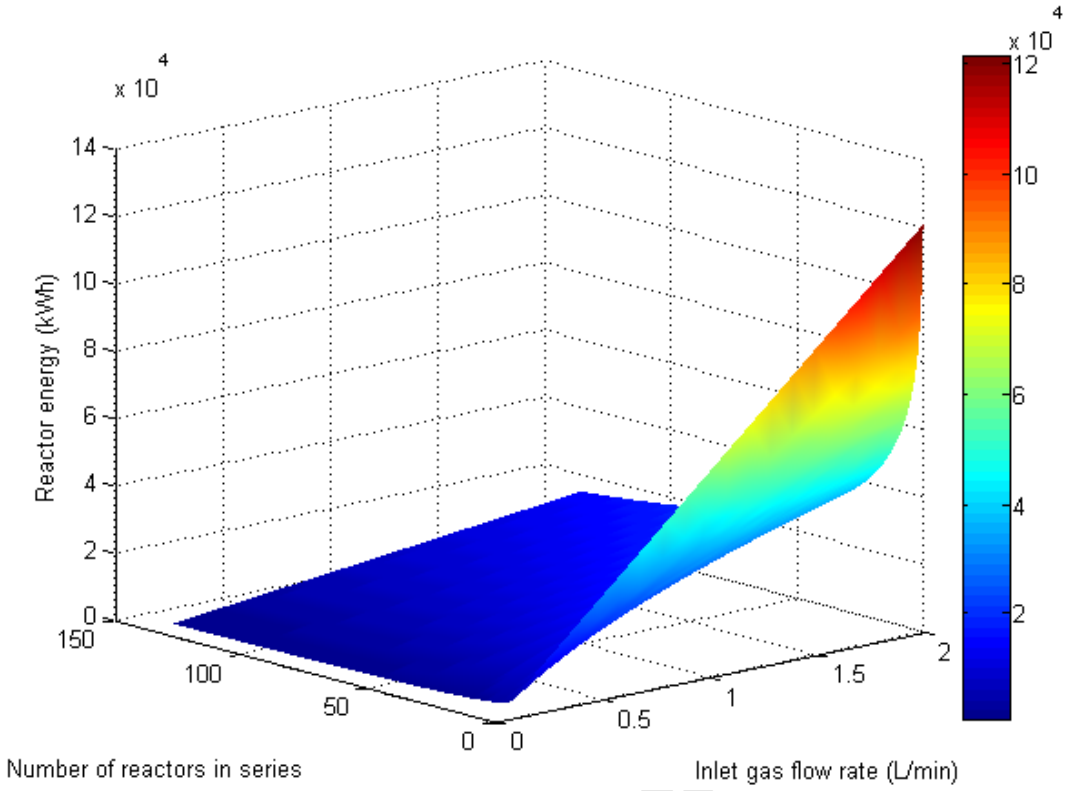

Figure 4-10 Reactor energy (kWh) for varying number of reactors in series and inlet gas flow rates within a reduced range.

4.6. Life Cycle Analysis

4.6.1. Methodology

Following comparison of performance data and inventory data generated for the biodiesel flow-sheet presented in Figure 3.1, further comparison between species was carried out using the LCA methodology described in Section 3.5.

The system was defined as cradle-to-factory-gate production of algal biodiesel as shown in Figure 3-1, including the extraction and production of raw materials. Boundaries exclude facility construction and dismantling. A functional unit of 1000 kg of algal biodiesel was used.

4.6.2. Neutral Energy Scenario

For any algal bio-energy system to be considered, it must yield a positive energy balance. So, considering that the initial LCA was dominated by the reactor and its electricity related impacts, a further LCA is thus conducted here on a hypothetically optimised system. Here, we consider *Scenedesmus* sp., the species of choice in the above system, operating at a reactor efficiency such that the system is energy neutral. This system required a reactor efficiency of 16.07 W/m^3 (Section 4.4.2). For the sake of comparison, all species were investigated at a reactor efficiency of 16.07

W/m^3 in the LCA. As *C. vulgaris* and *T suecica* require maximum respective reactor energy efficiencies of 7.2 and 6.7 W/m^3 to be energy neutral, these species show a negative energy balance.

The resultant energy division for all three species at this reactor efficiency, shown in Figure 4-11 remains reactor dominant. This trend continues in the impact assessment (Figure 4-12), where the species with the largest energy requirement shows the largest impacts and vice versa. The global warming impacts, shown in Figure 4-13, are predominantly from electricity and the use of nitrogen fertiliser. This is supported by all concurrent algal oil LCA studies published to date, as discussed in Chapter 2. This is also in agreement with the findings of Harding (2009) for heterotrophic microbial systems, where it was shown that the environmental impact of large scale, low value, low concentration processes is strongly dependent on the bioreactor and, specifically, the energy requirements and supply of combined nitrogen for both the microbial growth and production of organic carbon source. In this case, this point is emphasised by the particularly energy intensive nature of air compression, which drives the airlift reactors used for cultivation. This, too, is in agreement with Harding (2009) who demonstrated that air compression is a major consideration, even in mechanically agitated aerobic bioreactors. Further, the productivity and output of the bioreactor influences the requirements of the downstream process through, for example, the volume to be processed based on product concentration (Harding 2008). Thus, optimising the reactor process, rather than the downstream processes, has a greater effect on environmental impact of the process as a whole.

Apart from the reactor energy optimisation, increased efficiency in the use of nitrogen fertiliser would afford both environmental and energy benefits over the product life cycle. Clarens *et al.* (2010) showed the use of wastewater as sources of nitrogen and phosphorous could afford a significant reduction in algal cultivation burdens.

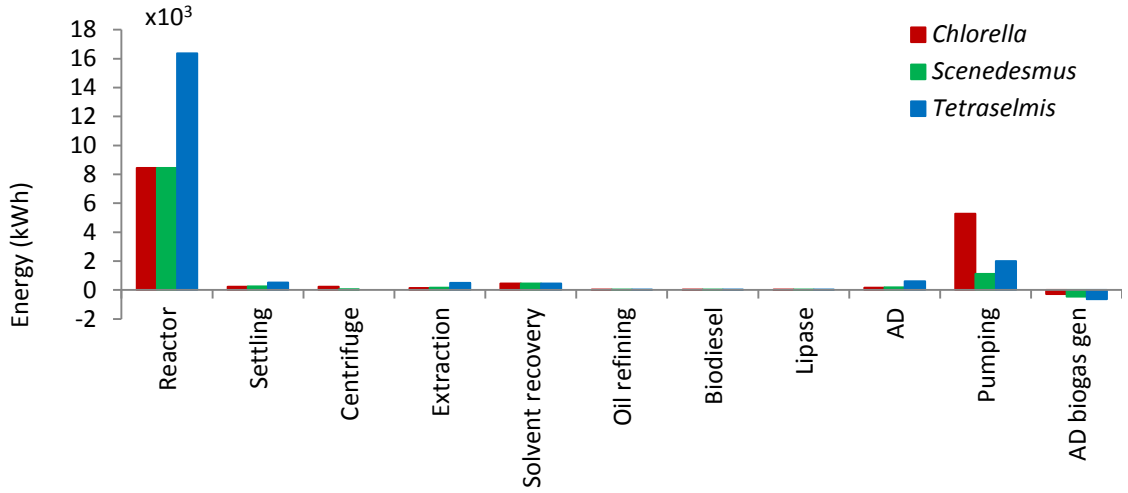

Figure 4-11 Fossil energy requirements for the production of biodiesel from *Chlorella vulgaris*, *Scenedesmus* sp. and *Tetraselmis suecica* at the point of highest instantaneous lipid productivity. Reactor efficiency of 16 W/m^3.

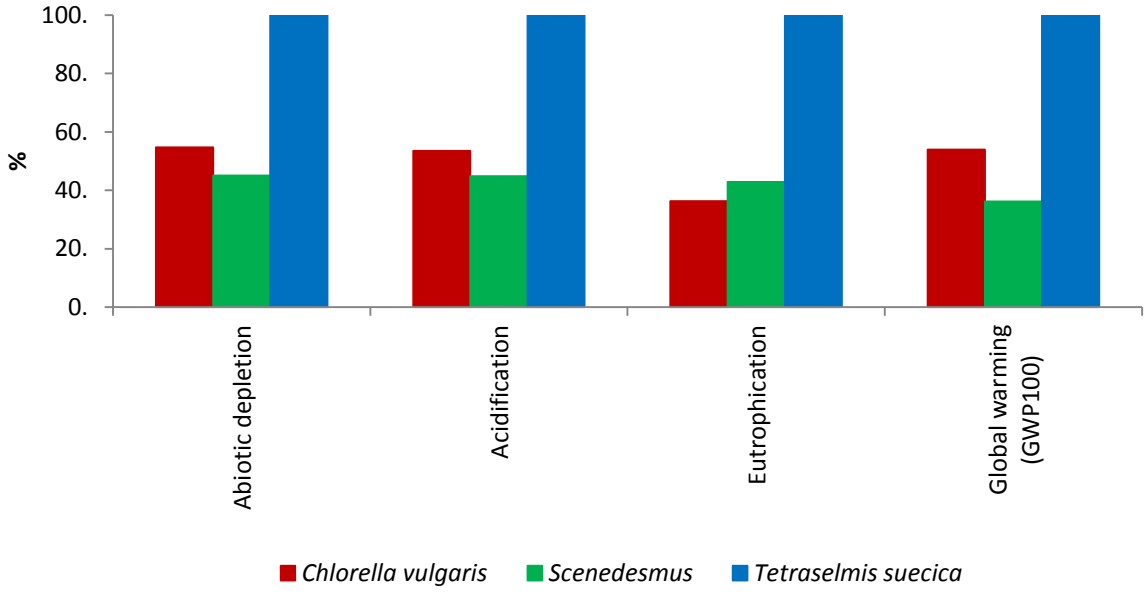

Figure 4-12 Life cycle impacts for the production of biodiesel from *Chlorella vulgaris*, *Scenedesmus* sp. and *Tetraselmis suecica* at the point of highest instantaneous lipid productivity. Reactor efficiency of 16 W/m^3.

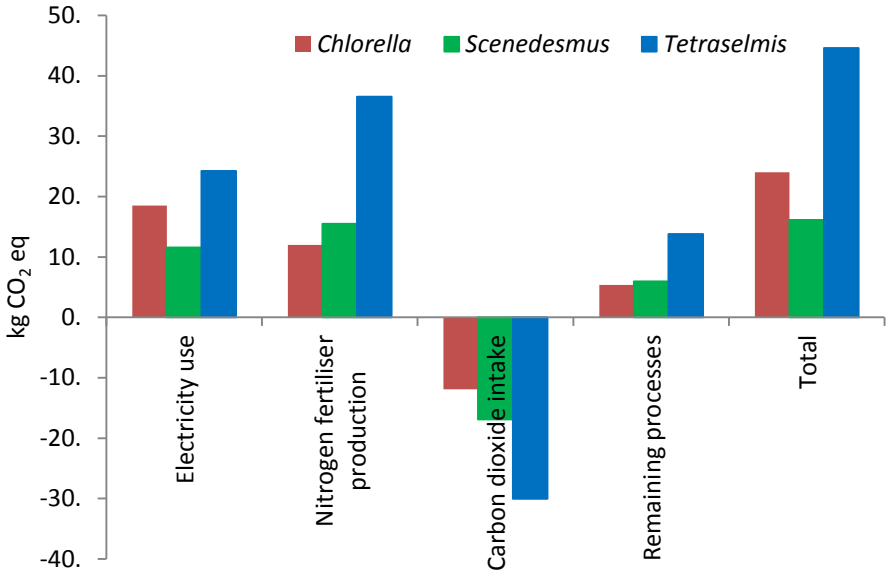

Figure 4-13 Global Warming potential for the production of biodiesel from *Chlorella vulgaris*, *Scenedesmus* sp. and *Tetraselmis suecica* at the point of highest instantaneous lipid productivity. Reactor efficiency of 16 W/m^3.

4.6.3. Digestate from Anaerobic Digestion used as a Soil Conditioner

The use of the residual biomass following anaerobic digestion deserves investigation. Previous studies have dealt with the digestate either considering it as waste (Campbell *et al.*, 2010), by recycling back to the growth medium (Collet *et al.*, 2010; Ras *et al.*, 2010; Stephenson *et al.*, 2010) or by considering it as soil conditioner (Finnveden *et al.*, 2005; Hospido *et al.*, 2010) and a by-product to the process. Recycling nitrogen and phosphorous present in the digestate and thereby displacing industrial fertiliser is an attractive possibility. This is possible as anaerobic digestion mineralises algal waste (Sialve *et al.*, 2009). However, limited data is available for the effect on algal growth of recycling the digestate to the reactor.

Here, a scenario is considered whereby the digestate was used as a fertiliser equivalent and by-product. The nitrogen and phosphorous content was calculated for an assumed 80% recovery. The system was expanded to displace the equivalent ammonium nitrate and phosphorous fertilisers. As there is no nitrogen or phosphorous contained in TAG, it can be assumed that a large proportion of the cell composition can be recovered.

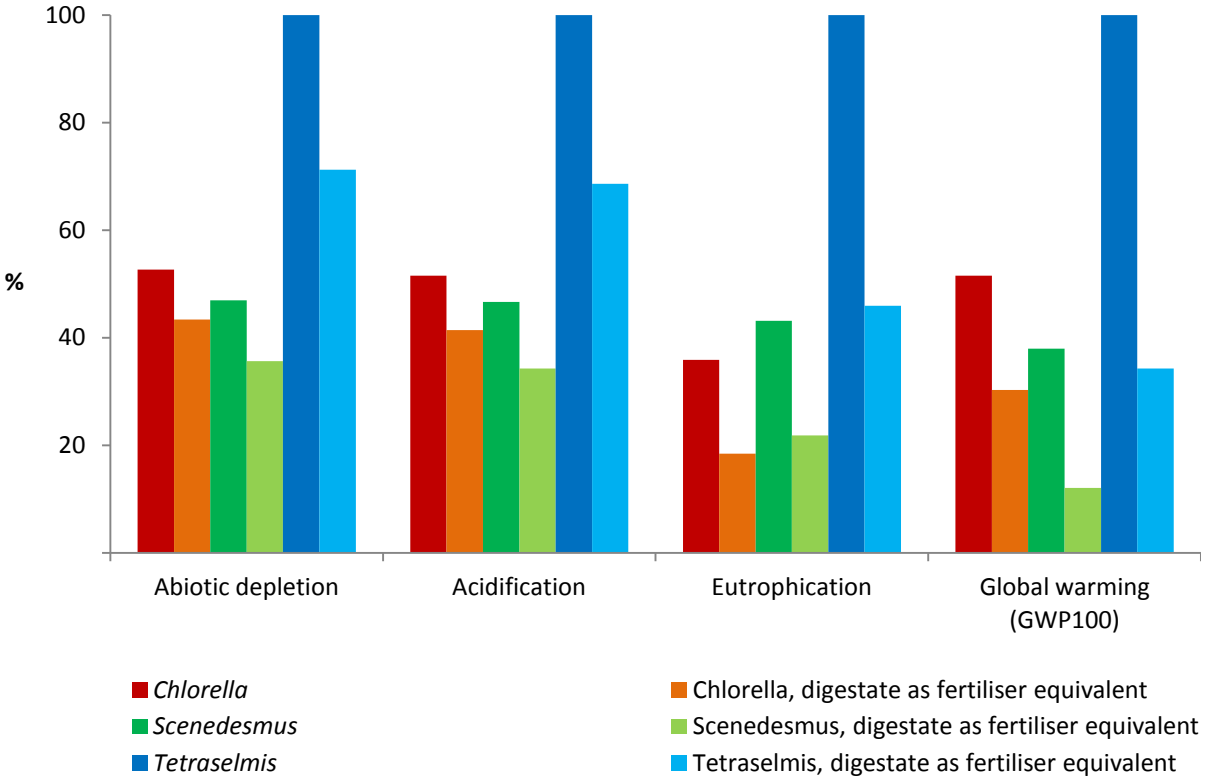

Figure 4-14 Life cycle impacts for the production of biodiesel from *Chlorella vulgaris*, *Scenedesmus* sp. and *Tetraselmis suecica* at the point of highest instantaneous lipid productivity where the digestate from anaerobic digestion is used as a soil conditioner. Reactor efficiency of 16 W/m^3.

As seen in Figure 4-14, all three species demonstrated significantly reduced impacts in all categories when the digestate was allocated as a soil conditioner. This enforces the need for further investigation into the use of waste water streams to provide the required nutrients for algal growth.

4.7. Conclusions

The environmental impact of the production of biodiesel from algae, using an airlift reactor system, modelled on a laboratory system, is predominantly due to reactor energy and nitrogen requirements. Reactor energy requirements in this system over-shadowed the species-specific settling benefits informing selection of the solid-liquid separation step. Nitrogen fertiliser related impacts can be significantly offset by recovering the digestate following anaerobic digestion and using it as a soil conditioner.

The reactor energy requirement is strongly dependent on lipid productivity. For a given system, this can be reduced either by optimising the performance of the reactor itself or by using a species of microalgae with high lipid productivity. The results show that the airlift system investigated is not feasible for the production of microalgal biomass as a feedstock for biodiesel. Two methods of increasing the reactor efficiency were investigated for *Scenedesmus* sp. at its maximum lipid

productivity: connecting reactors in series and variation in inlet gas flow rate. A minimum airflow rate of 0.6 L/min was calculated for a sufficiently short riser residence time. The number of reactors in series is restricted by the CO_2 mass transfer limitation before the dissolved oxygen concentration in the media reached inhibitory levels. The elevated cost associated with high pressure gas compression is expected to restrict the number of reactors in series before mass transfer limitation sets in.

The minimisation of reactor energy is key to the feasibility of algal biodiesel. A successful algal oil production system requires the optimisation of the reactor energy requirement through both lipid productivity and reactor efficiency. Further reactor configurations need to be investigated to determine the trade-off between the reactor used and growth optimisation.

5. Life-Cycle Comparison of Reactor Design

5.1. Introduction

As discussed in Section 1.4, there is disagreement in the literature over the choice of open or closed reactor systems for the cultivation of microalgal biodiesel. Open systems are cheaper both in terms of construction costs and energetic efficiency. This is particularly important given the low production cost required of fuel production (Sheehan *et al.*, 1998); however, they are constrained by productivities and biomass concentrations attainable as well as operation issues. On the other hand, closed photobioreactors achieve much higher biomass concentrations and productivities and allow for better control of the culture conditions (Chisti, 2007) at the cost of increased capital and operating costs.

A recent Life Cycle Assessment (LCA) study of aerobic heterotrophic microbial processes, conducted at the Centre for Bioprocess Engineering Research (CeBER), identified the bioreactor phase as a `hotspot' in large scale, low value, low concentration processes. This means that a small improvement in reactor performance could lead to a large improvement in overall environmental impacts through LCA scores (Harding, 2009). Such improvements could be made through the selection or optimisation of a favourable bioreactor configuration. Changes in algal growth parameters such as improved concentrations or productivities could also improve the system. As discussed in Section 4.4.1, a trade off exists between minimisation of reactor energy input and maximising microalgal oil productivity.

To this end, the growth of *Phaedodactylum tricornutum* was investigated in raceway ponds and horizontal and vertical tubular reactor systems. Justification for the choice of these species is given in Section 3.4 and centres on the availability of comparative data across these systems. The impact of reactor choice was investigated using a comparative energy analysis and LCA to determine the energetic balance and overall environmental impact of the production of 1000 kg of biodiesel in the chosen reactors and according to the flow-sheet shown in Figure 3-1, respectively.

This chapter aims to investigate the effect of reactor choice on the chosen flow-sheet (Figure 3-1) for the production of biodiesel and to explore the impact of changes to microalgal growth parameters for each reactor on a life cycle and system energy basis.

5.2. Methodology

Phaedodactylum tricornutum was used as the base case species in this chapter. The biochemical and elemental compositions of *P. tricornutum* were taken from studies by Mirón *et al.* (2003; 2002). While changes in the elemental composition of algae in response to nitrogen limitation have been reported (Griffiths et al., in prep), such data are not reported across reactor systems. For the sake of consistency, simultaneously occurring biomass concentrations and productivities were taken from the papers describing the closed reactor systems modelled in this study (Mirón *et al.*, 2003; Molina *et al.*, 2001). The corresponding air flow rates from the same papers were used in this study. For the raceway, a steady state biomass concentration of 0.5 g/L was selected, as done by Lardon *et al.* (2009). This is in agreement with Richmond *et al.* (2004b) who suggested that concentrations in raceway ponds do not exceed 0.6 g/L. The volumetric productivity of 0.07 g/L/day (21 g/m^2/day) used is in agreement with that achieved during the ASP (Sheehan *et al.*, 1998).

Table 5-1 Base case composition and culture parameters for the three reactor types investigated

	Units	Horizontal Tubular[a]	Draft tube airlift[b]	Raceway[c]
Biomass concentration	g/L	3.96	1	0.5
Biomass productivity	g/L/day	1.9	0.3	0.07
Protein	%	55	55	55
Carbohydrate	%	10	10	10
Lipid	%	21	21	21
Pigment	%	2	2	2
C	-	0.492	0.492	0.492
H	-	0.063	0.063	0.063
N	-	0.008	0.008	0.008
Reactor Energy	W/m^3	114	159	2

Figure 4-1 outlines the steps taken in order to achieve the goals of this chapter. From the data shown in Table 5-1, a continuous culture algal production reactor was simulated and the simulation model used to calculate the material and energy inputs and outputs required across the process flow-sheet for the production of the functional unit of biodiesel. The outputs from the model were then used to compare the reactors on an energy (Section 5.4) and life cycle basis (Section 5.5). Following this, the effect of reactor configuration, biomass concentration, biomass productivity and lipid content were investigated for each reactor in Section 5.6.

The soil conditioner resulting from anaerobic digestion is allocated as a non-impacting flow so that the effects of fertiliser use can be more clearly seen.

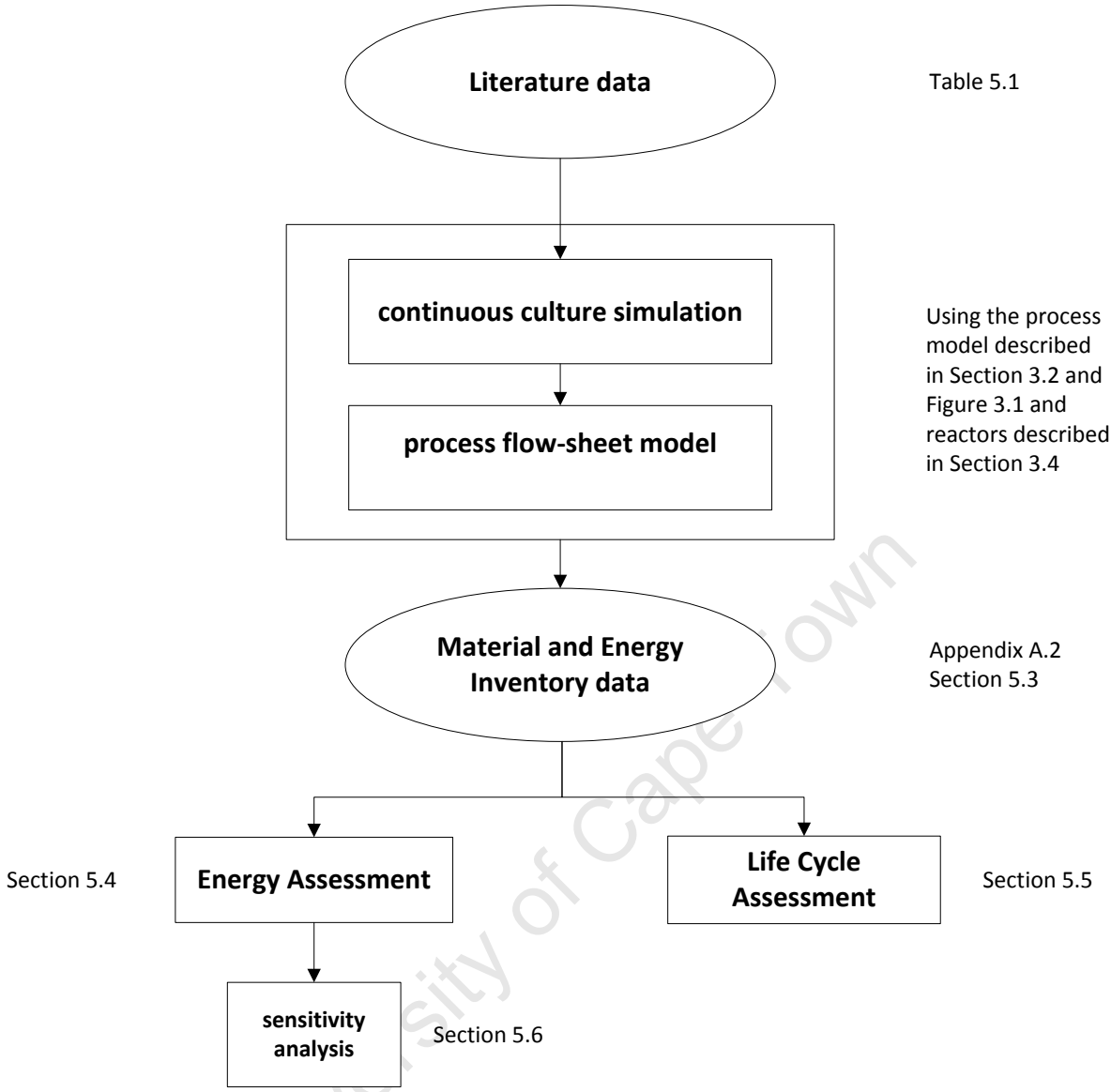

Figure 5-1 Flow-diagram illustrating the procedure followed to achieve the results of Chapter 5

5.3. Material and Energy Inventory Data

As in Chapter 4, for each set of conditions investigated in each reactor, the process simulation model described in Section 3.2 was used to generate the composition of each of the process flow streams in Figure 3-1. Tabulated stream compositions are given in Appendix A.2 for the growth of *P. tricornutum* in each of the three reactors. These stream tables were used to create the inventory table shown in Table 5-2 for each reactor. Table 5-3 shows the contributions of the individual process units. These data are used in the energy analyses in Section 5.4 and as input to the LCA in Section 5.5.

Table 5-2 Material and energy inventory data for *P. tricornutum* grown in raceway ponds, vertical and horizontal tubular reactors

	Raceway ponds		*Vertical Tubular Airlift Reactors*		*Vertical Tubular Airlift Reactors*	
Biomass Concentration (g/L)	0.103		0.63		0.83	
Biomass Productivity (g/L/day)	0.27		0.37		0.45	
Lipid content (%)	0.22		0.18		0.071	
	Input kg/day	Output kg/day	Input kg/day	Output kg/day	Input kg/day	Output kg/day
water	2680000	2680000	1350000	1350000	359000	359000
cells	0	129	0	129	0	129
ammonium nitrate	153	88.4	153	88.4	153	88.4
triple super phosphate	63.4	36.6	63.4	36.6	63.4	36.6
potassium chloride	26.9	0	26.9	0	26.9	0
Aluminium sulphate	0	0	0	0	0	0
Hexane	49.1	0	49.1	0	49.1	0
Phosphoric acid	10.8	0	10.8	0	10.8	0
Caustic soda	67.9	0	67.9	0	67.9	0
Methanol	111	2.4	111	2.4	111	2.4
Biodiesel	0	1000	0	1000	0	1000
Glycerol	0	106	0	106	0	106
cooling water	120	120	120	120	120	120
Steam	1540	0	1540	0	1540	0
Glucose	5.76	0.0576	5.76	0.0576	5.76	0.0576
Yeast	3.84	0.192	3.84	0.192	3.84	0.192
precipitating chemical	2.4	2.4	2.4	2.4	2.4	2.4
CO_2	11900	65	11900	65	11900	8.32
Phosphates	0	1.44	0	1.44	0	1.44
Urea	2.9	0	2.9	0	2.9	0
Methane (STP)	0	18.2	0	18.2	0	18.2
Lime (floc)	3960	3960	1980	1980	500	500
Total Energy (kWh)	6730	0	85700	0	10600	0

Table 5-3 Total energy requirements and material flows through each process unit shown in Figure 3-1 for *P. tricornutum* grown in raceway ponds, vertical and horizontal tubular reactors

Unit	Raceway pond	Vertical tubular	Horizontal tubular
Reactor	4570	84200	9490
Settling	49.2	24.5	6.09
Centrifuge	251	251	251
Extraction	143	143	143
Solvent recovery	456	456	456
Oil refining	34.4	34.4	34.4
Biodiesel	34.1	34.1	34.1
Lipase	22.1	22.1	22.1
AD	166	166	166
Pumping	1150	585	160
AD biogas gen	-152	-152	-152

5.4. Energy Analysis

The total fossil energy requirements for the production of 1000 kg of biodiesel from *P. tricornutum* grown in raceway ponds and both vertical and horizontal tubular reactors are shown in Figure 5-2, compared with the energy contained in the biodiesel produced.

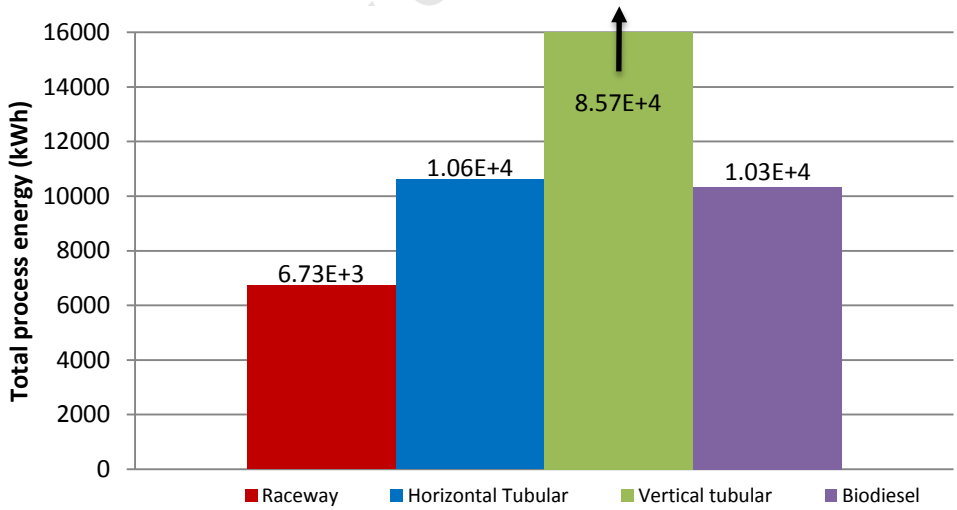

Figure 5-2 Total Fossil Energy requirements for the production of 1000 kg of biodiesel from *Phaedodactylum tricornutum* in raceway ponds, and horizontal tubular and draft tube airlift photobioreactors. Base case.

As expected, the raceway pond is far superior to the closed systems in terms of its energy balance, showing an NER of 1.5 (energy in biodiesel produced: fossil energy required). The horizontal tubular reactor system shows an approximately neutral energy balance (NER = 0.97), while the vertical tubular reactor shows a negative energy balance (NER = 0.12). Figure 5-3 demonstrates that this is attributed to the dominance of reactor energy in both the closed airlift driven systems. In the case of

the vertical tubular reactor, the reactor energy alone was approximately 8 times the energy value of the biodiesel produced. For this reason, it is not investigated further in the LCA component of this chapter, presented in Section 5.5. For the horizontal tubular reactor system, a more manageable reactor energy total was predicted due to its superior biomass productivity of 1.9 g/L/day compared to the 0.3 g/L/day in the vertical tubular reactors. Also of interest is the significance of pumping energy at the lower reactor concentrations achieved in the raceway in particular.

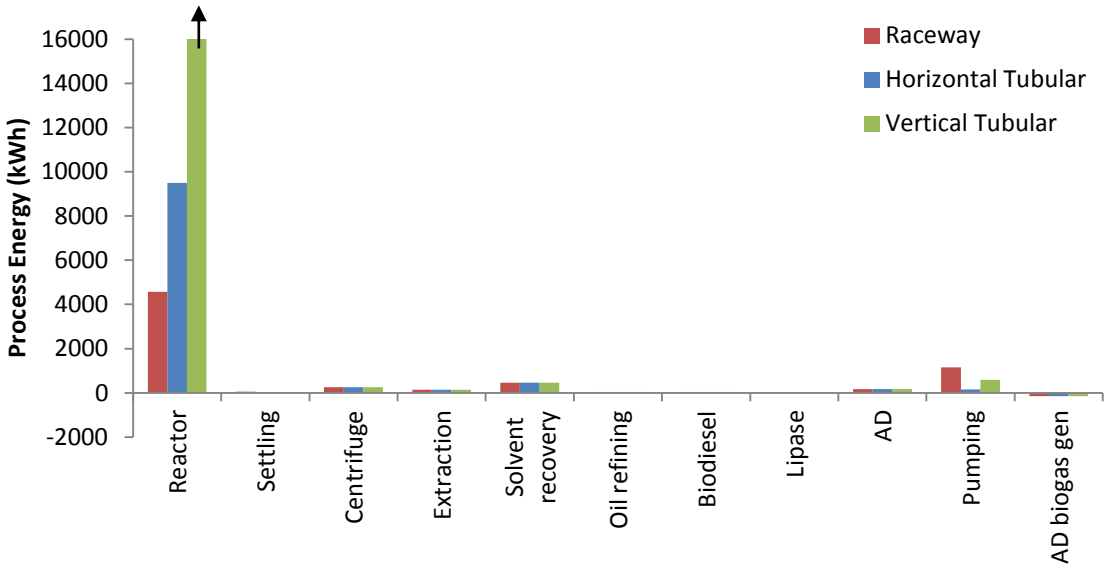

Figure 5-3 Fossil Energy requirements of the process units involved in the production of 1000 kg of biodiesel from *Phaedodactylum tricornutum* in raceway ponds, horizontal tubular and draft tube airlift photobioreactors. Base case scenario for flow-sheet given in Figure 3.1.

5.5. Life Cycle Assessment

5.5.1. Methodology

Life Cycle Analysis was performed as in Section 4.6. The system was defined as cradle-to-factory-gate production of algal biodiesel as shown in Figure 3-1, including the extraction and production of raw materials. Boundaries exclude facility construction and dismantling. A functional unit of 1000 kg of algal biodiesel was used.

The goal of this LCA is to assess the chosen process flow-sheet (Figure 3-1), in combination with the three reactor types, for the production of biodiesel from microalgae and to examine the effect of reactor choice on the environmental impact of the process.

5.5.2. Life Cycle Impact Assessment

The life cycle impacts of the production of biodiesel from algae grown in raceway and horizontal tubular bioreactors are shown in Figure 5-4. The impacts are largely proportional to the fossil energy

requirements of the reactor system. Greater energy leads to greater abiotic depletion and acidification impacts in the closed reactor, while a lesser energy requirement per unit product in raceway implies positive reduction in global warming. The other dominant impact shown in Section 4.6 is that of fertiliser use, but as the same species and thus elemental composition is assumed for each reactor, fertiliser impacts are the same.

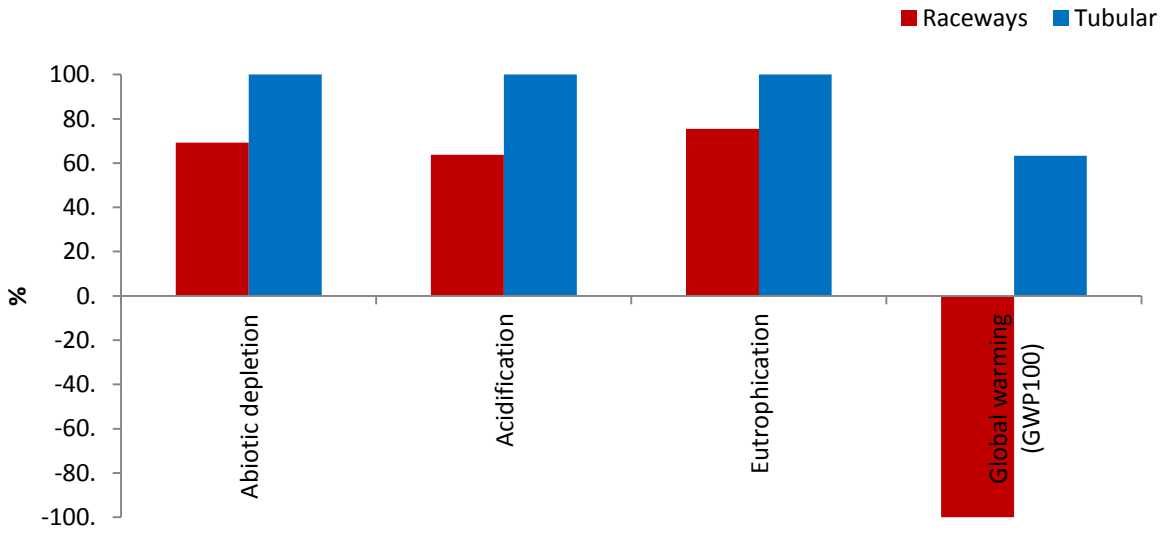

Figure 5-4 Normalised life cycle impacts for the production of biodiesel from *Phaedodactylum tricornutum*, cultivated in raceway and hortzontal tubular reactors for the production of 1000 kg of biodiesel. Base case scenario.

The global warming potential (GWP) impact category, which is of great interest in the study of microalgal biodiesel, is shown in more detail inFigure 5-5. GWP is lower in the raceway due to lower electricity requirements. The contribution of lime, used to assist in flocculation of the algae, to the overall GWP is noteworthy. The larger contribution in the case of the raceway was due to the lower biomass concentration exiting the reactor. The contribution of nitrogen fertiliser is significant, but less than for the species studied in Chapter 4. This is due to the particularly low nitrogen content of *P. tricornutum* (0.8%) compared to *Scenedesmus* sp. (9%). The typical chemical formula of algal biomass, $CH_{1.83}O_{0.48}N_{0.11}P_{0.01}$ corresponds to a 6% nitrogen content. This is an important result, suggesting that low nitrogen composition should be a factor in the choice of a species for algal biodiesel production. However, as algal composition is highly dependent on the growth environment, this is not a simple problem and would require further experimental study.

In addition to the much lower energy requirements of raceway cultivation over both closed reactor systems, Stephenson *et al.* (2010) also showed that the GWP associated with the manufacture of the horizontal tubular reactor's solar collector alone is roughly equal to the GWP of the entire cultivation stage of the raceway system.

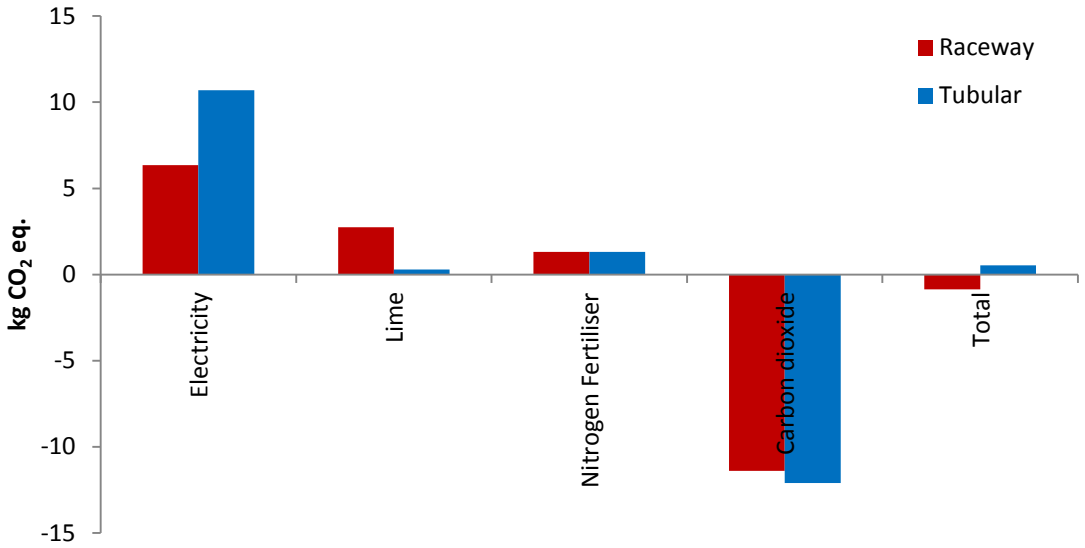

Figure 5-5 Contributions to the global warming potential impact category for raceway and horizontal tubular reactor systems.

5.6. Sensitivity Study

In the following sections, the key sensitivities to reactor performance are discussed. Changes affecting reactor performance are both a function of the bioreactor configuration and the algal species and are thus restricted by both the bioreactor and the metabolic limits of the species concerned. In this section, the focus is on the bioreactor configuration and operation.

5.6.1. Reactor Configuration and Specifications

As shown in Section 4.5.4, the energy requirement of airlift reactors is extremely sensitive to the inlet gas flow rate. Mirón *et al.* (2003) investigated the effects of shear stress on *P. tricornutum* in the vertical tubular reactor modelled in this study. The growth data used in this study were based on an inlet gas flow rate of 0.01 m/s. This translates to a draft tube residence time of 18 seconds. It was determined that above this airflow rate, cells were susceptible to aeration-associated hydrodynamic stress. Below this airflow rate, the algal growth rate may decline.

Molina et al. (2001) investigated the growth of *P. tricornutum* in a horizontal tubular reactor at various inlet gas flow rates. Flow rates resulting in circulation velocities of 0.17 m/s lead to culture death. This was postulated to be due to photo-oxidation effects owing to the longer circulation time. Circulation speeds of 0.35 and 0.5 m/s, however, achieved similar biomass productivities. As the horizontal tubular reactor in this study is based on the design of Molina *et al.*, a circulation speed of 0.35 m/s has been employed. Increasing this speed to 0.5 m/s would result in an increase in reactor power from 114 W/m^3 to 186 W/m^3.

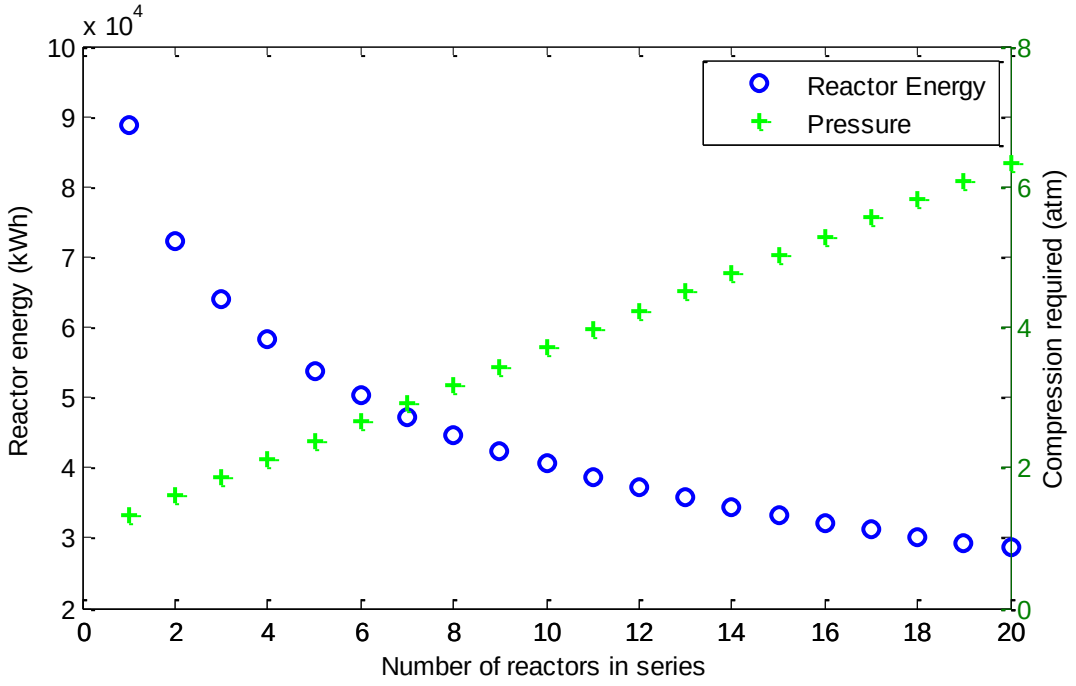

Figure 5-6 Reactor energy and corresponding air compression requirement for each respective vertical tubular reactor in series.

The other mode of decreasing overall reactor power in airlift reactors investigated in Chapter 4 was connecting reactors in series. Figure 5.6 shows the decrease in reactor energy and corresponding increase in pressure for an increasing number of reactors connected in series. Even with over 20 reactors in series and a resulting pressure of 6.3 atm, the resultant reactor energy remained more than twice the energy value of the produced biodiesel (NER < 0.5). Optimisation of this system is thus seemingly not achievable through a physical reactor optimisation alone. Further improvement may be attainable by optimisation of the culture conditions.

While mixing is the main contributor to reactor energy requirements, Stephenson *et al.* (2010) found that the environmental performance of biodiesel from microalgae cultivated in raceways was highly sensitive to the power required for compression of the flue gas. Consequently, it would be beneficial to use flue gases with higher concentrations of carbon dioxide. This would function to both reduce the volume of gas requiring compression and increase the rate of CO_2 mass transfer to the culture. Stephenson showed that if the concentration of CO_2 in the flue gas were reduced from 12.5% to 5%, the fossil-energy savings would fall from 85% to 45% and the GWP savings 78% to 47%, compared to fossil-derived diesel.

5.6.2. Algal Growth Parameters

5.6.2.1. Biomass Concentrations

Photoautotrophically grown algal cultures are by nature dilute. Even in more concentrated cultures, the change in volumetric power consumption of a given reactor is small as the density remains similar to that of water. A dilute culture simply means that a larger volume of fluid must be processed and there is thus an increased need for pumping (Figure 5-7). This translates to a larger overall power requirement and expense. This is consistent with the work of Harding (2009). The larger volumes resulting from low biomass concentrations also give rise to an increased requirement for flocculating agents. As seen in Figure 5-5, the production of such flocculating agents can form a significant contribution to the overall process burdens. The use of algal strains that concentrate well under free settling could eliminate this burden. As discussed in Chapter 4, both *T. suecica* and *Scenedesmus* sp. demonstrated good settling rates under laboratory conditions.

Biomass concentrations achievable in a given system are dependent on the light penetration through the culture. This, in turn, is dependent on the solar radiation available, which is a function of both climate and reactor configuration, and the degree of mixing, a function of reactor configuration.

Chisti (2007) gave the typical biomass concentration of 30 cm deep raceway cultures as 0.14 g/L, while Huntley and Redalje (2007) reported concentrations from 0.2 to 0.4 g/L. The biomass concentrations assumed in previous LCA's of raceway systems varied from 0.35 g/L to 1 g/L (Jorquera *et al.*, 2010; Stephenson *et al.*, 2010). The effect of biomass concentration is thus worthy of investigation.

From Figure 5-7 it can be seen that the pumping energy requirement decreases significantly, by an order of magnitude over the initial biomass concentration range from 0.1 to 0.5 g/L, after which the decrease in pumping energy per unit increase in biomass concentration is reduced. The total process energy largely reflects this result. A small decrease in the energy required for dewatering can be seen.

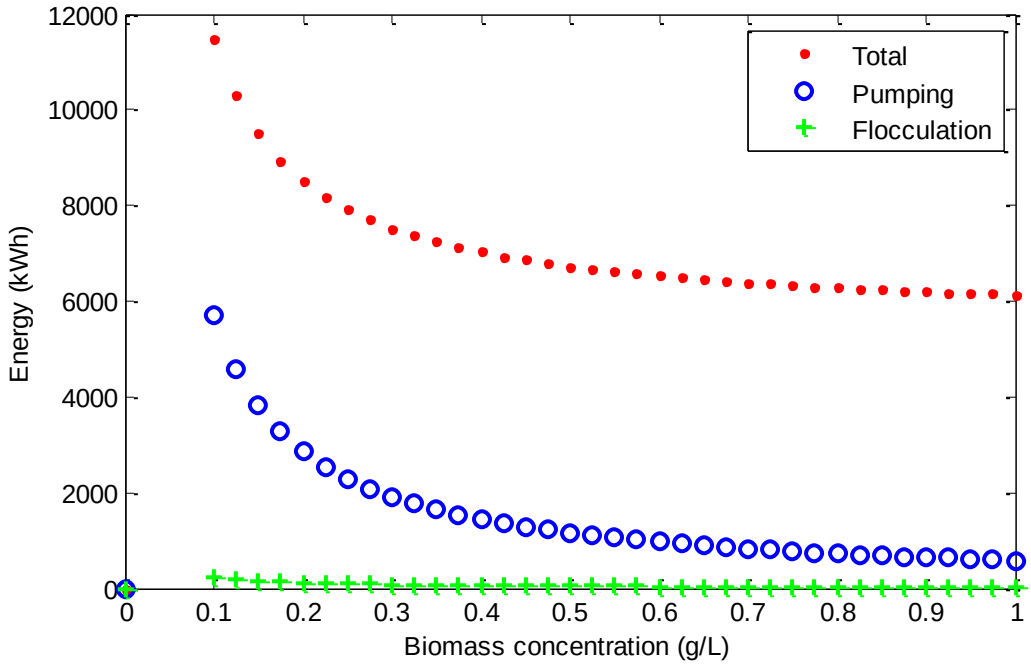

Figure 5-7 Total, pumping and flocculation energy requirements of biodiesel produced from *P. tricornutum* cultivated in raceway ponds over varying biomass concentrations. Base case scenario: 21% lipid content, 0.07 g/L/day.

5.6.2.2. Biomass Productivity

Considering first the raceway system, Richmond advocates that typical long term areal productivities of raceways are in the range of 12-13 g/m^2/day, while well-managed raceways could achieve seasonal productivities of 20-25 g/m^2/day and very short term maxima of 40 g/m^2/day (Richmond, 2004b). Lee *et al.* reported productivities of *Spirulina platensis* in raceway ponds in Israel of 27 g/m^2/day, while Huntley and Redalje (2007) reported average biomass productivities of 15 g/m^2/day, with a maximum of 36.4 g/m^2/day (Lee, 2001). Figure 5-8a shows that on increasing aerial productivity from 10 – 25 g/m^2/day, reactor energy requirement decreases by just less than half.

In all three reactor cases, increasing biomass productivity results in process energy reduction due to a decreased reactor requirement. The closed reactor systems show a more significant decrease over the achievable range for the given reactor system. Net productivities of 3.64 g/L/day have been reported for *Chlorella pyrenoidosa* in a 1.2 cm diameter tubular reactor in Singapore. Productivities for *P. tricornutum* of 2.7 g/L/day were reported in a 3.0 cm diameter tubular reactor in Almeira, Spain (Borowitzka, 1997). In the base case for this study, 6 cm diameter tubes are used, with a biomass productivity of 1.9 g/L/day. This lower productivity is presumably due to the increased tube diameter, allowing less light penetration. The surface-to-volume ratio has been cited as an important factor in tubular photobioreactor design (Sánchez Mirón *et al.*, 1999). However, the use of thinner tubes results in added expense, both financially and in terms of production energy and thus GWP.

The reduction in process energy achieved by increased productivity over the range from 1.9 to 3.5 g/L is minimal. Increasing the surface-to-volume ratio to increase productivity in this range thus could be counterproductive should the added expense outweigh the benefits of the increased productivity.

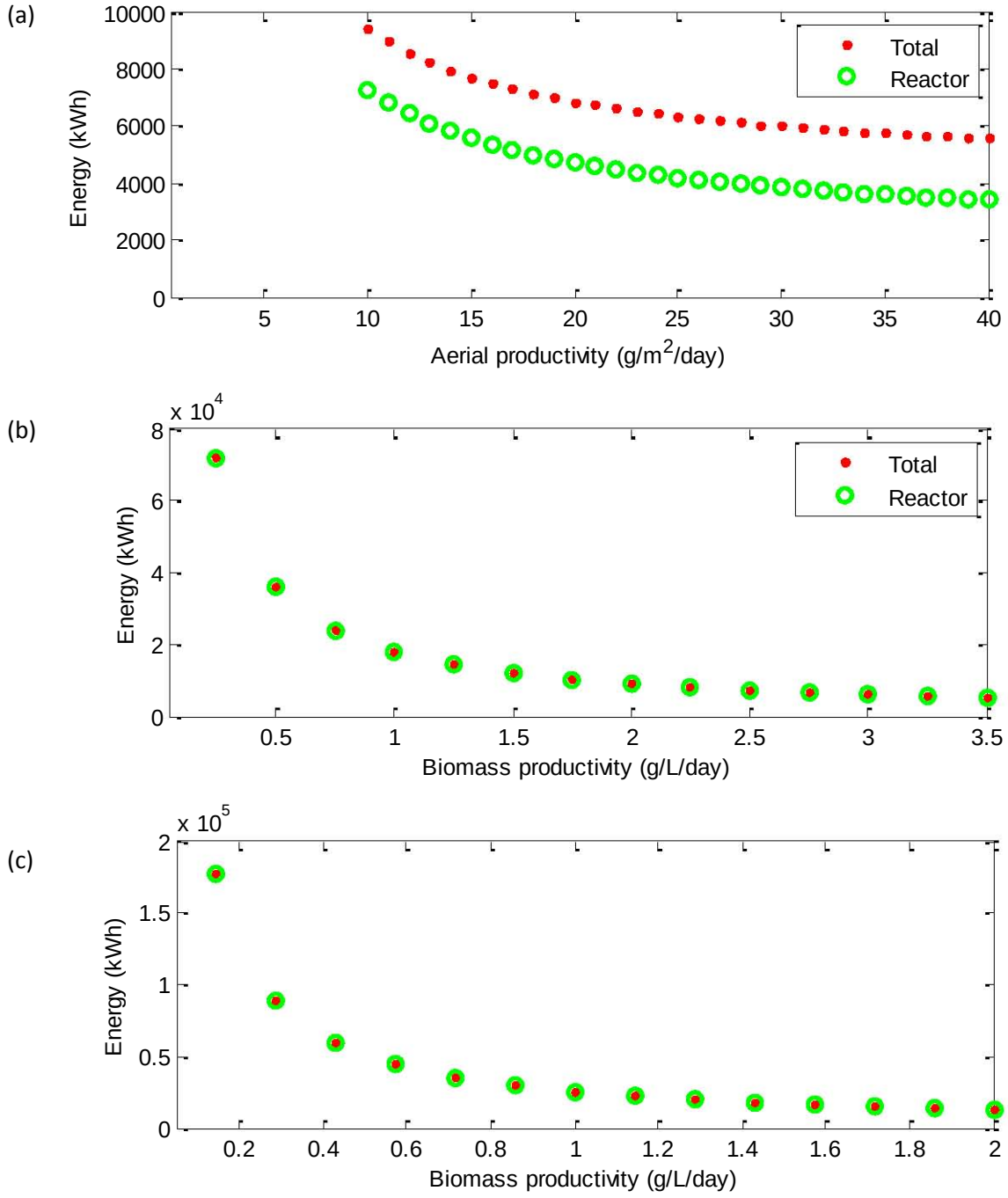

Figure 5-8 Total and reactor energy requirements over various values of aerial and biomass productivity in (a) a raceway pond (b) horizontal tubular reactors and (c) vertical tubular reactors. Base case scenario: 21% lipid content, biomass concentration 0.5 g/L in raceways, 3.96 g/L in horizontal tubular reactors and 1 g/L in vertical tubular reactors.

5.6.2.3. Lipid Content

Lipid content is a function of both the algal species and the growth conditions. Lipid contents of 20-50% are fairly common (Chisti, 2007). Particularly high lipid content often occurs at the expense of a lower growth rate. As seen in Figure 5-9, increased lipid content has multiple effects on the overall system. Reactor energy decreases as lower reactor volumes are required to produce the same amount of oil for biodiesel for a given biomass productivity. Pumping energy also shows a slight decrease due to the decreased volumes. On the other hand, higher lipid content means less non-lipid biomass and thus less energy payback through anaerobic digestion. From Figure 5-9 we can see that the higher the energy requirement of the reactor system, the greater the improvement achieved through increased lipid content. As the biomass productivity is kept constant, increased lipid content translates to increased lipid productivity. In all cases, the overall system energy shows a general decrease with increased lipid productivity.

Stephenson *et al.* (2010) noted that as the lipid concentration in cells increased from 20 to 60 %, the GWP savings of combusting biodiesel rather than fossil-derived diesel reduced from 118 to 64%. It was further advised that at very low lipid concentrations, oil extraction may be difficult and require a more energy intensive process.

5.6.2.4. Lipid Productivity

Lipid productivity has been proposed as the key variable to choosing a microalgal species for the production of microalgal biodiesel production (Griffiths & Harrison, 2009; Rodolfi *et al.*, 2009). It is calculated as the product of the species' biomass productivity and lipid content.

The effect of lipid productivity on the efficiency of biodiesel production from microalgae in the three reactor systems investigated in this dissertation is shown in Figure 5-10. For each system, the effect of increasing biomass productivity on overall energy is shown for three different lipid contents. The energy value of the biodiesel produced is shown. The raceway, as expected, displays a positive energy balance for all three lipid contents over the reasonable range of aerial productivities (10-25 g/m^2/day). A lipid productivity of greater than 0.005 g/L/day is expected to lead to a positive energy balance at a biomass concentration of 0.5 g/L. In the raceway base case, lipid productivity is 0.015 g/L/day. Cultivation in horizontal and vertical tubular reactors is expected to require lipid productivities above 0.4 and 0.5 g/L/day respectively at the concentrations of ~4 and 1 g/L to yield a positive energy balance. In the base case, these reactors displayed lipid productivities of 0.4 and 0.06 g/L/day. Vertical tubular reactors are therefore well short of the requirements for large scale biodiesel production, while horizontal tubular reactors under conditions investigated are marginal and raceways are feasible.

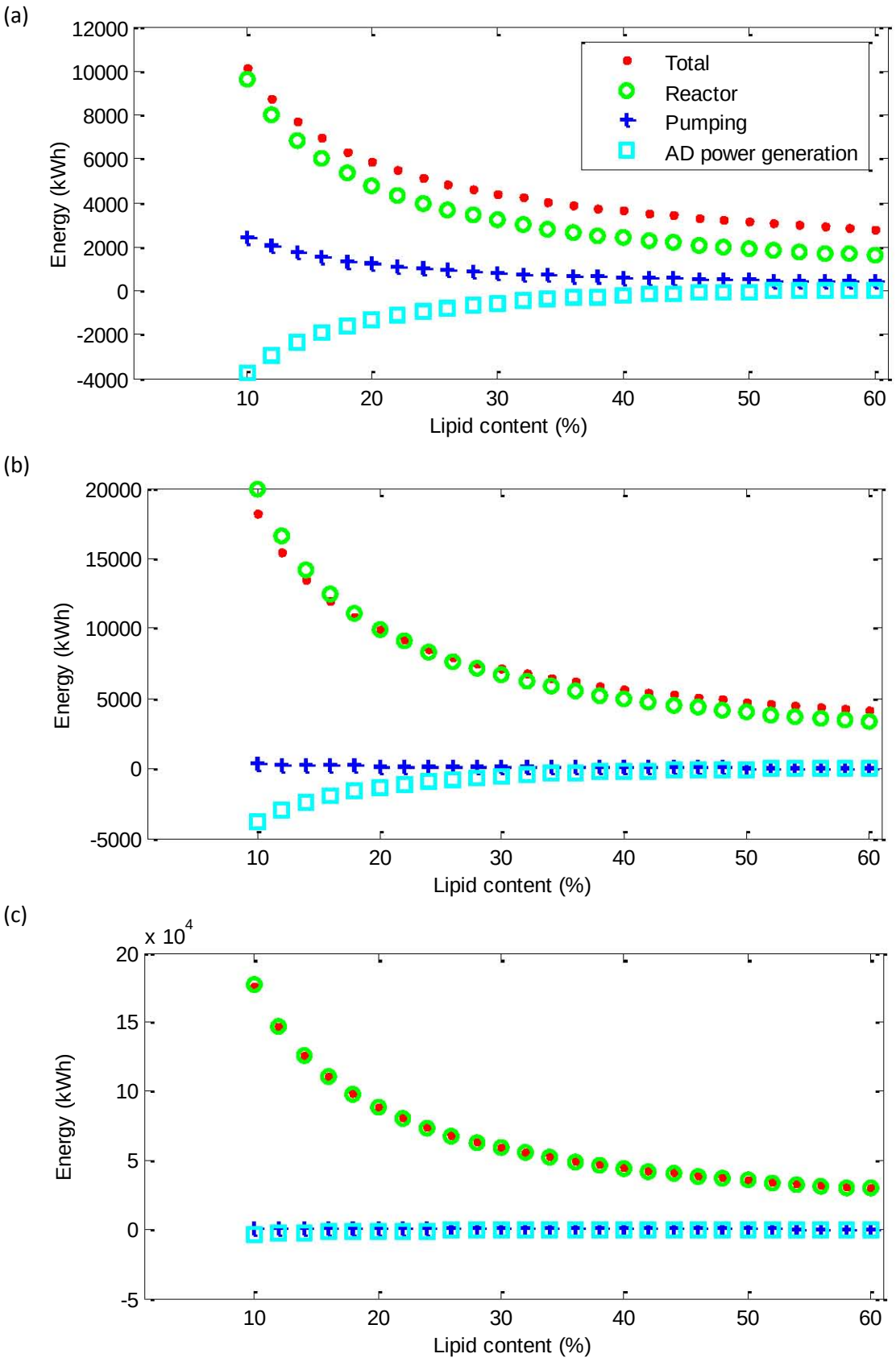

Figure 5-9 Total reactor and pumping energy requirements and energy payback through anaerobic digestion over various lipid contents in (a) raceway ponds (b) horizontal tubular reactors and (c) vertical tubular reactors. Base case scenario: productivities of 0.07 g/L/day at 0.5 g/L in raceways, 1.9 g/L/day at 3.96 g/L in horizontal tubular reactors and 0.3 g/L/day at 1 g/L in vertical tubular reactors.

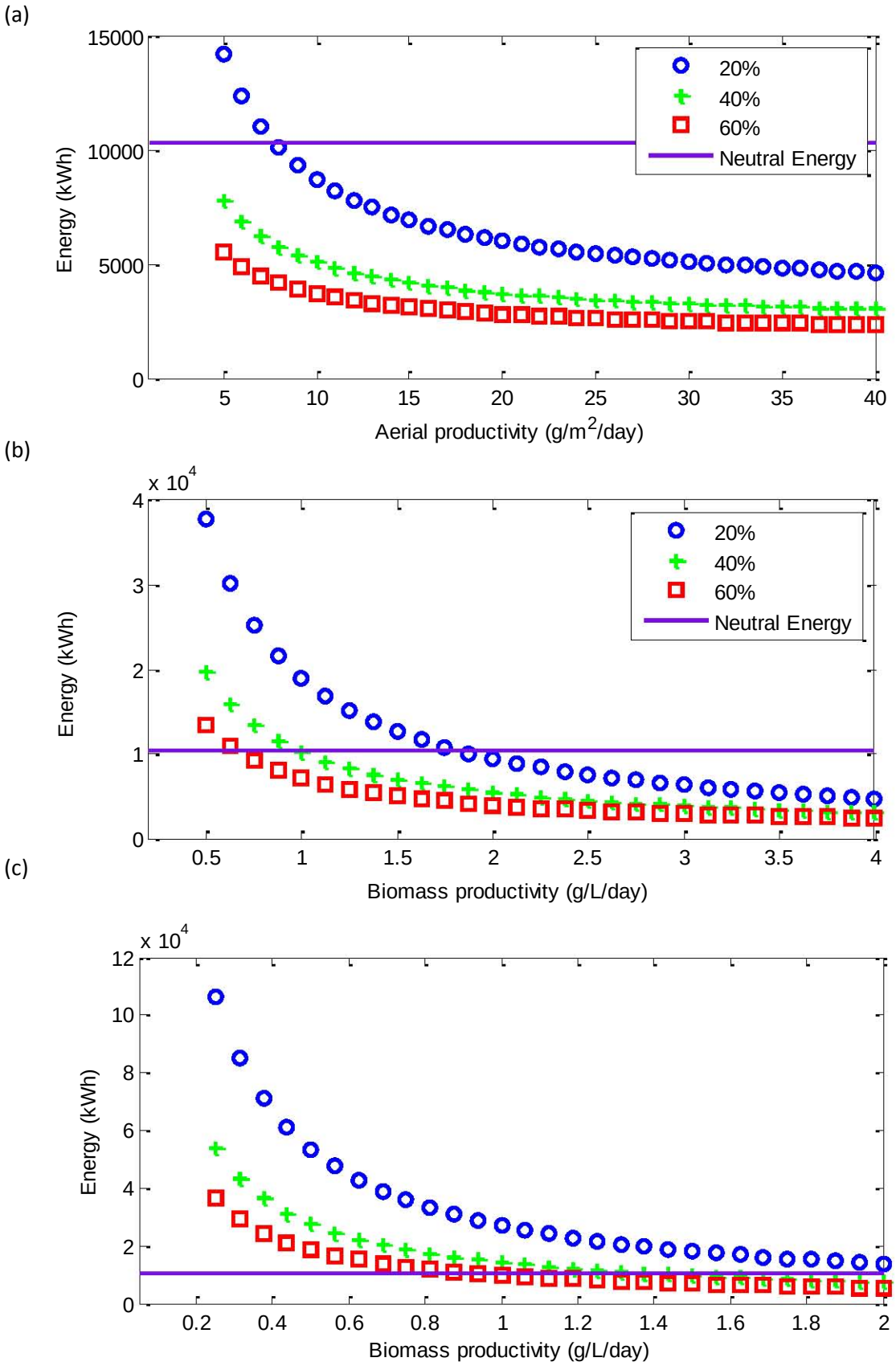

Figure 5-10 Total energy requirements various biomass productivities for lipid contents of 20, 40 and 60% in (a) raceway ponds (b) horizontal tubular reactors and (c) vertical tubular reactors. Base case scenario: biomass concentration 0.5 g/L in raceways, 3.96 g/L in horizontal tubular reactors and 1 g/L in vertical tubular reactors.

As mentioned earlier, the performance of the bioreactor is highly dependent on environmental conditions. Stephenson *et al.* (2010) noted that in the UK, the growing season is limited as the biomass and lipid productivity are both highly dependent on the temperature of the culture. Algal oil production is thus far more likely to be successful in regions with subtropical climates and low rainfall such as Israel, Hawaii and parts of Australia and South Africa.

5.7. Conclusions

As noted in Chapter 4, the energetic and environmental burdens of a microalgal biodiesel production facility are highly dependent on reactor performance. Thus both species choice and reactor configuration are key components to the success of such a facility.

The investigation of three possible reactor configurations has shown the raceway pond to be the most energetically favourable, showing an overall process energy gain of 4666 kWh/1000 kg of biodiesel in the base case, corresponding to an NER of 1.5. Further sensitivity analysis revealed that the raceway, despite low concentrations and productivities, is viable under the entire range of reasonable conditions. This, combined with its undisputed economic advantage, make it the current system of choice for algal biofuel production.

Horizontal tubular reactors were the more favourable of the two closed systems investigated, with a process energy gain of 782 kWh in the base case. The vertical tubular reactors investigated showed a vastly unfavourable energy balance. The much superior performance of the horizontal tubular reactors can largely be attributed to the much higher biomass productivity achieved in thinner tubes which allow for better light penetration.

For all systems, reactor energy was the dominant contributor to the overall process energy. At low biomass concentrations, particularly in raceways, the increased volumes to be processed can lead to a significant pumping energy requirement. In addition, a dilute slurry exiting the reactor phase has an increased flocculent requirement with respect to a more concentrated slurry, impacting the life cycle of the process. This encourages the use of algal strains that concentrate well under free settling.

Both increase in biomass productivity and lipid content have been shown to result in improvements in the total energy balances of all three systems. Raceways, horizontal and vertical tubular reactors were estimated to require lipid productivities above 0.005, 0.4 and 0.5 g/L/day respectively at the base case concentrations to afford an overall energy benefit. In the base case system, raceway ponds showed a lipid productivity of 0.015 g/L/day, well above of the required value.

Biodiesel production is highly dependent on bioreactor performance, both in terms of the bioreactor configuration and species specific characteristics. For the production of microalgal biodiesel in raceway ponds, the process appears energetically favourable, to minimise environmental burden and to be technically feasible.

6.Conclusions

This study has investigated the environmental feasibility of microalgal biodiesel through energy analysis and Life Cycle Assessment (LCA) to assess the system dependence on bioreactor design and operation in terms of overall environmental impact. Specifically, the effect of species choice and reactor type was examined.

The major findings of the thesis are presented in Section 6.1. In Section 6.2, findings are linked to the key questions of this thesis. Recommendations for future work are given in Section 6.3.

6.1. Major Findings

The species study, presented in Chapter 4, probed the feasibility of algal biodiesel for the chosen flow-sheet (Figure 3-1) using laboratory data for *Chlorella vulgaris*, *Scenedesmus* sp. and *Tetraselmus suecica*, grown in 3.2 L CeBER vertical tubular airlift reactors. In all cases, the production of biodiesel in the chosen system under its standard operating conditions on the laboratory scale yielded a negative energy balance, with the process energy requirements, additional to those supplied through biogas generated from waste algal biomass, being at least three times greater than the energy value of the biodiesel produced. Reactor energy was the dominant contributor to the energy requirement of the process. This showed the laboratory airlift reactor configuration to be entirely unfavourable for scale up for the production of microalgal biodiesel due to the energetic expense for air compression. However they remain appropriate defined systems for the generation of biological data.

A sensitivity study was conducted on the airlift reactors. This showed airflow rate and connecting reactors in series to offer order of magnitude reductions in reactor energy input required per unit volume mixed. These are thus identified as key operational variables.

For each of the three species, investigated over a range of simultaneously occurring biomass productivities, biomass concentrations and lipid contents, the minimum process energy requirement corresponded to the point of highest lipid productivity. Closer inspection revealed that lipid productivity was inversely proportional to reactor energy. Thus, a small increase in lipid productivity, would afford a significant change in reactor energy under conditions of high power input per unit volume. Given the dominance of the reactor contribution to the system energy balance, marginally superior lipid productivity outweighed any increase in DSP energy requirements as a result of lower biomass concentration. This reinforced lipid productivity as the key variable in microalgal species

choice for the production of biodiesel. *Scenedesmus* sp. exhibited the highest lipid productivity and thus the lowest overall process energy requirement for the production of 1000 kg biodiesel. The lipid productivity of 0.067 g/L/day, achieved by *Scenedesmus* sp., would require the power input per unit volume to decrease from 229 W/m^3 to ~16 W/m^3 to achieve a neutral energy scenario. Alternatively, if power input per unit volume were to remain unchanged, the lipid productivity would need to increase from 0.067 g/L/day to 0.19 g/L/day. From the 55 species documented in the 2009 review of Griffiths and Harrison, the highest lipid productivity calculated was 0.164 g/L/day with the freshwater species, *Ettlia oleoabundans*. For the optimisation of any algal bioenergy system, a balance must be found between increased reactor efficiency and lipid productivity. This is dependent on both the algal species and the reactor configuration.

Life Cycle Assessment was performed on a hypothetically optimised reactor system, where the airlift reactor was assumed to operate at power input per unit volume of 16 W/m^3 such that the system was energy neutral. Results agreed with previous LCAs, showing that fossil energy and fertiliser requirement were the key contributors to all impact categories. Allocation of the digestate following anaerobic digestion as fertiliser equivalent, thereby displacing industrial fertiliser was shown afford reductions for all species in all impact categories by as much as half. This supports further study into the use of wastewater and recycle of digestate back to the cultivation unit.

Chapter 5 investigated the production of algal oil from *Phaedodactylum tricornutum* in raceway ponds and horizontal and vertical tubular reactor systems integrated into the process flow-sheet. The raceway pond system showed a net energy ratio (NER) > 1 (energy in biodiesel produced: fossil energy required = 1.5), while the horizontal tubular reactor system showed a narrowly positive energy balance (NER = 0.97). The 60 L vertical tubular reactor, which was similar in configuration to the 3.2 L airlift reactors investigated in Chapter 4, showed a unrealistic negative energy balance (NER = 0.12). This indicates that this reactor configuration is not feasible for an algal biodiesel production system.

Life cycle impacts of the production of microalgal biodiesel using raceways showed lower impacts compared to that using horizontal tubular reactors. Notably, raceway systems showed a favourable score in the global warming impact category due to the CO_2 utilised for growth. While horizontal tubular reactors also utilised CO_2, this benefit was offset by the large reactor energy requirement.

The effect of varying algal biomass concentration, biomass productivity and lipid content in the three reactor configurations was investigated. At a biomass concentration of 0.1 g/L in raceway ponds, pumping energy contributed about half the total fossil energy requirement of the process owing to the high volumes resulting. This pumping energy requirement decreased by an order of magnitude

as the biomass concentration increased from 0.1 to 0.5 g/L. Further increase in biomass concentration showed a less pronounced decrease in pumping energy.

In all three reactor cases, increases in biomass productivity, lipid content and lipid productivity resulted in process energy reduction. This was due to a decreased reactor volume required and, to a lesser extent, pumping requirement.

From the analysis of lipid productivity, it would appear that cultivation in raceway ponds is both realistic and achievable as, despite low concentrations and productivities, the system provided a net energy gain under the entire range of reasonable conditions.

Overall, the energetic and environmental burdens of the microalgal biodiesel production facility were shown to be highly dependent on reactor performance, with both species choice and reactor configuration as key components to the success of such a facility. Further, life cycle assessment (LCA) was demonstrated to provide useful insight into environmental burden impacts and is an essential part of process development in immature technology

6.2. Findings Related to Key Questions

The key questions of this thesis, posed in Section 1.7 are stated and addressed in this section.

1. Is the production of algal biodiesel environmentally feasible?

The production of algal biodiesel was shown to be environmentally feasible if microalgae are cultivated in raceways over the entire range of reasonable conditions. Cultivation in the configuration of vertical tubular airlift reactor examined by this thesis was shown to be entirely infeasible. Cultivation in the horizontal tube photobioreactor demonstrated that, through ongoing process improvement, environmentally feasible algal biodiesel production may be attainable.

2. How does the reactor unit contribute to the energetic and environmental burden relative to the remainder of the process?

In all cases, the reactor was shown to be the dominant contributor the overall system energy requirement and environmental burden. At biomass concentrations below 0.5 g/L for cultivation in raceway ponds, pumping energy was also shown to be noteworthy, but to a lesser extent to that of reactor energy.

3. How does the environmental impact of biofuel production differ depending on the microalgal species used?

In general, species with higher lipid productivities were shown to result in decreased overall process energy requirements and thus, lower environmental impacts. Additionally, where lime was used to flocculate biomass, it was shown to contribute significantly to the global warming impact category where raceways gave a final biomass concentration of 0.5 g/l exiting the reactor. This advocates the use, within reason, of species that settle well under gravity without the addition of chemicals and the avoidance of very low biomass concentrations.

4. How does the environmental impact of biofuel production differ depending on the bioreactor used for algal growth?

The reactor has a critical influence on environmental impact of biofuel production as it represents the largest energy requirement of the process. Comparison across reactor types illustrated that the magnitude of the reactor energy requirement is not necessarily the critical factor, rather the ratio between this energy requirement and the energy generated through the algal system. Where the power input per unit volume is too large, the resultant overall fossil energy requirement was shown to cause such systems to be infeasible i.e. an NER less than 1. This occurs where the maximum attainable lipid productivity cannot meet the reactor energy input, whereas reactors with low energy input such as the raceway were shown to be able to accommodate lower lipid productivities.

5. What are the key contributors to the environmental impact of algal biodiesel production?

Fossil energy and fertiliser requirement were shown to be the dominant contributors to the environmental impact of the process. This finding is supported by concurrent algal biodiesel LCA studies

6. What operating variables most influence changes to the energetic and environmental impact of the overall process?

This study reinforces lipid productivity as the key variable in species choice. The reactor energy requirement was shown to be inversely proportional to lipid productivity. Thus, when reactor energy is large, small changes in lipid productivity can result in order of magnitude reductions in overall system energy. When reactor power per unit volume is lower, changes to the lipid productivity are less significant in their effect on overall system energy.

As mentioned in (2) above, biomass concentration influences reactor volume required and through this, pumping energy. At low biomass concentrations in the range 0.1 to 0.5 g/L, influence on pumping energy was notable.

For airlift reactor systems, airflow rate and connecting reactors in series were identified as key operational variables, offering order of magnitude reductions in reactor energy input required per unit volume mixed.

6.3. Future Work

The research findings have highlighted a number of questions which require additional study, beyond the scope of this thesis. These require further research in the following areas:

- Decoupling the relationship between lipid productivity and reactor energy.
- Exploring the link between light energy and reactor energy consumption, following the findings of this thesis, where the horizontal tubular airlift reactor, consisting of an airlift system and solar receiver showed a far superior energy balance to the vertical tubular airlift reactor, which did not have the benefit of the solar receiver for increased light capture.
- Exploring possible locations for the production of microalgal biodiesel, both in terms of climate considerations and proximity to power plants from which waste CO_2 could be utilised. This is particularly relevant given the added burden when compressed liquefied CO_2 is used.
- Consideration of process economics and, in particular, the production of valuable co-products. While tubular reactors are more expensive to construct and operate, if coupled with a valuable co-product, they may become more desirable. This is more possible in closed systems.
- Pilot and demonstration scale facilities operated for an extended period of time (at least a year, to cover all four seasons). Current large scale data are limited largely to Aquatic Species Program results.
- Toxicity studies to consider the effect of recycling the post-anaerobic digestion digestate back to the growth phase to displace chemical fertilisers and thus decrease the overall environmental burden.

7. References

Aden, A., Ruth, M., Ibsen, K., Jechura, J., Neeves, K., Sheehan, J., Wallace, B., Montague, L., Slayton, A. & Lukas, J. 2002. *Lignocellulosic biomass to ethanol process design and economics utilizing co-current dilute acid prehydrolysis and enzymatic hydrolysis for corn stover. NREL Technical Report, NREL/TP-510-32438.*

Anderson, R.A. 2005. Algal Culturing Techniques. 1st Edition. Elsevier, London.

Bailey, J. & Ollis, D. 1977. Biochemical Engineering Fundamentals. McGraw- Hill, Inc, New York.

Basson, M.S., Van Niekerk, P.H. & Van Rooyen, J.A. 1997. *Overview of Water Resources Availability and Utilisation in South Africa.* Pretoria, South Africa: Department of Water Affairs and Forestry.

Batan, L., Quinn, J., Willson, B. & Bradley, T. 2010. Net Energy and Greenhouse Gas Emission Evaluation of Biodiesel Derived from Microalgae. *Environmental Science & Technology.* 44(20):7975-7980.

Becker, E.W. 1994. Microalgae: biotechnology and microbiology. Cambridge University Press, New York.

Bello, R.A. 1985. Gas holdup and overall volumetric oxygen transfer coefficient in airlift contactors. *Biotechnology & Bioengineering.* 27(3):369-381.

Benedict, R.P. 1980. Fundamentals of pipe flow. Wiley-Interscience, New York.

Benemann, J. & Oswald, W.J. 1996.
Systems and Economic Analysis of Microalgae Ponds for Conversion of CO_2 to Biomass. Pittsburgh Energy Technology Center: U.S. DOE.

Benitez, J. 2002. Principles and Modern Applications of Mass Transfer Operations. 2nd Edition. Wiley, New York.

Borowitzka, 1997. Microalgae for aquaculture: opportunities and constraints. *Journal of Applied Phycology.* 9(5):393-401.

Borowitzka, M.A. 1988. Microalgal Biotechnology. Cambridge University Press, Cambridge.

Bouterfas, R., Belkoura, M. & Dauta, A. 2002. Light and temperature effects on the growth rate of three freshwater algae from a eutrophic lake. *Hydrobiologia.* (489):207-217.

Calderbank, P.H. & Moo-Young, M.B. 1961. The continuous phase heat and mass transfer properties of dispersions. *Chemical Engineering Science.* 16:39-54.

Camacho, F.G., Gómez, A.C., Sobczuk, T.M. & Grima, E.M. 2000. Effects of mechanical and hydrodynamic stress in agitated, sparged cultures of Porphyridium cruentum. *Process Biochemistry.* 35(9):1045-1050.

Campbell, P.K., Beer, T. & Batten, D. 2010. Life cycle assessment of biodiesel production from microalgae in ponds. *Bioresource Technology.* In Press, Corrected Proof.

Carvalho, 2006. Microalgal reactors: a review of enclosed system designs and performances. *Biotechnology Progress.* 22(6):1490-506.

Chen, F. 1996. High cell density culture of microalgae in heterotrophic growth. *Trends in Biotechnology.* 14(11):421-426.

Chisti, Y. 1989. Airlift Bioreactors. Elsevier, New York.

Chisti, Y. 2007. Biodiesel from microalgae. *Biotechnology Advances.* 25(3):294-306.

Chisti, Y. 2002. *Mass Transfer.* John Wiley & Sons, Inc.

Chisti, Y. 2008. Biodiesel from microalgae beats bioethanol. *Trends in Biotechnology.* 26(3):126-131.

Clarens, A.F., Resurreccion, E.P., White, M.A. & Colosi, L.A. 2010. Environmental life cycle comparison of algae to other bioenergy feedstocks. *Environmental Science & Technology.* 44(5):1813.

Collet, P., Hélias, A., Lardon, L., Ras, M., Goy, R. & Steyer, J. 2010. Life-cycle assessment of microalgae culture coupled to biogas production. *Bioresource Technology.* In Press, Accepted Manuscript.

Curran, M.A. 2000. Life cycle assessment: An international experience. *Environmental Progress.* 19(2):65-71.

Evans, A., Strezov, V. & Evans, T.J. 2009. Assessment of sustainability indicators for renewable energy technologies. *Renewable and Sustainable Energy Reviews.* 13(5):1082-1088.

Fargione, 2008. Land clearing and the biofuel carbon debt. *Science.* 319(5867):1235.

Finnveden, G., Johansson, J., Lind, P. & Moberg, Å. 2005. Life cycle assessment of energy from solid waste—part 1: general methodology and results. *Journal of Cleaner Production.* 13(3):213-229.

Geider, R.J. & La Roche, J. 2002. Redfield revisited: variability of C:N:P in marine microalgae and its biochemical basis. *European Journal of Phycology.* 37(01):1.

Gibbs, H., Johnston, M., Foley, J., Holloway, T., Monfreda, C., Ramankutty, N. & Zaks, D. 2008. Carbon payback times for crop-based biofuel expansion in the tropics: the effects of changing yield and technology. *Environmental Research Letters.* 3(3):034001.

Griffiths, M.J. 2011. Optimising microalgal lipid for biodiesel production. Thesis submitted for the degree of Doctor of Philosophy. University of Cape Town.

Griffiths, M.J. 2009. Unpublished data from CeBER.

Griffiths, M.J., van Hille, R.P. & Harrison, S.T.L. 2011. Lipid productivity, settling potential and fatty acid profile of eleven microalgal species grown under nitrogen replete and limited conditions. *Journal of Applied Phycology.* Accepted.

Griffiths, M.J. & Harrison, S.T.L. 2009. Lipid productivity as a key characteristic for choosing algal species for biodiesel production. *Journal of Applied Phycology.* 21(5):493-507.

Guinée, J.B. 2002. Handbook on Life Cycle Assessment: Operational Guide to the ISO Standards. Springer, New York.

Harding, K.G. 2009. *A Generic Approach to Environmental Assessment of Microbial Bioprocesses through Life Cycle Assessment.* Thesis submitted for the degree of Doctor of Philosophy. Cape Town, South Africa: University of Cape Town.

Harding, K.G., Dennis, J.S., von Blottnitz, H. & Harrison, S.T.L. 2008. A life-cycle comparison between inorganic and biological catalysis for the production of biodiesel. *Journal of Cleaner Production.* 16(13):1368-1378.

Harvey, A.P., Mackley, M.R. & Stonestreet, P. 2001. Operation and Optimization of an Oscillatory Flow Continuous Reactor. *Industrial & Engineering Chemistry Research.* 40(23):5371-5377.

Henderson, R., Parsons, S.A. & Jefferson, B. 2008. The impact of algal properties and pre-oxidation on solid–liquid separation of algae. *Water Research.* 42(8-9):1827-1845.

Hills, J.H. 1976. The operation of a bubble column at high throughputs : I. Gas holdup measurements. *The Chemical Engineering Journal.* 12(2):89-99.

Hospido, A., Carballa, M., Moreira, M., Omil, F., Lema, J.M. & Feijoo, G. 2010. Environmental assessment of anaerobically digested sludge reuse in agriculture: Potential impacts of emerging micropollutants. *Water Research.* 44(10):3225-3233.

Huntley, M. & Redalje, D. 2007. CO 2 mitigation and renewable oil from photosynthetic microbes: A new appraisal. *Mitigation and Adaptation Strategies for Global Change.* 12(4):573-608.

Illman, A.M., Scragg, A.H. & Shales, S.W. 2000. Increase in Chlorella strains calorific values when grown in low nitrogen medium. *Enzyme and Microbial Technology.* 27(8):631-635.

Janssen, 2003. Enclosed outdoor photobioreactors: light regime, photosynthetic efficiency, scale-up, and future prospects. *Biotechnology & Bioengineering.* 81(2):193-210.

Jorquera, O., Kiperstok, A., Sales, E.A., Embiruçu, M. & Ghirardi, M.L. 2010. Comparative energy life-cycle analyses of microalgal biomass production in open ponds and photobioreactors. *Bioresource Technology.* 101(4):1406-1413.

Jury, C., Benetto, E., Koster, D., Schmitt, B. & Welfring, J. 2010. Life Cycle Assessment of biogas production by monofermentation of energy crops and injection into the natural gas grid. *Biomass and Bioenergy.* 34(1):54-66.

Kadam, K.L. 2002. Environmental implications of power generation via coal-microalgae cofiring. *Energy.* 27(10):905-922.

Kaltschmitt, M., Reinhardt, G.A. & Stelzer, T. 1997. Life cycle analysis of biofuels under different environmental aspects. *Biomass and Bioenergy.* 12(2):121-134.

Kaparaju, P., Serrano, M., Thomsen, A.B., Kongjan, P. & Angelidaki, I. 2009. Bioethanol, biohydrogen and biogas production from wheat straw in a biorefinery concept. *Bioresource Technology.* 100(9):2562-2568.

Kim, S. & Dale, B.E. 2005. Life cycle assessment of various cropping systems utilized for producing biofuels: Bioethanol and biodiesel. *Biomass and Bioenergy.* 29(6):426-439.

Langley, N.M. 2010. *Strategies for Carbon Dioxide Delivery to Microalgal Cultures and their Potential for the Reduction of Emissions.* Thesis submitted for the degree of Master of Science in Engineering. Cape Town, South Africa: University of Cape Town.

Lardon, L., Helias, A., Sialve, B., Steyer, J. & Bernard, O. 2009. Life-Cycle Assessment of Biodiesel Production from Microalgae. *Environmental Science & Technology.* 43(17):6475-6481.

Larson, E.D. 2006. A review of life-cycle analysis studies on liquid biofuel systems for the transport sector. *Energy for Sustainable Development.* 10(2):109-126.

Lechón, Y.e.a. 2005. Life cycle analysis of wheat and barley crops for bioethanol production in Spain. *International Journal of Agricultural Resources, Governance and Ecology.* 4(2):113-122.

Lee, 2001. Microalgal mass culture systems and methods: Their limitation and potential. *Journal of applied phycology.* 13(4):307.

Levin, G.V., Clendenning, J.R., Gibor, A. & Bogar, F.D. 1962. Harvesting of algae by froth flotation. *Applied and Environmental Microbiology.* 10(2):169-175.

Li, 2008. Biofuels from microalgae. *Biotechnology Progress.* 24(4):815-820.

Liu, D. & Liptak, B.G. 1997. Environmental Engineering Handbook. 2nd Edition. Lewis Publishers, New York.

Mirón, A.S., García Camacho, F., Contreras Gómez, A., Molina Grima, A. & Chisti, Y. 2000. Bubble-column and airlift photobioreactors for algal culture. *AIChE Journal.* 46(9):1872-1887.

Mirón, A.S., García, M.C.C., Gómez, A.C., Camacho, F.G., Grima, E.M. & Chisti, Y. 2003. Shear stress tolerance and biochemical characterization of Phaeodactylum tricornutum in quasi steady-state continuous culture in outdoor photobioreactors. *Biochemical Engineering Journal.* 16(3):287-297.

Molina Grima, E., Belarbi, E.-., Acién Fernández, F.G., Robles Medina, A. & Chisti, Y. 2003. Recovery of microalgal biomass and metabolites: process options and economics. *Biotechnology Advances.* 20(7-8):491-515.

Molina Grima, E., Fernández, F.G.A., García Camacho, F. & Chisti, Y. 1999. Photobioreactors: light regime, mass transfer, and scaleup. *Journal of Biotechnology.* 70(1-3):231-247.

Molina, E., Fernández, J., Acién, F.G. & Chisti, Y. 2001. Tubular photobioreactor design for algal cultures. *Journal of Biotechnology.* 92(2):113-131.

Najafpour, G.D. 2007. Biochemical Engineering and Biotechnology. Elsevier, Burlington.

Panichelli, L. 2009. Life cycle assessment of soybean-based biodiesel in Argentina for export. *The International Journal of Life Cycle Assessment.* 14(2):144.

Perry, R.H. & Green, D.W. 1997. *Perry's Chemical Engineers' Handbook.* 7th. McGraw-Hill.

Piek, A. 2010. GEA Westfalia Separator Group GmbH.

Poitrat, E. 1999. The potential of liquid biofuels in France. *Renewable Energy.* 16(1-4):1084-1089.

Pulz, 2001. Photobioreactors: production systems for phototrophic microorganisms. *Applied Microbiology and Biotechnology.* 57(3):287-293.

Ras, M., Lardon , L., Sialve, B., Bernet, N. & Steyer, J. 2010. Experimental study on a coupled process of production and anaerobic digestion of Chlorella vulgaris. *Bioresource Technology.* In Press, Accepted Manuscript.

Richardson, J.F., Harker, J.H. & Backhurst, J.R. 2002. Particle Technology and Separation Processes. Volume 2. 5 Edition. Elsevier.

Richmond, A. 2004a. Principles for attaining maximal microalgal productivity in photobioreactors: an overview. *Hydrobiologia.* 512(1):33-37.

Richmond, A. 2004b. Handbook of microalgal culture biotechnology and applied phycology. Blackwell Science, Oxford OX UK Ames Iowa USA.

Rodolfi, L., Zittelli, G.C., Bassi, N., Padovani, G., Biondi, N., Bonini, G. & Tredici, M.R. 2009. Microalgae for oil: Strain selection, induction of lipid synthesis and outdoor mass cultivation in a low-cost photobioreactor. *Biotechnology & Bioengineering.* 102(1):100-112.

Rosello Sastre, R., Csögör, Z., Perner-Nochta, I., Fleck-Schneider, P. & Posten, C. 2007. Scale-down of microalgae cultivations in tubular photo-bioreactors—A conceptual approach. *Journal of Biotechnology.* 132(2):127-133.

Samson, R. 1986. Detailed study of anaerobic digestion of Spirulina maxima algal biomass. *Biotechnology & Bioengineering.* 28(7):1014-1023.

Sánchez Mirón, A., Cerón García, M., García Camacho, F., Molina Grima, E. & Chisti, Y. 2002. Growth and biochemical characterization of microalgal biomass produced in bubble column and airlift photobioreactors: studies in fed-batch culture. *Enzyme and Microbial Technology.* 31(7):1015-1023.

Sánchez Mirón, A., Contreras Gómez, A., García Camacho, F., Molina Grima, E. & Chisti, Y. 1999. Comparative evaluation of compact photobioreactors for large-scale monoculture of microalgae. *Journal of Biotechnology.* 70(1-3):249-270.

Sazdanoff, N. 2006. *Modeling and Simulation of the Algae to Biodiesel Fuel Cycle.* Undergraduate. United States: Department of Mechanical Engineering, The Ohio State University.

Schenk, 2008. Second generation biofuels: High-efficiency microalgae for biodiesel production. *Bioenergy Research.* 1(1):20-43.

Scragg, A.H., Illman, A.M., Carden, A. & Shales, S.W. 2002. Growth of microalgae with increased calorific values in a tubular bioreactor. *Biomass and Bioenergy.* 23(1):67-73.

Searchinger, 2008. Use of US croplands for biofuels increases greenhouse gases through emissions from land-use change. *Science.* 319(5867):1238-1240.

Sheehan, J., Dunahay, T., Benemann, J. & Roessler, P. 1998. *A look back at the U.S. Department of Energy's Aquatic Species Program: Biodiesel from Algae. Close-Out report.* Golden, Colorado, U.S.A.: National Renewable Energy Lab, Department of Energy.

Sialve, B., Bernet, N. & Bernard, O. 2009. Anaerobic digestion of microalgae as a necessary step to make microalgal biodiesel sustainable. *Biotechnology Advances.* 27(4):409-416.

Sinnott, R.K. 1999. Coulson and Richardson's Chemical Engineering. Volume 6. 3rd Edition. Butterworth – Heinemann Ltd, Oxford, U.K.

Stephenson, A.L. 2009. *The Sustainability of First- and Second-Generation Biofuels using Life Cycle Analysis.* Thesis submitted for the degree of Doctor of Philosophy. United Kingdom: University of Cambridge.

Stephenson, A.L., Kazamia, E., Dennis, J.S., Howe, C.J., Scott, S.A. & Smith, A.G. 2010. Life-Cycle Assessment of Potential Algal Biodiesel Production in the United Kingdom: A Comparison of Raceways and Air-Lift Tubular Bioreactors. *Energy & Fuels.* 43(17):4062-4077.

Talbot, P., Gortares, M.P., Lencki, R.W. & de la Noüe, J. 1991. Absorption of CO_2 in algal mass culture systems: A different characterization approach. *Biotechnology & Bioengineering.* 37(9):834-842.

Taylor, B. 2009. University of Cambridge.

Ugwu, C.U., Aoyagi, H. & Uchiyama, H. 2008. Photobioreactors for mass cultivation of algae. *Bioresource Technology.* 99(10):4021-4028.

Ugwu, C.U. 2005. Light/dark cyclic movement of algal culture (Synechocystis aquatilis) in outdoor inclined tubular photobioreactor equipped with static mixers for efficient production of biomass. *Biotechnology Letters.* 27(2):75-78.

Ugwu, C.U., Ogbonna, J.C. & Tanaka, H. 2005. Characterization of light utilization and biomass yields of Chlorella sorokiniana in inclined outdoor tubular photobioreactors equipped with static mixers. *Process biochemistry.* 40(11):3406.

Uihlein, A. & Schebek, L. 2009. Environmental impacts of a lignocellulose feedstock biorefinery system: An assessment. *Biomass and Bioenergy.* 33(5):793-802.

Vasudevan, P. & Briggs, M. 2008. Biodiesel production-current state of the art and challenges. *Journal of Industrial Microbiology Biotechnology.* 35(5):421-430.

Vunjak-Novakovic, G., Kim, Y., Wu, X., Berzin, I. & Merchuk, J.C. 2005. Air-Lift Bioreactors for Algal Growth on Flue Gas: Mathematical Modeling and Pilot-Plant Studies. *Industrial & Engineering Chemistry Research.* 44(16):6154-6163.

Waites, M.J. 2001. Industrial microbiology: an introduction. Oxford : Blackwell Science, UK.

Wang, M. 1999. *GREET – Transportation Fuel-Cycle Model.* Center for Transportation Research, Energy Systems Division, Argonne National Laboratory: .

Weissman, J.C. & Goebel, R.P. 1987. *Design and Analysis of Microalgal Open Pond Systems for the Purpose of Producing Fuels.* Golden, CO: U.S. Department of Energy Solar Energy Research Institute.

Weissman, J.C. & Tillet, D.M. 1989. Design and operation of an outdoor microalgae test facility: Large-Scale System Results. NREP, Golden, CO.

Welty, J.R., Wicks, C.E., Wilson, R.E. & Rorrer, G. 2001. Fundamentals of momentum, heat and mass transfer. 4th Edition. John Wiley & Sons, New York.

Wijffels, R.H. 2008. Potential of sponges and microalgae for marine biotechnology. *Trends in Biotechnology.* 26(1):26-31.

Wu, X. & Merchuk, J.C. 2004. Simulation of algae growth in a bench scale internal loop airlift reactor. *Chemical Engineering Science.* 59(14):2899-2912.

Yang, J., Xu, M., Zhang, X., Hu, Q., Sommerfeld, M. & Chen, Y. 2011. Life-cycle analysis on biodiesel production from microalgae: Water footprint and nutrients balance. *Bioresource Technology.* 102(1):159-165.

Zhang, Y., Singh, S. & Bakshi, B.R. 2010. Accounting for Ecosystem Services in Life Cycle Assessment, Part I: A Critical Review. *Environmental Science & Technology.*

Zuber, N. & Findlay, J.A. 1965. Average volumetric concentration in two phase flow systems. *Journal of Heat Transfer.* 18:453-468.

A. Appendix

A.1. Data for Algal Process model

A.1.1. Biodiesel and Lipase production

Table A-1 Mass, energy and utility flows obtained by Harding (2009) for the production of 1 000 kg of biodiesel

Products		
Biodiesel	1000	kg
Glycerol	106	kg
Feed		
Oil	991	kg
MeOH	111	kg
Lipase	1.6	kg
Steam	1540	kg
Electricity	34.1	kWh
Water (process)	56.4	kg
Water (cooling)	97.4	kg
Waste		
MeOH	2.4	kg
Water	50.9	kg

Table A-2 Material, energy and utility flows for the production of lipase from *Candida antarctica* (Harding, 2009)

In		
Glucose	3.6	kg
Yeast	2.4	kg
Air	3.6	kg
Precipitating chemical	1.5	kg
Water	20.1	kg
Out		
Glucose	0.036	kg
Yeast	0.12	kg
Precipitating chemical	1.5	kg
Co2	5.2	kg
Phosphates	0.9	kg
Water	22.4	kg
Lipase	1	kg
Energy		
Electricity	35.4	MJ/kg lip
Steam (152°C, 3 bar)	14.3	MJ/kg lip
Total energy equivalent	49.7	MJ/kg lip
Cooling water	14	kg/kg lip

A.1.2. Experimental Growth and Composition Data

The literature study done by Griffiths and Harrison in 2009 concluded that there was a need for more experimental work to allow for comparison of species under similar growth conditions, regarding the trade off between growth rate and lipid content under nitrogen deprivation. In response, Griffiths *et al.* (2011) compared, under similar culture conditions, the lipid productivity, settling potential and fatty acid profile of 11 microalgal species, under both nitrogen sufficient and deficient conditions in airlift photobioreactors. Microalgae were grown in batch culture in 3.2 L vertical tubular airlift photobioreactors (shown in Figure 3-2). CO_2 enriched air was sparged at 2 $L.min^{-1}$ using a 0.29 % CO_2 concentration, shown to be non-carbon-limiting under these conditions (Langley, 2010). Constant light was provided at 250 $\mu mol.m^{-2}.sec^{-1}$ by three cool white 18W fluorescent light bulbs (Osram) at the reactor surface. Culture temperature was monitored daily and remained a constant 25°C ±1°C. These data were collected in conjunction with Griffiths and is reported in full in Griffiths et al. (2011).

The species showing with highest lipid productivity under nitrate deprivation were *Chlorella vulgaris* and *Scenedesmus* sp. *Cylindrotheca fusiformis*, *Spirulina platensis*, *Scenedesmus* and *Tetraselmis suecica* showed the fastest settling rates and highest biomass recoveries after 24 hours of gravity sedimentation. Experimental data generated for Griffiths et al. (2011), used as input to the present work, is shown in Table A.3 to A.5.

Table A-3 Daily growth data and biomass composition for *Chlorella vulgaris* grown under low nitrogen conditions

Day		0	0.5	0.8	1.5	1.9	2.5	3	3.8	4.9	5.8	6.8	7.6	8.9	9.7
Biomass concentration	g/L	0.03	0.10	0.10	0.26	0.41	0.51	0.37	0.52	0.64	0.69	0.74	0.79	0.82	0.82
Productivity	g/L/day	0.12	0.22	0.27	0.25	0.15	0.12	0.07	0.06	0.05	0.03	0.02	0.02	0.02	0.02
Protein	%	58	58	58	58	58	58	58	58	48	40	31	24	12	7
Carbohydrate	%	17	17	17	17	17	17	17	17	24	30	37	43	51	55
Lipid content	%	22	22	22	22	22	22	22	22	26	28	32	34	38	40
Pigment	%	3.37	4.4	5.38	4.9	4.4	4.7	4.97	3.45	1.61	1.26	1.11	0.98	0.89	0.79
C	-	0.54	0.54	0.54	0.54	0.54	0.54	0.54	0.54	0.55	0.55	0.55	0.55	0.56	0.56
H	-	0.08	0.08	0.08	0.08	0.08	0.08	0.08	0.08	0.08	0.08	0.08	0.08	0.09	0.09
N	-	0.09	0.09	0.09	0.09	0.09	0.09	0.09	0.09	0.08	0.06	0.05	0.04	0.02	0.01

Table A-4 Daily growth data and biomass composition for *Scenedesmus* sp. grown under low nitrogen conditions

Day		0.3	0.8	1.1	1.8	2.2	2.8	3.3	4.1	5.2	6.1	7.1	7.9	9.2	10.0	11.0
Biomass concentration	g/L	0.08	0.22	0.30	0.44	0.63	0.85	0.98	1.22	1.36	1.51	1.71	1.72	1.76	1.54	1.70
Productivity	g/L/day	0.20	0.24	0.32	0.35	0.37	0.30	0.23	0.20	0.16	0.12	0.08	0.08	0.03	0.08	0.02
Protein	%	52	52	52	52	52	52	52	52	44	37	30	24	14	8	0.02
Carbohydrate	%	18	18	18	18	18	18	18	18	24	29	35	39	46	50	56
Lipid content	%	18	18	18	18	18	18	18	18	21	23	26	28	31	33	36
Pigment	%	5.1	5.1	4.7	4.2	3.0	3.0	1.7	2.4	1.7	0.7	0.6	0.5	0.4	0.4	0.3
C	-	0.60	0.60	0.60	0.60	0.60	0.60	0.60	0.60	0.64	0.67	0.71	0.75	0.80	0.83	0.87
H	-	0.07	0.07	0.07	0.07	0.07	0.07	0.07	0.07	0.07	0.07	0.07	0.08	0.08	0.08	0.08
N	-	0.088	0.088	0.088	0.087	0.087	0.087	0.086	0.086	0.072	0.061	0.048	0.039	0.024	0.014	0.003

Table A-5 Daily growth data and biomass composition for *Tetraselmis suecica* grown under low nitrogen conditions

Day		0.7	0.9	1.7	2.0	2.7	2.9	3.8	4.7	5.7	6.8	7.7	8.8
Biomass concentration	g/L	0.29	0.43	0.83	0.92	1.28	1.34	1.49	1.98	1.99	2.07	2.02	2.05
Productivity	g/L/day	0.46	0.49	0.45	0.36	0.30	0.32	0.24	0.21	0.01	0.02	0.01	0.02
Protein	%	60	55.6	51.2	52.8	54.5	50.7	46.9	46.0	40.4	42.3	42.1	41.8
Carbohydrate	%	25	28.3	31.6	30.3	29.1	31.9	34.8	35.5	39.6	38.2	38.3	38.6
Lipid content	%	4.0	5.5	7.1	6.5	5.9	7.3	8.6	8.9	10.9	10.2	10.3	10.4
Pigment	%	1.54	1.18	0.81	0.97	1.13	0.82	0.51	0.58	1.10	0.41	0.57	0.36
C	-	0.45	0.45	0.45	0.45	0.45	0.45	0.46	0.46	0.46	0.46	0.46	0.46
H	-	0.06	0.07	0.07	0.07	0.07	0.07	0.07	0.07	0.07	0.07	0.07	0.07
N	-	0.10	0.09	0.08	0.09	0.09	0.08	0.08	0.07	0.07	0.07	0.07	0.07

A.2. Material and Energy Inventory Data

Selected material inventories, generated using the simulation model, are shown here. Figure A-1 shows the process flow-sheet. Table A-6 shows the composition of each stream for *Scenedesmus* sp grown at the point of highest instantaneous lipid productivity. Table A-7, A-8 and A-9 show the composition of each stream for *Phaedodactylum tricornutum* grown in raceway ponds, horizontal and vertical tubular reactor systems respectively.

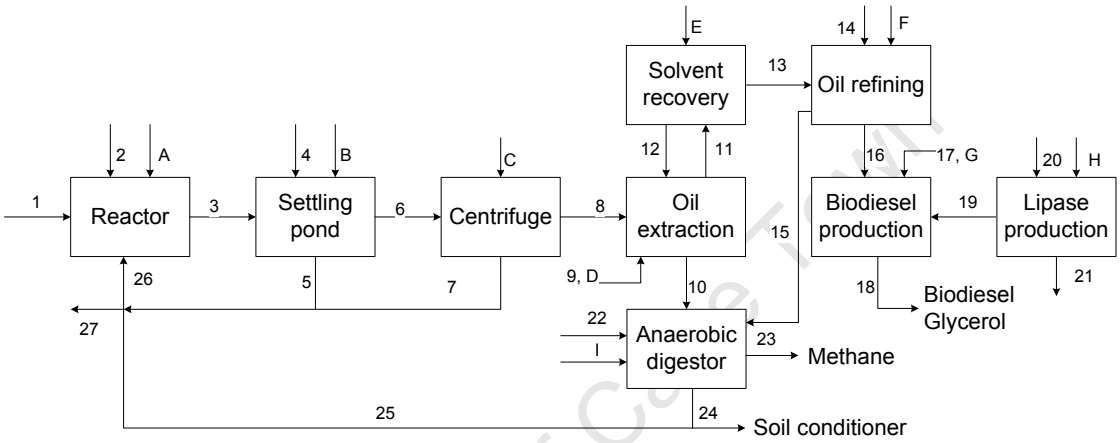

Figure A-1 Process Flow-sheet for the system investigated in Chapters 4 and 5. Annotations 1-24 refer to flows and A-I to energy inputs.

Table A-6 Composition of the streams in the process flow diagram, Figure A-1, for the production of 1000 kg of biodiesel from *Scenedesmus* sp. grown at the point of highest instantaneous lipid productivity in the laboratory airlift reactors described in Section 3.4.2

Flows (kg/day)	1	2	3	4	5	6	7	8	9
Water	2620000	0	13000000	0	12900000	64200	29400	34800	0
Cells	0	0	8130	0	813	7320	366	6950	0
Ammonium nitrate	2120	0	0	0	0	0	0	0	0
Triple super phosphate	878	0	0	0	0	0	0	0	0
Potassium chloride	372	0	0	0	0	0	0	0	0
Aluminium sulphate	0	0	0	0	0	0	0	0	0
Hexane	0	0	0	0	0	0	0	0	57.3
Phosphoric acid	0	0	0	0	0	0	0	0	0
NaOh	0	0	0	0	0	0	0	0	0
Methanol	0	0	0	0	0	0	0	0	0
Biodiesel	0	0	0	0	0	0	0	0	0
Glycerol	0	0	0	0	0	0	0	0	0
Cooling water	0	0	0	0	0	0	0	0	0
Steam	0	0	0	0	0	0	0	0	0
Glucose	0	0	0	0	0	0	0	0	0
Yeast	0	0	0	0	0	0	0	0	0
Precipitating chemical	0	0	0	0	0	0	0	0	0
CO_2	0	17800	0	0	0	0	0	0	0
Phosphates	0	0	0	0	0	0	0	0	0
Urea	0	0	0	0	0	0	0	0	0
Methane (STP)	0	0	0	0	0	0	0	0	0
Lime (flocculent)	0	0	0	0	0	0	0	0	0
TAG	0	0	0	0	0	0	0	0	0
Chlorophyll	0	0	0	0	0	0	0	0	0
Lipase	0	0	0	0	0	0	0	0	0
Total	2630000	17800	13000000	0	12900000	71500	29800	41700	57.3

Flows (kg/day)	10	11	12	13	14	15	16	17	18
Water	34800	0	0	0	134	0	0	56.4	50.9
Cells	5780	0	0	0	0	0	0	0	0
Ammonium nitrate	0	0	0	0	0	0	0	0	0
Triple super phosphate	0	0	0	0	0	0	0	0	0
Potassium chloride	0	0	0	0	0	0	0	0	0
Aluminium sulphate	0	0	0	0	0	0	0	0	0
Hexane	0	11500	11400	57.3	0	28.6	28.6	0	0
Phosphoric acid	0	0	0	0	1.23	0	0	0	0
NaOh	0	0	0	0	3.68	0	0	0	0
Methanol	0	0	0	0	0	0	0	111	2.4
Biodiesel	0	0	0	0	0	0	0	0	1000
Glycerol	0	0	0	0	0	0	0	0	106
Cooling water	0	0	0	0	0	0	0	97.4	97.4
Steam	0	0	0	0	0	0	0	1540	0
Glucose	0	0	0	0	0	0	0	0	0
Yeast	0	0	0	0	0	0	0	0	0
Precipitating chemical	0	0	0	0	0	0	0	0	0
CO_2	0	0	0	0	0	0	0	0	0
Phosphates	0	0	0	0	0	0	0	0	0
Urea	0	0	0	0	0	0	0	0	0
Methane (STP)	0	0	0	0	0	0	0	0	0
Lime (flocculent)	0	0	0	0	0	0	0	0	0
TAG	0	1000	0	1000	0	10	991	0	0
Chlorophyll	0	167	0	167	0	163	3.34	0	0
Lipase	0	0	0	0	0	0	0	0	0
TOTAL	40500	12600	11400	1230	138	202	1020	1800	1260

Flows (kg/day)	19	20	21	22	23	24	25	26	27
Water	0	32.2	35.8	0	0	0	34800	10400000	2590000
Cells	0	0	0	0	0	0	0	943	236
Ammonium nitrate	0	0	0	0	0	1160	0	0	0
Triple super phosphate	0	0	0	0	0	480	0	0	0
Potassium chloride	0	0	0	0	0	0	0	0	0
Aluminium sulphate	0	0	0	0	0	0	0	0	0
Hexane	0	0	0	0	0	0	0	0	0
Phosphoric acid	0	0	0	18.2	0	0	0	0	0
NaOh	0	0	0	122	0	0	0	0	0
Methanol	0	0	0	0	0	0	0	0	0
Biodiesel	0	0	0	0	0	0	0	0	0
Glycerol	0	0	0	0	0	0	0	0	0
Cooling water	0	22.4	22.4	0	0	0	0	0	0
Steam	0	0	0	0	0	0	0	0	0
Glucose	0	5.76	0.0576	0	0	0	0	0	0
Yeast	0	3.84	0.192	0	0	0	0	0	0
Precipitating chemical	0	2.4	2.4	0	0	0	0	0	0
CO_2	0	0	8.32	0	0	0	126	0	0
Phosphates	0	0	1.44	0	0	0	0	0	0
Urea	0	0	0	5.47	0	0	0	0	0
Methane (STP)	0	0	0	0	53.9	0	0	0	0
Lime (flocculent)	0	0	0	0	0	0	0	0	0
TAG	0	0	0	0	0	0	0	0	0
Chlorophyll	0	0	0	0	0	0	0	0	0
Lipase	1.6	0	0	0	0	0	0	0	0
TOTAL	1.6	66.6	70.6	145	53.9	1640	34900	10400000	2590000

Table A-7 Composition of the streams in the process flow diagram, Figure A-1, for the production of 1000 kg of biodiesel from *Phaedodactylum tricornutum* grown in the raceway ponds described in Section 3.4.1.

Flows (kg/day)	1	2	3	4	5	6	7	8	9
Water	2680000	0	13300000	0	13000000	309000	279000	29800	0
Cells	0	0	6600	0	330	6270	314	5960	0
Ammonium nitrate	153	0	0	0	0	0	0	0	0
Triple super phosphate	63.4	0	0	0	0	0	0	0	0
Potassium chloride	26.9	0	0	0	0	0	0	0	0
Aluminium sulphate	0	0	0	0	0	0	0	0	0
Hexane	0	0	0	0	0	0	0	0	49.1
Phosphoric acid	0	0	0	0	0	0	0	0	0
NaOH	0	0	0	0	0	0	0	0	0
Methanol	0	0	0	0	0	0	0	0	0
Biodiesel	0	0	0	0	0	0	0	0	0
Glycerol	0	0	0	0	0	0	0	0	0
Cooling water	0	0	0	0	0	0	0	0	0
Steam	0	0	0	0	0	0	0	0	0
Glucose	0	0	0	0	0	0	0	0	0
Yeast	0	0	0	0	0	0	0	0	0
Precipitating chemical	0	0	0	0	0	0	0	0	0
CO_2	0	11900	0	0	0	0	0	0	0
Phosphates	0	0	0	0	0	0	0	0	0
Urea	0	0	0	0	0	0	0	0	0
Methane (STP)	0	0	0	0	0	0	0	0	0
Lime (flocculent)	0	0	0	3960	0	3960	0	3960	0
TAG	0	0	0	0	0	0	0	0	0
Chlorophyll	0	0	0	0	0	0	0	0	0
Lipase	0	0	0	0	0	0	0	0	0
TOTAL	2680000	11900	13300000	3960	13000000	319000	280000	39700	49.1

Flows (kg/day)	10	11	12	13	14	15	16	17	18
Water	29800	0	0	0	125	0	0	56.4	50.9
Cells	4860	0	0	0	0	0	0	0	0
Ammonium nitrate	0	0	0	0	0	0	0	0	0
Triple super phosphate	0	0	0	0	0	0	0	0	0
Potassium chloride	0	0	0	0	0	0	0	0	0
Aluminium sulphate	0	0	0	0	0	0	0	0	0
Hexane	0	9820	9770	49.1	0	24.5	24.5	0	0
Phosphoric acid	0	0	0	0	1.15	0	0	0	0
NaOH	0	0	0	0	3.44	0	0	0	0
Methanol	0	0	0	0	0	0	0	111	2.4
Biodiesel	0	0	0	0	0	0	0	0	1000
Glycerol	0	0	0	0	0	0	0	0	106
Cooling water	0	0	0	0	0	0	0	97.4	97.4
Steam	0	0	0	0	0	0	0	1540	0
Glucose	0	0	0	0	0	0	0	0	0
Yeast	0	0	0	0	0	0	0	0	0
Precipitating chemical	0	0	0	0	0	0	0	0	0
CO_2	0	0	0	0	0	0	0	0	0
Phosphates	0	0	0	0	0	0	0	0	0
Urea	0	0	0	0	0	0	0	0	0
Methane (STP)	0	0	0	0	0	0	0	0	0
Lime (flocculent)	3960	0	0	0	0	0	0	0	0
TAG	0	1000	0	1000	0	10	991	0	0
Chlorophyll	0	95.3	0	95.3	0	93.4	1.91	0	0
Lipase	0	0	0	0	0	0	0	0	0
TOTAL	38600	10900	9770	1150	129	128	1020	1800	1260

Flows (kg/day)	19	20	21	22	23	24	25	26	27
Water	0	32.2	35.8	0	0	0	29800	10600000	2650000
Cells	0	0	0	0	0	0	0	515	129
Ammonium nitrate	0	0	0	0	0	88.4	0	0	0
Triple super phosphate	0	0	0	0	0	36.6	0	0	0
Potassium chloride	0	0	0	0	0	0	0	0	0
Aluminium sulphate	0	0	0	0	0	0	0	0	0
Hexane	0	0	0	0	0	0	0	0	0
Phosphoric acid	0	0	0	9.67	0	0	0	0	0
NaOH	0	0	0	64.5	0	0	0	0	0
Methanol	0	0	0	0	0	0	0	0	0
Biodiesel	0	0	0	0	0	0	0	0	0
Glycerol	0	0	0	0	0	0	0	0	0
Cooling water	0	22.4	22.4	0	0	0	0	0	0
Steam	0	0	0	0	0	0	0	0	0
Glucose	0	5.76	0.0576	0	0	0	0	0	0
Yeast	0	3.84	0.192	0	0	0	0	0	0
Precipitating chemical	0	2.4	2.4	0	0	0	0	0	0
CO_2	0	0	8.32	0	0	0	56.7	0	0
Phosphates	0	0	1.44	0	0	0	0	0	0
Urea	0	0	0	2.9	0	0	0	0	0
Methane (STP)	0	0	0	0	18.2	0	0	0	0
Lime (flocculent)	0	0	0	0	0	0	3960	0	3960
TAG	0	0	0	0	0	0	0	0	0
Chlorophyll	0	0	0	0	0	0	0	0	0
Lipase	1.6	0	0	0	0	0	0	0	0
TOTAL	1.6	66.6	70.6	77	18.2	125	33800	10600000	2650000

Table A-8 Composition of the streams in the process flow diagram, Figure A-1, for the production of 1000 kg of biodiesel from *Phaedodactylum tricornutum* grown in the vertical tubular airlift reactors described in Section 3.4.3

Flows (kg/day)	1	2	3	4	5	6	7	8	9
Water	1350000	0	6640000	0	6330000	309000	279000	29800	0
Cells	0	0	6600	0	330	6270	314	5960	0
Ammonium nitrate	153	0	0	0	0	0	0	0	0
Triple super phosphate	63.4	0	0	0	0	0	0	0	0
Potassium chloride	26.9	0	0	0	0	0	0	0	0
Aluminium sulphate	0	0	0	0	0	0	0	0	0
Hexane	0	0	0	0	0	0	0	0	49.1
Phosphoric acid	0	0	0	0	0	0	0	0	0
NaOH	0	0	0	0	0	0	0	0	0
Methanol	0	0	0	0	0	0	0	0	0
Biodiesel	0	0	0	0	0	0	0	0	0
Glycerol	0	0	0	0	0	0	0	0	0
Cooling water	0	0	0	0	0	0	0	0	0
Steam	0	0	0	0	0	0	0	0	0
Glucose	0	0	0	0	0	0	0	0	0
Yeast	0	0	0	0	0	0	0	0	0
Precipitating chemical	0	0	0	0	0	0	0	0	0
CO_2	0	11900	0	0	0	0	0	0	0
Phosphates	0	0	0	0	0	0	0	0	0
Urea	0	0	0	0	0	0	0	0	0
Methane (STP)	0	0	0	0	0	0	0	0	0
Lime (flocculent)	0	0	0	1980	0	1980	0	1980	0
TAG	0	0	0	0	0	0	0	0	0
Chlorophyll	0	0	0	0	0	0	0	0	0
Lipase	0	0	0	0	0	0	0	0	0
TOTAL	1350000	11900	6650000	1980	6330000	317000	280000	37700	49.1

Flows (kg/day)	10	11	12	13	14	15	16	17	18
Water	29800	0	0	0	125	0	0	56.4	50.9
Cells	4860	0	0	0	0	0	0	0	0
Ammonium nitrate	0	0	0	0	0	0	0	0	0
Triple super phosphate	0	0	0	0	0	0	0	0	0
Potassium chloride	0	0	0	0	0	0	0	0	0
Aluminium sulphate	0	0	0	0	0	0	0	0	0
Hexane	0	9820	9770	49.1	0	24.5	24.5	0	0
Phosphoric acid	0	0	0	0	1.15	0	0	0	0
NaOH	0	0	0	0	3.44	0	0	0	0
Methanol	0	0	0	0	0	0	0	111	2.4
Biodiesel	0	0	0	0	0	0	0	0	1000
Glycerol	0	0	0	0	0	0	0	0	106
Cooling water	0	0	0	0	0	0	0	97.4	97.4
Steam	0	0	0	0	0	0	0	1540	0
Glucose	0	0	0	0	0	0	0	0	0
Yeast	0	0	0	0	0	0	0	0	0
Precipitating chemical	0	0	0	0	0	0	0	0	0
CO_2	0	0	0	0	0	0	0	0	0
Phosphates	0	0	0	0	0	0	0	0	0
Urea	0	0	0	0	0	0	0	0	0
Methane (STP)	0	0	0	0	0	0	0	0	0
Lime (flocculent)	1980	0	0	0	0	0	0	0	0
TAG	0	1000	0	1000	0	10	991	0	0
Chlorophyll	0	95.3	0	95.3	0	93.4	1.91	0	0
Lipase	0	0	0	0	0	0	0	0	0
TOTAL	36600	10900	9770	1150	129	128	1020	1800	1260

Flows (kg/day)	19	20	21	22	23	24	25	26	27
Water	0	32.2	35.8	0	0	0	29800	5290000	1320000
Cells	0	0	0	0	0	0	0	515	129
Ammonium nitrate	0	0	0	0	0	88.4	0	0	0
Triple super phosphate	0	0	0	0	0	36.6	0	0	0
Potassium chloride	0	0	0	0	0	0	0	0	0
Aluminium sulphate	0	0	0	0	0	0	0	0	0
Hexane	0	0	0	0	0	0	0	0	0
Phosphoric acid	0	0	0	9.67	0	0	0	0	0
NaOH	0	0	0	64.5	0	0	0	0	0
Methanol	0	0	0	0	0	0	0	0	0
Biodiesel	0	0	0	0	0	0	0	0	0
Glycerol	0	0	0	0	0	0	0	0	0
Cooling water	0	22.4	22.4	0	0	0	0	0	0
Steam	0	0	0	0	0	0	0	0	0
Glucose	0	5.76	0.0576	0	0	0	0	0	0
Yeast	0	3.84	0.192	0	0	0	0	0	0
Precipitating chemical	0	2.4	2.4	0	0	0	0	0	0
CO_2	0	0	8.32	0	0	0	56.7	0	0
Phosphates	0	0	1.44	0	0	0	0	0	0
Urea	0	0	0	2.9	0	0	0	0	0
Methane (STP)	0	0	0	0	18.2	0	0	0	0
Lime (flocculent)	0	0	0	0	0	0	1980	0	1980
TAG	0	0	0	0	0	0	0	0	0
Chlorophyll	0	0	0	0	0	0	0	0	0
Lipase	1.6	0	0	0	0	0	0	0	0
TOTAL	1.6	66.6	70.6	77	18.2	125	31800	5290000	1320000

Table A-9 Composition of the streams in the process flow diagram, Figure A-1, for the production of 1000 kg of biodiesel from *Phaedodactylum tricornutum* grown in the horizontal tubular airlift reactors described in Section 3.4.2

Flows (kg/day)	1	2	3	4	5	6	7	8	9
Water	359000	0	1680000	0	1370000	309000	279000	29800	0
Cells	0	0	6600	0	330	6270	314	5960	0
Ammonium nitrate	153	0	0	0	0	0	0	0	0
Triple super phosphate	63.4	0	0	0	0	0	0	0	0
Potassium chloride	26.9	0	0	0	0	0	0	0	0
Aluminium sulphate	0	0	0	0	0	0	0	0	0
Hexane	0	0	0	0	0	0	0	0	49.1
Phosphoric acid	0	0	0	0	0	0	0	0	0
NaOH	0	0	0	0	0	0	0	0	0
Methanol	0	0	0	0	0	0	0	0	0
Biodiesel	0	0	0	0	0	0	0	0	0
Glycerol	0	0	0	0	0	0	0	0	0
Cooling water	0	0	0	0	0	0	0	0	0
Steam	0	0	0	0	0	0	0	0	0
Glucose	0	0	0	0	0	0	0	0	0
Yeast	0	0	0	0	0	0	0	0	0
Precipitating chemical	0	0	0	0	0	0	0	0	0
CO_2	0	11900	0	0	0	0	0	0	0
Phosphates	0	0	0	0	0	0	0	0	0
Urea	0	0	0	0	0	0	0	0	0
Methane (STP)	0	0	0	0	0	0	0	0	0
Lime (flocculent)	0	0	0	500	0	500	0	500	0
TAG	0	0	0	0	0	0	0	0	0
Chlorophyll	0	0	0	0	0	0	0	0	0
Lipase	0	0	0	0	0	0	0	0	0
TOTAL	359000	11900	1680000	500	1370000	316000	280000	36300	49.1

Flows (kg/day)	10	11	12	13	14	15	16	17	18
Water	29800	0	0	0	125	0	0	56.4	50.9
Cells	4860	0	0	0	0	0	0	0	0
Ammonium nitrate	0	0	0	0	0	0	0	0	0
Triple super phosphate	0	0	0	0	0	0	0	0	0
Potassium chloride	0	0	0	0	0	0	0	0	0
Aluminium sulphate	0	0	0	0	0	0	0	0	0
Hexane	0	9820	9770	49.1	0	24.5	24.5	0	0
Phosphoric acid	0	0	0	0	1.15	0	0	0	0
NaOH	0	0	0	0	3.44	0	0	0	0
Methanol	0	0	0	0	0	0	0	111	2.4
Biodiesel	0	0	0	0	0	0	0	0	1000
Glycerol	0	0	0	0	0	0	0	0	106
Cooling water	0	0	0	0	0	0	0	97.4	97.4
Steam	0	0	0	0	0	0	0	1540	0
Glucose	0	0	0	0	0	0	0	0	0
Yeast	0	0	0	0	0	0	0	0	0
Precipitating chemical	0	0	0	0	0	0	0	0	0
CO_2	0	0	0	0	0	0	0	0	0
Phosphates	0	0	0	0	0	0	0	0	0
Urea	0	0	0	0	0	0	0	0	0
Methane (STP)	0	0	0	0	0	0	0	0	0
Lime (flocculent)	500	0	0	0	0	0	0	0	0
TAG	0	1000	0	1000	0	10	991	0	0
Chlorophyll	0	95.3	0	95.3	0	93.4	1.91	0	0
Lipase	0	0	0	0	0	0	0	0	0
TOTAL	35200	10900	9770	1150	129	128	1020	1800	1260

Flows (kg/day)	19	20	21	22	23	24	25	26	27
Water	0	32.2	35.8	0	0	0	29800	1320000	329000
Cells	0	0	0	0	0	0	0	515	129
Ammonium nitrate	0	0	0	0	0	88.4	0	0	0
Triple super phosphate	0	0	0	0	0	36.6	0	0	0
Potassium chloride	0	0	0	0	0	0	0	0	0
Aluminium sulphate	0	0	0	0	0	0	0	0	0
Hexane	0	0	0	0	0	0	0	0	0
Phosphoric acid	0	0	0	9.67	0	0	0	0	0
NaOH	0	0	0	64.5	0	0	0	0	0
Methanol	0	0	0	0	0	0	0	0	0
Biodiesel	0	0	0	0	0	0	0	0	0
Glycerol	0	0	0	0	0	0	0	0	0
Cooling water	0	22.4	22.4	0	0	0	0	0	0
Steam	0	0	0	0	0	0	0	0	0
Glucose	0	5.76	0.0576	0	0	0	0	0	0
Yeast	0	3.84	0.192	0	0	0	0	0	0
Precipitating chemical	0	2.4	2.4	0	0	0	0	0	0
CO_2	0	0	8.32	0	0	0	56.7	0	0
Phosphates	0	0	1.44	0	0	0	0	0	0
Urea	0	0	0	2.9	0	0	0	0	0
Methane (STP)	0	0	0	0	18.2	0	0	0	0
Lime (flocculent)	0	0	0	0	0	0	500	0	500
TAG	0	0	0	0	0	0	0	0	0
Chlorophyll	0	0	0	0	0	0	0	0	0
Lipase	1.6	0	0	0	0	0	0	0	0
TOTAL	1.6	66.6	70.6	77	18.2	125	30300	1320000	330000

A.3. Determination of the Additional Pipe Length in Horizontal Tubular Airlift Reactor Due to Bends in the Solar Collector

The horizontal tubular photobioreactor shown in Figure 3-3 was assumed to consist of a 180° pipe bend every 10 m of solar collector as well as two 90° bends which connect the solar collector to the air-lift column. The additional equivalent pipe length owing to losses over bends in the pipe was determined using Equations A-1 - A-3, where K is the loss coefficient, calculated for each respective bend (Benedict, 1980). The additional lengths for each bend were then added to give the total additional length due to losses over pipe bends.

A-1

A-2

where: α = coefficient

Ω = angle of the bend (°)

r = internal radius of the pipe

R_b = bend radius (sum of the external diameter of the solar collector pipe and the distance between adjacent tubes on the horizontal plane = 0.09 m)

Re = Reynolds number

The additional pipe length, L_{eq} was then calculated for each bend, expressed as a number of pipe diameters:

A-3

Here, f_{pipe} was determined from the Colebrook equation for a smooth pipe for the specific Reynold's number.

A.4. Laboratory Airlift Reactor Sensitivity Calculations

A.4.1. Liquid Circulation in Airlift Bioreactors

As discussed in Section 4.4.2, it is important to keep the riser residence time (dark period) under 6 seconds so as not to negatively affect the algal growth rate. The riser residence time, t_r can be calculated using the below equations.

Following the calculation of the gas hold-ups in the riser and downcomer regions and U_{Lr} as described in Section 3.2.3, the overall gas hold-up could be calculated:

A-4

where: ε = overall gas hold-up

ε_r & ε_d = gas hold-ups in riser and downcomer

A_r & A_d = cross-sectional areas of the riser and downcomer (m^2)

The sparged liquid height, h_D can then be solved for using Equation A-5.

A-5

where: h_L = unsparged liquid height (m)

U_{Lr} can then be solved for iteratively using Equations 3-53-4-3-6.

The superficial liquid velocity in the downcomer, j_{Ld} was calculated by continuity using the following equation:

A-6

The circulation times in the riser could then be calculated in Equations A-7.

A-7

A.4.2. Gas-Liquid Mass Transfer

As described in Section 4.4.1, it is essential that the k_La of the system is sufficient to support the required growth rate. Additionally, at low airflow rates and high numbers of reactors in series, it is possible that the level of dissolved oxygen may reach inhibitory levels. Therefore, for the sensitivity study, as the number of reactors in series was changed or the airflow rate varied, the dissolved oxygen level in the media and both the required k_La and that of the system were calculated as described below.

The rate of CO_2 consumed (dCO_2) and O_2 generated (dO_2) could be calculated from the algal growth rate and carbon content of the biomass. This allowed for the calculation of the airflow rate, Q_g and partial pressure of CO_2 in the gas phase, P_{CO2} through the final reactor in series.

The CO_2 saturation concentration in the liquid is directly proportional to the partial pressure of CO_2 in the gas stream and was calculated using Henry's law, as shown in Equation **Error! Reference ource not found.** (Chisti, 2002).

A-8

where: H = Henry's law constant (l.Pa/g)

Following this, the k_La required to support the growth rate could be calculated using Equation 1.1.

To determine the k_La of the system, the chemical and physical properties of the system were estimated. Further, the mean bubble diameter, d_b was taken to be 2 mm, as determined by Langley *et al.* (2010) by analysis of photographic evidence.

$D_{CO2.H2O}$ =	diffusivity of CO_2 in H_2O	=	1.77×10^{-9} m^2/s	
P_{H2O} =	density of H_2O	=	1000 kg/m^3	
μ_{H2O} =	viscosity of H_2O	=	0.001 kg/m/s	
Δρ =	difference between H_2O and air density	=	998.8 kg/m^3	

Considering the total photobioreactor volume, V_R of 3.2 L and the overall gas hold-up, ε as calculated in Equation A-4, the following could be calculated:

A-9

A-10

A-11

A-12

where: A_b = surface area of one bubble (m)

V_b = volume of one bubble (m^3)

N_b = number of bubbles in the reactor

$A_{i,total}$ = total gas-liquid interfacial area (m^2)

The following correlation, suggested by Calderbank and Moo-Young (1961), was used to estimate the k_La for the transfer of a sparingly soluble solute from a swarm of bubbles, with a mean bubble diameter of less than 2.5 mm, into a solvent (Welty *et al.*, 2001). This required calculation of the Grashof (Gr) and Schmidt (Sc) numbers in Equations A-13 and A-14 respectively, towards the calculation of the overall mass transfer coefficient in Equation A-15.

A-13

A-14

A-15

Towards the calculation of the dissolved oxygen concentration in the reactors, the partial pressure of O_2 in the gas phase, P_{O2} through the final reactor in series, could be calculated as for CO_2. This allowed for calculation of the O_2 saturation concentration in the liquid using Henry's law, as shown for CO_2 in Equation **Error! Reference source not found.**.

Equation A-16 has been shown to be accurate in to converting $k_La(CO_2)$ to $k_La(O_2)$ (Chisti, 2002; Talbot *et al.*, 1991).

A-16

where: $D_{O2.H2O}$ = diffusivity of O_2 in H_2O

Thus, the O_2 saturation concentration, oxygen mass transfer coefficient and the rate of oxygen mass transfer, taken from the growth rate, were used in Equation 1.1. to solve for the dissolved oxygen concentration in the media.